

# **HUMAN RESPONSIVE DAYLIGHTING IN OFFICES a gaze-driven approach for dynamic discomfort glare assessment**

THÈSE N° 6660 (2015)

PRÉSENTÉE LE 19 JUIN 2015

À LA FACULTÉ DE L'ENVIRONNEMENT NATUREL, ARCHITECTURAL ET CONSTRUIT  
LABORATOIRE INTERDISCIPLINAIRE DE PERFORMANCE INTÉGRÉE AU PROJET  
PROGRAMME DOCTORAL EN GÉNIE CIVIL ET ENVIRONNEMENT

ÉCOLE POLYTECHNIQUE FÉDÉRALE DE LAUSANNE

POUR L'OBTENTION DU GRADE DE DOCTEUR ÈS SCIENCES

PAR

**Mandana SAREY KHANIE**

acceptée sur proposition du jury:

Prof. M. Bierlaire, président du jury  
Prof. M. Andersen, Dr J. Wienold, directeurs de thèse  
Prof. C. Schierz, rapporteur  
Dr M. Knoop, rapporteuse  
Prof. S. Süssstrunk, rapporteuse  
Prof. Prof. W. Einhäuser-Treyer, rapporteur



ÉCOLE POLYTECHNIQUE  
FÉDÉRALE DE LAUSANNE

Suisse  
2015



# HUMAN RESPONSIVE DAYLIGHTING IN OFFICES

A GAZE-DRIVEN APPROACH FOR DYNAMIC DISCOMFORT GLARE ASSESSMENT

THIS IS A TEMPORARY TITLE PAGE

Thèse n. 6660 2015

présenté le 19 June 2015

à la Faculté de l'Environnement Naturel, Architectural et Construit

Laboratoire interdisciplinaire de performance intégrée au projet [LIPID]

Programme doctoral en Génie-civil et environnement [EDCE]

École Polytechnique Fédérale de Lausanne

pour l'obtention du grade de Docteur ès Sciences

par



**MANDANA SAREY KHANIE**

acceptée sur proposition du jury:

Prof. Michel Bierlaire, président du jury

Prof. Marilyne Andersen, directeur de thèse,

Dr. -ing. Jan Wienold, co-directeur de thèse

Prof. Christoph Schierz, rapporteur

Dr. Martine Knoop, rapporteur

Prof. Wolfgang Einhäuser, rapporteur

Prof. Sabine Süssstrunk, rapporteur

Lausanne, EPFL, 2015



L'architecture est jugée par les yeux qui voient, par la tête qui tourne, par les jambes qui marchent. L'architecture n'est pas un phénomène synchronique, mais successif, fait de spectacles s'ajoutant les uns aux autres et se suivant dans temps et l'espace, comme d'ailleurs le fait la musique. **Architecture is judged with searching eyes, with a moving head, with moving legs. Architecture is not a synchronous phenomenon, but rather a succession of one drama after another, consecutive in time and space, in much the same way as music is structured.**

*Le Corbusier*



# Abstract

This dissertation proposes a novel gaze-driven approach for dynamic discomfort glare assessments as a first step towards understanding human responsive comfort with respect to daylight. The objective was to observe the natural gaze behaviour in relation to glare for office spaces with the conditions implicitly constrained by real world luminous conditions. In the existing visual comfort models human behaviour is not sufficiently considered. These models employ only subjective assessments, which lack an objective understanding of the factors affecting the perceptual mechanism of light-induced visual discomfort. They so far have not integrated the inter-dependencies of visual discomfort perception and human gaze responses and have been limited to a fixed-gaze assumption directed towards the office task area.

In this dissertation, a gaze-driven approach is developed and adopted in the discomfort glare assessments. The assessments were done in a series of experiments in simulated office setting under different lighting conditions where participants' gaze responses with means of mobile eye-tracking as well as their subjective assessments were recorded while monitoring photometric quantities relevant to visual comfort using high dynamic range luminance imaging. Integration of the luminance images coupled with eye tracking enabled us to obtain the gaze-centred luminance fields, which gives a better estimate of actual luminance values perceived by the eye, used as a basis to investigate the gaze direction dependencies of visual comfort.

This PhD dissertation describes different stages of conception of this novel dynamic discomfort glare assessment method. In the experimental phase, two pilot studies were made for proper integration of the adopted methods and techniques into discomfort glare assessments. Development of several routines, algorithms and tools to identify and translate the gaze directions in order to derive the actual luminance field perceived by the participants were needed to achieve this goal. A final comprehensive experimental phase was realised to investigate gaze behaviour in response to light. As a first validation step, the gaze-driven approach was compared to the fixed-gaze approach. Then the effects of different luminance levels as well as different view outside the window on the dynamic shifts of the gaze were investigated. The developed approach demonstrates the need to integrate gaze direction patterns into visual comfort assessments, which move us beyond the existing assumption of a fixed-gaze direction towards a gaze responsive comfort.

**Key words:** *Daylighting, Discomfort glare, Gaze Direction, HDR imaging, Mobile eye-tracking*





# Résumé

Cette thèse propose une nouvelle approche pour une évaluation dynamique de l'inconfort visuel basée sur la direction de regard comme un premier pas vers une meilleure compréhension du confort et bien-être humains en ce qui concerne l'éclairage naturel. L'objectif est d'observer la direction du regard en lien avec l'éblouissement dans un espace de travail présentant des conditions implicitement limitées par l'état lumineux réel. Ces modèles n'ont à ce jour pas intégré les interdépendances entre cette perception et la direction du regard. Ils sont restés limités à l'hypothèse du regard fixe dirigé vers l'endroit du bureau lié à la tâche de l'occupant. Dans cette thèse, une approche basée sur le regard est développée et adoptée dans l'évaluation de l'éblouissement inconfortable. Nous dérivons la distribution de luminance dans le champ de vision (FOV) par rapport à la direction réelle du regard, ce qui nous donne une meilleure estimation des valeurs réellement perçues par l'œil. Les évaluations ont été menées via une série d'expériences dans un environnement simulant un bureau sous différentes conditions lumineuses. La réponse en terme du regard des participants a été enregistrée à l'aide d'un appareil mobile d'oculométrie. L'évaluation subjective des participants a aussi été enregistrée, et les valeurs photométriques pertinentes au confort visuel monitorées en utilisant la technique d'imagerie à grande gamme dynamique (HDR). L'intégration des images de luminance couplées à l'oculométrie permet d'obtenir les champs de luminance associés à la direction du regard. Une base de donnée unique a ainsi été créée comme pour étudier la dépendance entre la direction du regard et le confort visuel. Cette thèse de doctorat décrit les différentes phases de conception de cette nouvelle méthode dynamique. Dans la phase expérimentale, deux études pilotes ont été faites pour l'intégration adéquate des nouvelles méthodes et techniques dans l'évaluation de l'éblouissement inconfortable pour tenir compte des mesures de luminance réelles ressenties par les participants. Le développement de plusieurs routines, algorithmes et outils est décrit en détail. Une phase d'expérimentation finale a été réalisée pour étudier le comportement du regard en réponse à la lumière. Nous avons d'abord comparé cette nouvelle approche basée sur la direction du regard à celle basée sur l'hypothèse du regard fixe. Ensuite, nous avons étudié l'effet de différents niveaux de luminance et des vues sur l'extérieur sur les déplacements dynamiques du regard. L'approche développée démontre la nécessité d'intégrer la direction du regard dans l'évaluation du confort visuel, ce qui nous pousse au-delà de l'hypothèse actuelle d'une direction de regard fixe vers la notion d'une direction réactive au confort.

**Mots clés :** *lumière du jour, éblouissement inconfortable, direction du regard, imagerie à grande gamme dynamique (HDR), oculométrie mobile*



# Zusammenfassung

In dieser Dissertation wird eine neuartige Methodik für die dynamische psychologische Blendungsbewertung entwickelt, in der die Blickrichtung berücksichtigt wird. Dies ist ein erster Schritt hin zum Verständnis der subjektiven Wahrnehmungsbewertung im Bezug auf Tageslicht. Ziel der Arbeit war die Beobachtung des natürlichen Blickverhaltens in Büroarbeitsplätzen im Bezug auf tatsächliche Einstrahlungsverhältnisse. Vorhandene visuelle Komfortmodelle vernachlässigen den Zusammenhang zwischen der Wahrnehmung von visuellem Komfort (oder Unbehagen) und der Blickrichtung und verwenden anstatt dessen eine feste Blickrichtung - meist in Richtung des Tätigkeitsbereiches (z.B. im Büro). Eine Reihe von Nutzerversuchen wurden in büroähnlichen Versuchsräumen unter verschiedenen Lichtverhältnissen durchgeführt. Dabei wurden die Blickrichtungen der Versuchsteilnehmer mithilfe eines mobile Eye-Trackers aufgezeichnet. Des Weiteren wurden parallel dazu die subjektive Wahrnehmung der Teilnehmer erfasst und die relevanten lichttechnischen Größen unter Einbeziehung von Leuchtdichteaufnahmen aufgezeichnet. Die Kombination aus Leuchtdichteaufnahmen und Blickrichtungserfassung ermöglicht es eine blickrichtungsabhängige Leuchtdichteverteilung zu verwenden, die eine verbesserte Abschätzung der vom Auge wahrgenommenen Leuchtdichten liefert. Mithilfe dieses neuen Ansatzes wurde eine einzigartige Datengrundlage geschaffen, um die Abhängigkeit von Blickrichtung und visuellem Komfort weiter zu untersuchen. In der Arbeit werden die verschiedenen Phasen der Konzeption einer neuartigen dynamischen Blendungsbewertung dargestellt. In der experimentellen Phase wurden zwei Pilotstudien durchgeführt bei denen die neuen Methoden und Techniken in die Blendungsbewertung integriert wurden, um die durch die Teilnehmer wahrgenommenen Leuchtdichten zu berücksichtigen. Die Entwicklung verschiedener Routinen, Algorithmen und Werkzeuge zur Identifizierung und Transformierung der Blickrichtungen werden detailliert beschrieben. In einer abschließenden Experimentalphase wurde das Nutzerverhalten hinsichtlich Blickrichtung in Reaktion auf verschiedene Lichtsituationen untersucht. Als Erstes wird die neue entwickelte, durch die Blickrichtung bestimmte Methode mit der auf einer festen Blickrichtung basierenden verglichen. Anschließend untersuchten wir die Auswirkung unterschiedlicher Leuchtdichten sowie den Einfluss verschiedener Ausblicke aus dem Fenster auf die Veränderungen der Blickrichtung der Probanden. Die Ergebnisse veranschaulichen die Notwendigkeit zukünftig die Blickrichtung bei visuellen Komfortbewertungen mit zu berücksichtigen. Die Ergebnisse zeigen auch, dass die Annahme einer festen Blickrichtung nicht unbedingt zutrifft, sondern die Blickrichtung je nach Lichtsituation angepasst wird.

**Stichwörter:** *Tageslicht, psychologische Blendung, Blickrichtung, HDR imaging, Eye-tracking*



# Acknowledgements

I am grateful for the many people who have supported me during my thesis work:

First and foremost I would like to thank Prof. Marilyne Andersen for believing in me and providing me with the opportunity to pursue my career to become a specialist in my field. I would like to thank you for your valuable criticism and scientific rigour. You have taught me the value of perfection and guide me through my journey to become a scientist architect.

Dr. Jan Wienold, I thank you for your feedback during these years and your supervision during my last year as co-supervisor.

Prof. Wolfgang Einhauser for believing in the interdisciplinary nature of this work and always having a big smile, a positive attitude and much fruitful advice.

My committee members Prof. Christoph Schiertz, Dr. Martine Knoop, Prof. Wolfgang Einhauser and Prof. Süsstrunk for the attention with which you read this thesis and the helpful questions and feedback that enhanced the quality of this work, and Prof. Michel Bierlaire for kindly accepting to direct the exam as the thesis jury president with great professionalism.

École Polytechnique Fédérale de Lausanne (EPFL) for having provided financial support and infrastructure for this project.

The Swiss National Science Foundation for a financial support that will allow me to advance this work in my Post-Doctoral study.

My dear eye tracking expert of all time Josef Stoll for his always direct criticism and for reminding me of my mathematical mistakes.

I would like to thank Professor Michael Bach and Dr. Marius 't Hart for their fruitful advice and comments early on that helped shape this project.

## Acknowledgements

---

I wish to thank Christian Reetz at PSE Freiburg for his technical contribution and valuable programming expertise in making the *NewView* tool. Sandra Mende for her assistance and contribution in the first experimental runs that we did together. Lucas Nainemoutou for helping me to sort thousands of images and Lena Kraeling for her assistance in recruiting 168 test persons for my last experiment.

I would also like to thank all those who made my PhD life the most fun, enjoyable and memorable years with all its ups and downs with their big hearts, great smiles and support:

Sweetest Emilie Nault, thank you for always helping me with my French. Maria Ámundadóttir and Jon Agustsson, for enjoyable companionship, amazing mountaineering, ski and climbing experiences. Siobhan Rockcastle for all the scientific and non-scientific discussions. My youngest and sweetest colleague Parag Rastogi (Thank you for the elephants!). And of course Monsieur Dr. Boris. And the very new members of the lab whom I exploited the last few months of my thesis for several proof readings: Giuseppe, Luisa, JD, Kynthia and Georgia.

Kai Pippo, for bringing me to the lighting world and Clara Fraenkel for her supervisions. My many friends who have always been there for me all 544+ of them. Hoda Y., Therese H., Cristina C., I am very happy to have you guys in my life. Mehrnaz H. for many projects that we finished together.

My very special thanks to my dearest parents: Farah for being a role model for me as an ambitious, successful and strong woman and Nosrat for his endless support, encouragement, enthusiasm and just being the Dad that he is. I love you both endlessly. My lovely sisters, Pantea for being such an angle in my life and Anahita Roxana who always cheers me up with her sweet laughs. Words can not express my gratitude so I will refrain from forcing them.

I am grateful for the granted access to Fraunhofer ISE test facilities and thank the ISE staff and non-ISE participants that took part in the experimental study. I hope you enjoyed the Steini<sup>2</sup>s on the ISE's rooftop.

This project was supported by the École Polytechnique Fédérale de Lausanne (EPFL)

*Lausanne, March 2015*

M. S.

# List of Publications

The results of this PhD research project have been published in the following publications:

## Journal Papers

**(Manuscript Accepted for Publication)**

**M. Sarey Khanie, J. Stoll, W. Einhäuser, J. Wienold, M. Andersen.** Gaze driven approach for estimating luminance values in the field of view for discomfort glare assessments. *Journal of Lighting Research and Technology*.

**(Manuscript in Preparation)**

**M. Sarey Khanie, J. Stoll, W. Einhäuser, J. Wienold, M. Andersen.** Dynamics of gaze direction in day lit office spaces. (Manuscript in Preparation to be submitted to *Journal of Lighting Research and Technology*.)

## Conference Papers

**(Pending papers)**

**M. Sarey Khanie, Y. Jia, J. Wienold, M. Andersen.** A sensitivity analysis on glare detection parameters. BS2015 - 15th International Conference of the International Building Performance Simulation Association, Hyderabad, India, 2015. (Accepted abstract, Paper under review)

**M. Sarey Khanie, J. Stoll, W. Einhäuser, J. Wienold, M. Andersen.** Gaze driven approach for discomfort glare assessments. The 28th SESSION of the CIE will take place in Manchester, United Kingdom, June 28 - July 4, 2015. (Accepted paper)

**(Presented work)**

**M. Sarey Khanie\*, J. Wienold, M. Andersen.** A sensitivity analysis on glare detection parameters (remote presentation). In: 13th International Radiance Workshop, London, UK, 2014.

## List of Publications

---

**J. Stoll, M. Sarey Khanie, S. Mende, J. Wienold, M. Andersen, W. Einhäuser\***. Real-world tasks with full control over the visual scene: combining mobile gaze tracking and  $4\pi$  light-field measurements. 17th EUROPEAN CONFERENCE ON EYE MOVEMENTS (ECEM), Lund, Sweden, 2013.

**M. Sarey Khanie\***, **J. Stoll, S. Mende, J. Wienold, W. Einhäuser, M. Andersen**. Uncovering relationships between view direction patterns and glare perception in a daylit workspace. LUXEUROPA, Krakow, Poland, 2013.

**M. Sarey Khanie\***, **J. Stoll, S. Mende, J. Wienold and W. Einhäuser, M. Andersen**. Investigation of gaze patterns in daylit workplaces: using eye-tracking methods to objectify view direction as a function of lighting conditions. CIE Centenary Conference "Towards a New Century of Light", Paris, France, 2013.

**M. Sarey Khanie\***, **M. Andersen, B. M. 't Hart, J. Stoll, W. Einhäuser**. Integration of Eye-tracking Methods in Visual Comfort Assessments. CISBAT 11: CleanTech for Sustainable Buildings - From Nano to Urban Scale, Lausanne, Switzerland, 2011.

\* presenter

## Posters

**M. Sarey Khanie and M. Andersen**. Understanding View Direction in Relation to Glare in Daylit Offices. VELUX Daylight symposium: New eyes on existing buildings, Copenhagen, 2013.

**J. Stoll, M. Sarey Khanie, S. Mende, M. 't Hart, M. Andersen, W. Einhäuser**. Combining wearable eye-tracking with  $4\pi$  light-field measurements: towards controlling all bottom-up and top-down factors driving overt attention during real-world tasks. 10th Göttingen Meeting of the German Neuroscience Society, Göttingen, Germany, 2013.

**M. Sarey Khanie, M. Andersen (Dir.)**. Towards a model for View Direction patterns as a function of light distribution. ENAC Research Day, Lausanne, Switzerland, 2011.

**M. Sarey Khanie and M. Andersen**. Model for view direction as a function of light distribution. Academic Forum of the 4th Velux Daylight Symposium, Lausanne, Switzerland, 2011.

**M. Sarey Khanie and M. Andersen**. Towards a refined understanding of comfort in workspaces. Swiss-Emirati Friendship Forum: UAE-Swiss Research Day 2011, Lausanne, Switzerland, 2011.



**Supervised Student Works**

**Y. Jia, M. Sarey Khanie (Dirs.), M. Andersen.** Sensitivity analysis on glare detection algorithm using High Dynamic Range imaging techniques for light rendering based tools. 2014. (3 months internship through Georgia Tech-EPFL student exchange program)

**S. J. Gochenour, M. L. Ámundadóttir, M. Sarey Khanie (Dirs.), M. Andersen.** Light-Syntax Zones in Daylit Café Spaces: A Novel Method for Understanding Occupancy. , 2014. (Master Thesis work)

**M. Niqui, M. Sarey Khanie (Dirs.), J. Huang, M. Andersen.** Responsive Systems: Light and Human Responsive Systems in Architecture. , 2012. (Master Thesis work)



# Contents

<b>Abstract</b>	<b>i</b>
<b>Acknowledgements</b>	<b>vii</b>
<b>List of Publications</b>	<b>ix</b>
<b>List of Figures</b>	<b>xvii</b>
<b>List of Tables</b>	<b>xxv</b>
<b>I Introduction</b>	<b>1</b>
I.1 Daylighting in Offices . . . . .	1
I.2 Bringing Discomfort Glare and Gaze Together . . . . .	2
I.3 Outline of the Study . . . . .	5
<b>II Discomfort Glare and Gaze:</b>	
<b>State of the Art</b>	<b>7</b>
II.1 Lighting and Discomfort Glare in Offices . . . . .	7
II.2 Discomfort Glare Models . . . . .	10
II.3 Gaze and Natural Behaviour in Relation to Glare . . . . .	14
II.4 View Outside the Window and Glare . . . . .	15
<b>III Methodology</b>	<b>17</b>
III.1 Experimental Strategy . . . . .	18
III.2 Experimental Set up . . . . .	19
III.2.1 Daylight Laboratory . . . . .	20
III.2.2 Photometric Measurements . . . . .	21
III.2.3 Visual Office Task: Development & Design . . . . .	22
III.2.4 Standardised Introduction . . . . .	26
III.2.5 Subjective Assessments: Development & Design . . . . .	28
III.3 HDR Imaging Techniques for Discomfort Glare Evaluations . . . . .	32
III.4 Mobile Eye-tracking Method & Measurements . . . . .	35
	<b>xiii</b>

## Contents

---

III.5	Analysis Methods . . . . .	36
<b>IV</b>	<b>A Novel Gaze-driven Approach</b>	<b>39</b>
IV.1	Step I: Gaze-in-world Directions . . . . .	40
IV.2	Step II: Identifying the Dominant Gaze Directions . . . . .	43
IV.2.1	Secondary and Tertiary Dominant Gaze Directions . . . . .	45
IV.2.2	Analysis of Secondary and Tertiary Dominant Gaze . . . . .	45
IV.3	Step III: Deriving Gaze-centered Luminance Images . . . . .	48
IV.4	Summary . . . . .	51
<b>V</b>	<b>Experimental Phase: Pilot Studies</b>	<b>53</b>
V.1	Experiment I: Integrating Eye-tracking Methods . . . . .	53
V.1.1	Set up . . . . .	53
V.1.2	Proof of Concept . . . . .	56
V.1.3	Conclusions of Experiment I . . . . .	59
V.2	Experiment II . . . . .	60
V.2.1	Set up . . . . .	61
V.2.2	Outcome I . . . . .	64
V.2.3	Outcome II . . . . .	67
V.2.4	Outcome III . . . . .	67
V.2.5	Conclusions of Experiment II . . . . .	69
V.3	Summary & Discussion . . . . .	70
<b>VI</b>	<b>Experimental Phase: Full Study</b>	<b>73</b>
VI.1	Experiment III: Investigating Gaze in Relation to Glare . . . . .	74
VI.1.1	Set up . . . . .	74
VI.1.2	Experimental Design . . . . .	76
VI.1.3	Lighting Conditions . . . . .	77
VI.1.4	Results: Gaze Behaviour in Different Lighting Conditions . . . . .	81
VI.2	Experiment IV: View Outside the Window . . . . .	88
VI.2.1	Experimental Design . . . . .	90
VI.2.2	Lighting Condition . . . . .	90
VI.2.3	Results: Gaze Dynamics & View Outside the Window . . . . .	91
VI.3	Summary & Discussion . . . . .	96
<b>VII</b>	<b>Gaze-driven vs. Fixed-gaze Approach in Glare Evaluations</b>	<b>99</b>
VII.1	Uncertainty Estimation . . . . .	101
VII.1.1	EyeSeeCam - Gaze Uncertainty . . . . .	101
VII.1.2	Gaze-Centred Luminance Image Uncertainty . . . . .	102

VII.2 Results: Gaze-driven Approach vs. Fixed-gaze Approach . . . . .	104
VII.3 Summary & Discussion . . . . .	110
<b>VIII Conclusion</b>	<b>111</b>
VIII.1 Achievements . . . . .	111
VIII.2 Main Findings and Discussion of Results . . . . .	112
VIII.3 Application and Use in Perspective . . . . .	115
VIII.4 Future steps . . . . .	120
<b>Appendices</b>	<b>123</b>
<b>A Questionnaire</b>	<b>125</b>
<b>B Office task sequence</b>	
<b>On paper example</b>	<b>133</b>
<b>C Nomenclature</b>	<b>141</b>
<b>Curriculum Vitae</b>	<b>157</b>



# List of Figures

I.1	<b>Discomfort glare depends on four physical quantities:</b> the illustrations on a fisheye luminance images show a) $L_s$ (luminance of glare source), b) $\omega_s$ (solid angle of source), c) $L_a$ (adaptation luminance), and d) $P_i$ (position index); where $\alpha$ is the angle from vertical plane of line gaze and $\beta$ is the angle between the gaze direction and the line between the eye and the glare source. . . . .	3
I.2	<b>Gaze direction:</b> Gaze direction is where we direct our gaze by mutually moving our body, head and eyes. . . . .	4
I.3	<b>Structure of the work</b> . . . . .	5
II.1	<b>Position Index angular description</b> . . . . .	9
II.2	<b>Position Index:</b> $Y$ is horizontal distance between source and gaze direction [mm], $H$ is vertical distance between source and gaze direction [mm] and $D$ is the distance between eye and plane of glare source [mm]. . . . .	9
III.1	<b>Schematic map of methods.</b> . . . . .	17
III.2	<b>Main facility and tools in the general set up:</b> a) the daylight laboratory which is an office like test facilities, b) the ESC worn by a subject, b) the two CCD cameras used in the experiments installed so as to be positioned above the participants head. . . . .	19
III.3	<b>Plan of the daylight laboratory:</b> the layout of the rooms, the position of the measurement devices and all the objects that were used in the experiment or were in the scene. . . . .	21
III.4	<b>Cameras comparison method:</b> by capturing images with each camera, a) C1: LMK 98 and, b) C2: LMK 98-4, c) the photometric output of the predefined region was then compared. . . . .	22
III.5	<b>Cameras positions:</b> a) the section showing the position of the CCD cameras and the approximate position of the EyeSeeCam mounted on the participants head, b) the two CCD cameras are installed above the participants head position with 90° of rotation from each other, c) the EyeSeeCam is equipped with three cameras, (1) Head-fixed scene camera, (2) & (3) Eye-tracking cameras. . . . .	22
III.6	<b>Task-supports:</b> a) screen, b) paper, c) phone. . . . .	23

## List of Figures

---

III.7	<b>Task sequence on screen:</b> a) input text justified in the screen centre; b) thinking phase with an off screen; c) the multi-choice question based on the content of the input text; d) a designated area was presented for typing. . . . .	25
III.8	<b>On-screen specification:</b> a) computer screen luminance variations during the on-screen task, b) the figure shows an upper corner section of one of the texts as displayed on the computer screen. Measures such as word, character and between line spacing as well as font size and font type was taken into consideration for a standardised visual task representation. These measures, shown in table III.8a, were set in the Adobe Flash software. . . . .	25
III.9	<b>Introductory phase:</b> a) the participants entered Room L and took position at seat 1. b) the response box . . . . .	27
III.10	<b>Glare ratings:</b> a) Hopkinson's glare scale, b) participants were asked to rate glare with the Likert scale after each phase. . . . .	30
III.11	<b>Continuous scale:</b> a) participants were asked to rate glare on a continuous glare scale with vertical representation before and after the experiment, b) the purpose fitness scale using a continuous itemised scale with vertical representation. The participants were instructed on how to use the scale. . . . .	31
III.12	<b>HDR luminance images:</b> a) physically-based renderings, b) an HDR image captured by a CCD camera equipped with fisheye lense,c) luminance value of pixel $L_j$ is calculated based on the recorded RGB values and its position is defined by three coordinates. . .	33
III.13	<b>Image processing for glare evaluation:</b> a) the algorithm searches the pixels column by column, b) . . . . .	34
III.14	<b>Image processing for glare evaluation:</b> Using <i>Evalglare</i> we measured 5 different thresholds and 3 different search radii to calculate the visual comfort models. a, b and c show three examples, where the glare sources found with 3 different combinations are highlighted. The colours don't have a meaning. . . . .	35
III.15	<b>EyeSeeCam calibration:</b> a) The seating position 100 [cm] from the opposite wall, b) five dots that are projected on the wall from the ESC, c) Participant wearing the eye-tracker and a headset at the desk position. . . . .	36
IV.1	<b>Generating a gaze-cantered luminance image.</b> . . . . .	39
IV.2	<b>The gaze-in-world coordinates are derived from:</b> a) the eye-in-head coordinates superimposition with the, b) head-in-room coordinates to derive, c) the gaze-in-world coordinates. . . . .	41
IV.3	<b>EyeSeeCam coordinate system:</b> a) EyeSeeCam coordinate system in the room and the rotation IMU, b) the spherical coordinates representing the horizontal and vertical angular definitions of the gaze vectors in the 3D space. . . . .	42



IV.4	<b>Gaze-in-world distributions:</b> a,b) a participant's gaze distribution binned during on-screen <i>Input</i> phase and <i>Thinking</i> phase; the x-axis and y-axis respectively correspond respectively to 180° horizontal gaze orientation and 90° vertical gaze orientation. . . .	44
IV.5	<b>Gaze-in-world distributions:</b> a histogram of gaze-in-world distribution; the x-axis corresponds to 180° horizontal gaze orientation; the y-axis and the colour bar shows the number of gaze encounters at each point in space; the dominant gaze direction with the highest number of encounters is shown with an arrow. . . . .	44
IV.6	<b>Primary, secondary &amp; tertiary gaze:</b> a) a participant's gaze allocations during a <i>Thinking</i> phase. Three dominant gaze directions are identified. b) 3D visualisation of the gaze allocations. . . . .	45
IV.7	<b>Primary, secondary and tertiary gaze:</b> a gaze-centred luminance image was developed with respect to each identified dominant gaze and processed, a) the primary dominant gaze, b) the secondary dominant gaze, c) and the tertiary dominant gaze. . . . .	46
IV.8	<b>Primary, secondary and tertiary gaze:</b> a) percentage of all cases of identified dominant gaze encounters ion comparison to the primary gaze, b) a boxplot showing the distribution of the vertical illuminance for primary , secondary and tertiary dominant gaze directions. . . . .	46
IV.9	<b>3D visualisation:</b> one participant's gaze allocations for each task phase using computer.	47
IV.10	<b>3D visualisation:</b> One participant's gaze allocations during each task phase using a headset. . . . .	47
IV.11	<b>Translating the gaze directions to the camera coordinates:</b> a) the coordinate system of the EyeSeeCam and <i>Radianc</i> e is shown, b) vector $\hat{v}$ is a gaze direction from the camera position that is looking in the same direction as $\hat{g}$ . . . . .	49
IV.12	<b>Gaze intersection with the 3D geometry:</b> a) the resulting 3D representation of all gaze points from one participant over a minute of <i>Input</i> phase recorded with 221Hz sampling rate. . . . .	50
IV.13	<b>Luminance images:</b> a) participant's view, and b) window's view, c) resulting image for a dominant gaze direction. . . . .	50
IV.14	<b>Merging the two luminance images:</b> a) the overlapping Pixels at the border of the lens within a 2° range, here highlighted in red, were removed, b, c) each single image is rotated, so that the image's view direction property is pointed to the centre of the image, the black areas are the regions that were not captured by either camera, d) The areas that were not captured by any camera are highlighted in red. . . . .	51
V.1	<b>Plan of the daylight laboratory for experiment I:</b> the layout of the rooms, location of the participant during the test procedure, the position of the measurement devices and all the objects that were used or were in the scene in the first pilot study. . . . .	54

## List of Figures

---

V.2	<b>Set up and main measurements:</b> a) a participant being introduced to the experiment. b) the two cameras were installed side by side, here the possibility of getting a 360° image by rotating one of the cameras by 180° was tested, c) earlier version of ESC used in these experiments. . . . .	54
V.3	<b>Façades considered in the pilot study:</b> a) FS1: clear sky condition with no direct sunlight in the room, b) FC2: clear sky condition with venetian blind half way down, c) FC3: clear sky condition with direct sunlight in the room, d) FC4: clear sky condition with the sun in the FOV. . . . .	55
V.4	<b>Processed images:</b> To evaluate each condition one image per task phase was processed, a-b) coloured patches show the identified glare sources. . . . .	57
V.5	<b>Results:</b> illuminance at the vertical level [lux] of each participant (at the assumed eye position at camera C2 position) measure per each façade configuration are shown. . .	58
V.6	<b>Results:</b> a) horizontal variance between all four façades b) horizontal variance between two façade configurations: "2: dark and high contrast" "4: bright and extreme contrast".	58
V.7	<b>Plan of the daylight laboratory for experiment II:</b> the layout of the rooms, location of the participant during the test procedure, the position of the measurement devices and all the objects that were in the scene during these experiments. . . . .	60
V.8	<b>Test procedure:</b> a schematic representation of the test procedure of the experiment .	61
V.9	<b>Luminance images processed:</b> a) on-screen task, b) on-paper task, c) on phone task. The reference task area is marked in blue and the detected glare sources are highlighted.	62
V.10	<b>Luminance contrast during different task activities:</b> box-plot representation of the contrast and its variation. The box represents 50% of the data and the outer borderlines 95% of the data. a) During the on-screen activity's <i>Thinking</i> phase, the screen turns off which significantly lowers the general luminance contrast. b) Certain large variations of contrast can be seen due to participants' position changes while working with paper. c) The inconsistencies seen in the previous task activities are not visible in this phase. The screen is off and the participant holds a stable position. . . . .	63
V.11	<b>The two view outside the window:</b> a) southwest orientation b) west orientation. . . .	64
V.12	<b>Results overview:</b> a) <i>Input</i> phase b) <i>Thinking</i> phase, c) <i>Response</i> phase, d) <i>Interaction</i> phase . . . . .	65
V.13	<b>Results overview:</b> a) dominant gaze distribution for all participants and for the four phases of the trial; view southwest and west are shown with two colours , b, c) the gaze direction distribution behaves independently of view outside the window for different ranges of visual engagement in the office task . . . . .	67
V.14	<b>Daylight conditions:</b> glare evaluations were used for refining the groupings: a) low contrast, b) high contrast; c, d) the box-plot shows illuminance variations reaching the eye at a vertical level. . . . .	68

V.15	<b>Results overview:</b> during the a) <i>Input</i> phase the gaze directions are more focused on the task area under both light conditions, whereas during the b) <i>Thinking</i> phase the gaze direction is more dispersed over the space. . . . .	69
V.16	<b>Results overview:</b> the mean and radial standard deviations of the gaze orientations are compared for the three task-supports under the two lighting conditions during: a) the <i>Input</i> phase, b) the <i>Thinking</i> phase. The origin is at the border of inside and outside at the corner of the room (Figure: V.17b). . . . .	71
V.17	<b>Results overview:</b> a) $E_v$ for the two lighting conditions, b) the mean gaze orientation is illustrated: when the participants are not engaged in visually demanding task and the presence of the task-support is minimal, the gaze orients towards the view outside, but this tendency is less in high contrast lighting conditions. . . . .	71
VI.1	<b>Plan of the daylight laboratory for final experiments:</b> the layout of the rooms, location of the participant during the test procedure, the position of the measurement devices and all the objects that were used in the experiment or were in the scene. . . . .	74
VI.2	<b>Test Procedure:</b> a diagram showing the flow of the test procedure with different data collection and experimental trial phases for each participant . . . . .	75
VI.3	<b>Simulations for the foreseen experimental:</b> daylight condition categorisation based on the direct sunlight geometry . . . . .	77
VI.4	<b>Daylight conditions:</b> based on the sun-patch geometry variations for southwest orientation, a) August, b) September; Daylight saving time has not been considered. Numbers 1-8 corresponds to number shown in figure VI.3. Number (9) is the sunset and (10) is after sunset conditions. . . . .	78
VI.5	<b>Daylight conditions:</b> based on the sun-patch geometry variations for west orientation, a) August, b) September; Daylight saving time has not been considered. Numbers 1-8 corresponds to number shown in figure VI.3. Number (9) is the sunset and (10) is after sunset conditions. . . . .	78
VI.6	<b>Lighting conditions:</b> the plot shows the distribution of a) the vertical illuminance at the vertical level at the position of camera C2 and b) the distribution of average luminance in the room for each lighting condition. . . . .	79
VI.7	<b>Six lighting conditions were considered in these experiments:</b> a) LC1: Clear sky with no direct sunlight, b) LC2: clear sky with direct sunlight on the wall opposite to the participant, c) LC3: clear sky with direct sunlight on desk, d) LC4: clear sky with sun in the scene, e) LC5: overcast sky, f) LC6: artificial light. . . . .	80
VI.8	a) the graph compares the average glare source size and brightness under different lighting conditions. The diameter of each circle is proportional to the average solid angle of the glare sources. b) the screen-centre axis and the outside axis are marked on the plan of the test-room. . . . .	81

## List of Figures

---

VI.9	<b>Gaze dynamics &amp; lighting conditions:</b> grouped data for the 6 lighting conditions during phase a-d) while working with monitor . . . . .	82
VI.10	<b>Gaze dynamics &amp; lighting conditions:</b> grouped data for the 6 lighting conditions during phase a-d) while working with phone. . . . .	83
VI.11	<b>3D visualisation:</b> the colour correspond to the 6 lighting conditions and the size of the spheres correspond to the duration of the fixation on the same point. . . . .	84
VI.12	<b>Gaze dynamics &amp; <math>E_v</math>:</b> Gaze orientation is shown in relation to $E_v$ variation. . . . .	85
VI.13	<b>View Type 1:</b> a mixture of nature and built environment on two orientations under overcast sky conditions. . . . .	88
VI.14	<b>View Type 2 :</b> a combination of containers and build environment in close distance under overcast sky conditions. . . . .	88
VI.15	<b>View Type 3 :</b> the window was blocked by a black cover and the venetian bliss were closed blocking light and view from the outside. . . . .	89
VI.16	<b>Lighting conditions:</b> a) overcast sky, b) electrical lighting . . . . .	90
VI.17	<b>Gaze patterns &amp; view outside the window:</b> a-d) while working with monitor . . . . .	91
VI.18	<b>Gaze patterns &amp; view outside the window:</b> a-d) while working with phone . . . . .	92
VI.19	<b>Gaze behaviour under free exploration tasks:</b> each data point represents one participants dominant gaze. the size of the data points corresponds to the fixation duration. . . . .	93
VI.20	<b>Gaze dynamics &amp; view:</b> a panorama picture of the room from the point of view of the participant. The three prominent fixation regions a1- a3 are noted on the image. . . . .	94
VI.21	<b>Gaze behaviour under free exploration tasks:</b> a) View-type 1, b) View-type 2, c) View-type 3. . . . .	94
VI.22	Horizontal. . . . .	95
VI.23	Vertical. . . . .	95
VI.24	Duration. . . . .	96
VII.1	<b>Gaze-centred luminance images evaluated by <i>Evalglare</i>:</b> left column) The gaze distribution of one participant during the four phases of the on-screen work is shown and the most dominant gaze $\vec{v}_1$ is marked, right column) the gaze-driven FOV luminance image corresponding to $\vec{v}_1$ in each phase as processed by <i>Evalglare</i> . . . . .	100
VII.2	<b>Fixed-gaze luminance images evaluated by <i>Evalglare</i>:</b> a) the reference region are marked in blue; when the monitor was off during the <i>Thinking</i> phase, the keyboard region was set as reference, b) during the on-phone task the average luminance of the scene was considered as the threshold reference. This setting was the same for all the phases including the <i>Thinking</i> phase. The highlighted areas in are the potential glare sources. . . . .	101
VII.3	<b>Camera position deference:</b> a) the Ideal position b) The 65 [mm] disposition, c-d) the images were processed using <i>Evalglare</i> and analysed using <i>Matlab</i> . . . . .	103

VII.4	<b>Illuminance at the vertical level for gaze-driven vs. fixed-gaze approach:</b> on-screen a) <i>Input</i> phase & b) <i>Thinking</i> phase, c) on-phone <i>Thinking</i> phase, d) free exploration phase which is the on-screen and on-phone <i>Thinking</i> phase combined; an observable a grey area is marked on the graph. . . . .	104
VII.5	<b>The graphs demonstrate gaze-driven vs. fixed-gaze <math>E_v</math> approach:</b> a) the median and standard deviation of gaze-driven values $E_{vg}$ and fixed FOV values $E_{vf}$ for above and below the grey area are shown, b) the graph is a box plot comparing the distribution of the $E_{vg}$ and $E_{vf}$ for higher and lower values than the grey area. . . . .	105
VII.6	<b>Interaction plots:</b> a) Interaction diagram corresponding to $E_v$ for gaze-driven and fixed-gaze approach, b) Interaction diagram for $E_v$ corresponding to different lighting conditions: The lines are not parallel, which means that there is an interaction between the two factors. . . . .	106
VII.7	<b>Gaze-driven vs. fixed-gaze approach for central vision:</b> luminance at the central vision [ $\text{cd}/\text{m}^2$ ] during <i>Thinking</i> phase a) when working on screen, b) when working on-phone. 107	
VII.8	<b>Gaze-driven vs. fixed-gaze approach for DGP:</b> a) <i>Input</i> phase on-screen task and b) <i>Thinking</i> phase on-screen task. . . . .	109
VII.9	<b>Gaze-driven vs. fixed-gaze approach for DGI:</b> a) <i>Input</i> phase on-screen task and b) <i>Thinking</i> phase on-screen task. . . . .	109
VIII.1	<b>Gaze avoidance:</b> significant statistical relation between the luminance variations and shift of gaze as a foothold for further development of a gaze direction model . . . . .	115
VIII.2	<b>Gaze avoidance:</b> a concept for a gaze responsive model to predicts the gaze response to independent variables glare impact and view. . . . .	116
VIII.3	<b>Future perspective:</b> Gaze shifts as a response to the glare impact at different times of the day. The cyan spheres represent the gaze direction intersection with the geometry. The potential glare sources are highlighted in yellow. The variations in the glare source colour correspond to the glare source intensity. . . . .	118
VIII.4	<b>Future perspective:</b> Gaze response to glare impact are visualised over time. . . . .	119



# List of Tables

II.1	Commonly known discomfort glare models . . . . .	13
III.1	Comparison of the two CCD cameras C1: LMK98 & C2: LMK98-4 . . . . .	22
III.2	Office task sequence specifications . . . . .	24
III.3	On-screen specifications . . . . .	24
V.1	Office task sequence specifications . . . . .	54
V.2	Façade & lighting condition specifications . . . . .	56
V.3	Three-way ANOVA results . . . . .	59
V.4	Two-way ANOVA results: left eye . . . . .	59
V.5	Office task sequence specifications . . . . .	62
VI.1	Office task sequence specifications . . . . .	74
VI.2	Experimental protocol with achieved sample sizes for all conditions . . . . .	76
VI.3	Average measurements of all participants' data. . . . .	79
VI.4	$\bar{L}_s$ : Average luminance value of glare sources found in each phase [cd/m <sup>2</sup> ] . . . . .	81
VI.5	3-way ANOVA on unequal sample sizes on horizontal variance . . . . .	86
VI.6	3-way ANOVA on unequal sample sizes on vertical variance . . . . .	86
VI.7	3-way ANOVA on unequal sample sizes on radial standard deviation . . . . .	87
VI.8	Experimental protocol with achieved sample sizes for all conditions . . . . .	90
VI.9	One-way ANOVA . . . . .	95
VI.10	One-way ANOVA . . . . .	95
VI.11	One-way ANOVA . . . . .	96
VII.1	Two-way ANOVA results . . . . .	106





# I Introduction

"Observe the light and admire its beauty. Close your eyes and look:

What you have seen doesn't exist anymore, and what you will see does not yet exist."

*Leonardo da Vinci*

## I.1 Daylighting in Offices

If correctly integrated, daylight is a component of building design which has both aesthetical values and energy saving benefits. Daylight is the most prominent architectural element in producing visual impressions [1] and providing a character to a space [2] by revealing and structuring built volumes and forms. The qualities of daylight enhance appraisal and acceptability of the space [3, 4, 5] while elevating the occupants' well-being and health [6, 7, 8]. Numerous surveys show a strong preference for views and daylight instead of electric lighting [9, 10] with, potentially, a positive impact on productivity and performance [11].

The relation between light and energy has led to different building concepts throughout history. In a brief overview, daylight —being a primary architectural form-giver for centuries—was introduced to buildings in a new way in the mid-19th century which changed the definitions of light and space use. Wide spans of glazing became a possible façade solution and open spaces with thin walls and columns replaced the earlier massiveness of architecture. In the beginning of the 20th century, architecture was about finding new meanings, forms and possibilities, and little attention was paid to energy use. During the post war Era, fluorescent lamps found their way into buildings as a cheap lighting solution. Many buildings were constructed with few windows and thus used air-conditioning and electrical lighting excessively. It was in the 70's, as a result of the oil crisis, that Daylighting was again seen as a solution, this time to reduce the use of electrical lighting. Today, electrical lighting alone is responsible for almost a quarter (24.2%) of the electricity requirements in non-residential sector (excluding households) [12].

## Chapter I. Introduction

---

This is considerable when the large demand for office buildings is taken into account, and emphasises the importance of efficient Daylighting, which has energy saving potentials estimated up to 80% [13].

These benefits, however, can only be gained when human comfort in built environments is ensured. Remarkably, the question of what these human needs are is far from answered [14] and our understanding of human responses to light [15, 16] in built environments is limited [17, 18].

The most basic of these needs is visual comfort, which in its definition is still ambiguous [19], as it is not directly observable. The most simplified understanding of visual comfort is to eliminate discomfort, which by nature is independent of comfort perception [20]. Moreover, individual differences and preferences are vast and one's comfort and wellbeing is shaped by temporary conditions, taste, fatigue and previous experience [21, 22]. Among light-induced discomforts specific to office buildings, the most commonly experienced, yet one of the least understood visual discomforts, is known as discomfort glare. Discomfort glare can change our motivation and mood, especially if the work is prolonged. Considering the substantial proportion of daily office tasks involving visual activities, there is a strong need for a refined understanding of this discomfort glare phenomenon in order to optimise Daylighting and lighting strategies that support human responsive design for workspaces (e.g. façade and shading system integration in interior space design). Enhanced human comfort and performance, and ultimately building performance, are in line with this perspective.

### I.2 Bringing Discomfort Glare and Gaze Together

Ensuring visually comfortable lighting solutions in indoor environments currently revolves mainly around minimising the periods of visual discomfort caused by light [19, 5]. Despite numerous efforts to develop discomfort glare models, mainly through subjective assessment studies (self-evaluated using questionnaires), predicting visual discomfort in indoor environments still presents important challenges when determining a lighting or daylighting scheme in building design. These existing models are very similar to each other, as they share the same basic form for a specific field of view (FOV). This form accounts for four main physical quantities in relation to subjective judgment of the sensation of discomfort. The four physical quantities are the luminance of the glare source ( $L_s$ ), the solid angle of the glare source subtended at the eye ( $\omega_s$ ), the discomfort sensation that the glare source induces based on its angular position in the FOV with respect to the gaze direction ( $P_i$ ) and the adaptation luminance ( $L_a$ ) (Figure: I.1 a-d). A major limitation shared by existing discomfort glare models lies in the neglect of the fundamentals of human response from the point of view of our visual system. A prominent model limitation is the high dependency of the discomfort glare on the gaze direction and its dynamic shifts. The assumption behind these models is that the gaze direction is fixed and is directed towards the task area. Gaze direction is where we direct our gaze by mutually moving our body, head and eyes (Figure: I.2). Depending on our seating position and

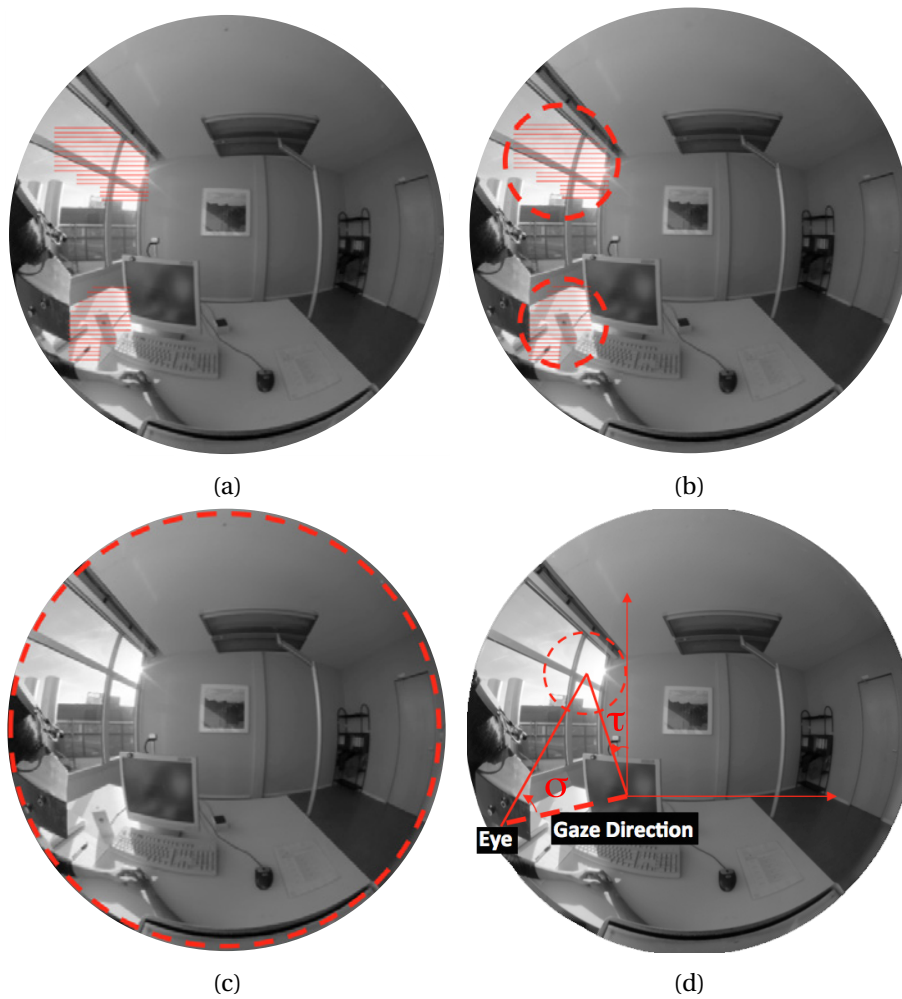


Figure I.1 – **Discomfort glare depends on four physical quantities:** the illustrations on a fisheye luminance images show a)  $L_s$  (luminance of glare source), b)  $\omega_s$  (solid angle of source), c)  $L_a$  (adaptation luminance), and d)  $P_i$  (position index); where  $\alpha$  is the angle from vertical plane of line gaze and  $\beta$  is the angle between the gaze direction and the line between the eye and the glare source.

gaze direction, light distribution in our FOV can vary from interesting highlights to disturbing contrast variations. The latter situation fosters discomfort glare, which causes discomfort without necessarily impairing our vision of objects [23]. Shifts in gaze direction will have a strong impact on the basic shared quantities for discomfort glare evaluation. The assumed position of the glare source [24, 25] and the luminance distribution across different parts of the FOV [26] are highly dependent on gaze direction and if ignored could cause uncertainties in the existing models [27]. The sensation of discomfort varies greatly depending on the angular displacement of the glare source from the gaze direction [24, 28, 25]. The gaze shifts also result in changes of overall light levels entering the eye, requiring the visual system to adapt its sensitivity to light [18]. Therefore, gaze shifts have implications on adaptation levels [29] and, consequently, on the subjective response to glare sensation [30]. Dynamic gaze shifts of gaze

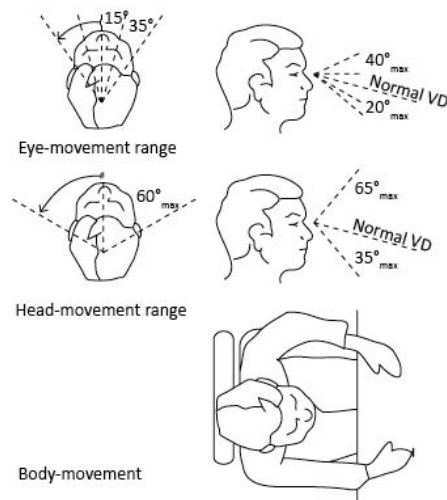


Figure I.2 – **Gaze direction:** Gaze direction is where we direct our gaze by mutually moving our body, head and eyes.

potentially have a significant influence on glare evaluation outcomes. On the other hand, natural visual behaviour associated with glare is unknown. Few studies have investigated the relationship between gaze shifts and building-induced visual context, such as the presence of windows [17] or light [18, 15]. Some studies suggest that gaze directions extend over different regions of space on vertical and horizontal planes, and thus, are not solely fixed on a certain area [31]. In other studies, the necessity of limited luminance ratios at workplaces have been underlined for minimising performance losses due to a re-adaptation process caused by the dynamics of gaze direction [18]. The adaptive capability of gaze shifts in response to uncomfortable conditions was also acknowledged (somewhat arbitrarily) by extending gaze directions to a predefined angular range rather than to a unique gaze direction [32]. The most recent studies with focus on lighting and gaze allocation have been limited to urban street [33, 34] or pedestrian lighting [35, 36]. To the author's knowledge, no study has gone so far as to relate the actual gaze direction to light-induced discomfort perception.

Extreme luminance in different parts of the FOV can generate negative individual responses either by attracting the eye towards excessively bright areas [37] or by inducing continuous eye deviation, as with similar neurophysiological pathways such as photophobia [38]. In turn, recent eye-tracking studies done with static images of natural scenes have shown participants' tendency to avoid bright and dark stimulus regions and to instead direct gaze to regions of medium luminance [15, 16]. In any case, the hypothesis is that certain ranges of luminance values cause certain gaze direction shifts, thus creating predictable gaze patterns.

### I.3 Outline of the Study

To investigate if certain ranges of luminance values cause certain gaze direction shifts, several potential questions need to be addressed: does considering gaze in glare assessments make a difference? Are there observable relation between lighting and dynamics of gaze? Is this relation independent of the view outside of the window? To answer these questions the following three core hypotheses will be tested:

Hypothesis 1) Dynamic gaze luminance measurements are different than the fixed-gaze measurements

Hypothesis 2) Luminance distributions in the FOV have an effect on gaze shifts

Hypothesis 3) The view outside the window has an effect on gaze shifts

To examine these hypotheses, a new gaze-driven approach was introduced instead of the existing fixed-gaze approach, in order to estimate the luminance distribution in the FOV for discomfort glare assessments in office spaces. In this approach, mobile eye-tracking methods were employed in the discomfort glare assessment in addition to the subjective assessment completed with questionnaires. Figure I.3 illustrates the structure of the work presented in this dissertation. The structure of the dissertation is based on a development phase followed by a processing phase and is concluded in results and future steps.

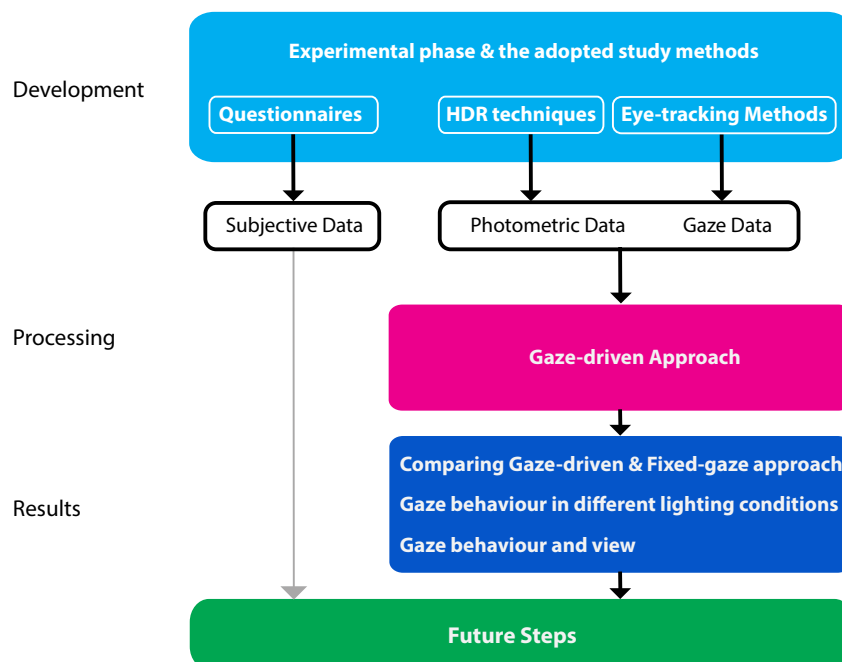


Figure I.3 – Structure of the work

## Chapter I. Introduction

---

The development phase included performing experiments under daylight conditions with integrated measurement methods: subjective assessments through questionnaires, photometric measurements using CCD cameras and HDR imaging processing methods, and gaze responses using mobile eye-tracking methods. In parallel to these experiments, a new gaze-driven approach was developed to derive gaze-centred luminance images. The gaze-centred luminance images were generated in three steps. The obtained luminance images are an accumulation of luminance values received at the eye of the participant at each gaze allocation. During the processing phase, after an extensive and careful data preparation, the photometric data and the gaze data were processed using the new gaze-driven approach.

The processed data was then evaluated to verify the three main hypotheses. The first step was to compare the newly developed gaze-driven approach with the existing fixed-gaze approach. The gaze behaviour in relation to light was then investigated. This was followed by investigation on relation between gaze and the view outside the window.

The structure of the dissertation is as follow:

**Chapter II** gives an overview of the existing discomfort glare models. Gaze natural behaviour and its relation to glare are reviewed.

**Chapter III** gives a background on methods employed and their integration into this study.

**Chapter IV** provides a detailed description of the novel gaze-driven approach that is developed to extract gaze dependent luminance distributions from photometric measurements.

**Chapter V** provides a detailed description of the two performed experiments that served as pilot studies.

**Chapter VI** explains the final experimental strategy which was developed based on two pilot studies. Additionally, the results that compare the gaze-driven and the fixed-gaze approaches are presented. Gaze behaviour in different lighting conditions and in relation to the view outside the window is investigated and the results are described.

The main results of the study are presented here as well. These results compare the gaze-driven and the fixed-gaze approaches at the first stage. Gaze behaviour in different lighting conditions and in relation to the view outside the window is investigated and the results are presented.

**Chapter VII** estimates the uncertainties in the newly developed gaze-driven approach and compares this approach to the existing fixed-gaze approach.

**Chapter VIII** concludes the thesis by summarising the main achievements of the work. A summary of findings of this dissertation are presented and discussed, and possibilities of future avenues for human responsive daylighting in offices are put into perspective. Additionally, the future steps to overcome the limitations of this study are listed.

# II Discomfort Glare and Gaze:

## State of the Art

### II.1 Lighting and Discomfort Glare in Offices

The illumination conditions in a room can create situations that reduce visibility and create visual discomfort in a daylit office environment. One of these discomforting situations is known as glare. It is usually marked by behaviours such as blinking, looking away or shielding the eyes when encountering extreme contrast intensities, and if persistent results in visual fatigue. Glare was recognised as a visual phenomenon in the scientific literature for the first time in 1910 when it was characterised as "a more or less serious discomfort" [37]. This vague definition was later categorised as a range from temporary visual reduction to extreme situations such as retinal damage of the eye. Today, however, we have a better understanding of different types of glare sensation based on their spatial and temporal characteristics and by their degree of seriousness [38]. These different types can be categorised into two main temporal groups: rare and commonly experienced [39]. Glare sensations such as flash blindness, paralysing glare, distracting glare and retinal damage glare fall into the first group, whereas conditions such as dazzle or saturation glare, adaptation glare, veiling glare (reflection), disability glare, and discomfort glare are more commonly experienced.

Disability glare and veiling glare are caused by contrast reduction on either the retina or the surface of the object such as on a computer screen or a glossy paper. Whereas disability and veiling glare are easier to recognise and quantify, discomfort glare, having been studied for more than 50 years, is less understood. This type of glare is a distracting or uncomfortable situation which interferes with the perception of visual information, but it does not significantly reduce the ability to see the information needed for visual activities [23].

There is a general consensus that glare is one of the main causes of building occupant interactions with shading, and thus a major source of potential dissatisfaction for the building occupants [40, 11, 41]. The initial challenge of this phenomenon is that it only creates subjective negative responses with no immediate visual strain and no known physiological origins [19]. Studies have associated discomfort

## Chapter II. Discomfort Glare and Gaze: State of the Art

---

glare with certain pupil fluctuation [42] and activities of the facial muscles in the vicinity of the eye [43]. However, it is uncertain whether or not these physiological observations are indications of a general discomfort, or whether they are created by the actual discomfort glare sensation [38, 44].

So far, conventional human assessments have been used to quantify discomfort glare by means of questionnaires with a focus on negative responses. Most of these studies that have led to the development of mathematical models for discomfort glare quantification were done under electrical lighting conditions, with the exception of one project which was done under daylight conditions [45]. Despite biased subjective responses when a view out of a window is available (resulting in higher glare tolerance) [46], or task difficulty is increased (resulting in lower glare tolerance) [47, 48], or task type [49], attempts to quantify discomfort glare have led to the development of a series of different models for visual comfort predictions in indoor spaces. Each of these glare models evaluate glare differently but they share a basic trend and draw upon the same four physical quantities: luminance of the glare source ( $L_s$ ), the solid angle of the glare source subtended at the eye ( $\omega_s$ ), the discomfort sensation the glare source induces based on its angular position in the FOV with respect to the gaze direction ( $P_i$ ) and the adaptation luminance ( $L_a$ ) and the model-specific parameters ( $e_{1-4}$ ) [19] (equation II.1).

$$\text{Glare sensation} = \frac{L_s^{e_1} \cdot \omega_s^{e_2}}{L_a^{e_3} \cdot P_i^{e_4}} \quad (\text{II.1})$$

$L_s$	Luminance of a glare source [cd/m <sup>2</sup> ]
$\omega_s$	Solid angle of source subtended at the eye [sr]
$L_a$	Adaptation Luminance
$P_i$	Position Index of source $i$
$e_{1-4}$	Model-specific parameters > 0

This equation indicates that a brighter and larger source of glare in a high contrast room, which is closer to the gaze direction (within 10° but not at the gaze direction [25]), increases the risk of discomfort glare. Each component has a different exponent that varies for different discomfort glare equations. The exponents  $e_1$ ,  $e_2$  and  $e_3$ , seen in equation II.1, are best-fitted empirical values.

In the mentioned glare models exponent  $e_1$  is always greater than exponent  $e_2$ . The inverse relation between luminance of the source and the luminance of the background also indicates that higher background (or adaptation) luminance in the FOV can minimise the discomforting effect of a prominent focused (small-sized) glare source.

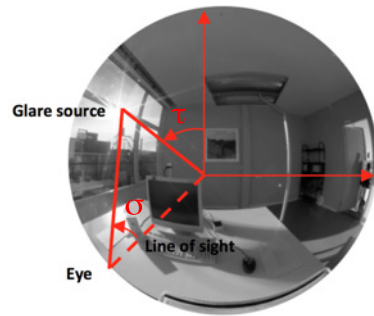
The Position Index ( $P_i$ ) value is used in most of the common glare models with an exponent  $e_4$  between 1 and 2.  $P_i$  is a complex equation which shows the change in discomfort based on the angular displacement of the glare source from a gaze line [24]. It also highlights the sensitivity of different parts of the FOV to discomfort sensation [50, 25]. Guth and Luckiesh did their measurements on the



## II.1. Lighting and Discomfort Glare in Offices

upper part of the visual field since their main intention was to assess the glare sensation created by an artificial light source which was mainly installed on the ceiling and above the line of sight (equation II.2, Figure: II.1).

$$Index P_i = (35.2 - 0.31889\tau - 1.22e^{\frac{-2\tau}{9}}) \times 10^{-3} \times \sigma + (21 + 0.26667\tau - 0.002963\tau^2) \times 10^{-5} \times \sigma^2 \quad (II.2)$$

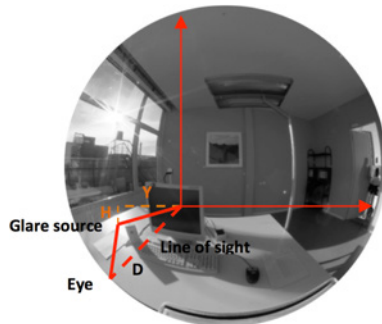


Where

$\tau$  = angle between the vertical plane of gaze direction and the glare source

$\sigma$  = angle between the gaze direction and the line between the eye the glare source

Figure II.1 – Position Index angular description



$$P_i = 1 + 0.8 \times R/D \quad [R < 0.6D]$$

$$P_i = 1 + 1.2 \times R/D \quad [R \geq 0.6D]$$

Where

$$R = \sqrt{(H^2 + Y^2)}$$

Figure II.2 – Position Index:  $Y$  is horizontal distance between source and gaze direction [mm],  $H$  is vertical distance between source and gaze direction [mm] and  $D$  is the distance between eye and plane of glare source [mm].

With respect to the glare caused by daylight from the windows, the lower part of the visual field has to be considered, given that the glare source can be located there or could extend to this part. As a result, this index was evaluated later on by Iwata and Tokura [50] for the lower part of the visual field. They showed that the sensation of glare is different in this part of the visual field.

Therefore, this index was evaluated later on by Iwata and Tokura [50] for the lower part of the visual field. They showed that the sensation of glare is different in this part of the visual field.

Einhorn then completed this finding with an analytical equation shown in Figure II.2. The limitation of these equations are that they are reliable within  $30^\circ$  from the gaze direction. A recent study [25] has

## Chapter II. Discomfort Glare and Gaze: State of the Art

---

proposed a new position index for glare sources positioned in the whole FOV. In their study, they have made measurements using a device called "Glare tester" which was designed specifically for developing a position index for whole FOV. The Glare-tester enabled placement of glare source ranging from 0 to 160,000 cd/m<sup>2</sup> generated by halogen lamps at different positions in the FOV creating a glare source of 0.0011 sr.

From those experiments it has been concluded that boundary of vision is not symmetrical in upper and lower visual field. The sensitivity to glare is higher in the lower part of the FOV. The differences between lower and upper part of the visual field increase as the light source moves farther from the line of sight [50]. The border line between comfort and discomfort luminance on the line of sight is not significantly different from Guth's measurements (2844 cd/m<sup>2</sup>) and it is 2590 cd/m<sup>2</sup>. One of the interesting results of this experiments is that eye as it is assumed in general is not most sensitive on the light of sight whereas the sensation of brightness is the highest at positions that deviate 10° from this line.

Glare source position in the FOV which is measured with respect to the line of gaze, hence, plays an important role in the discomfort sensation it induces. With a fixed-gaze assumption, this measure can not be properly calculated. Among glare indexes, described in next section, DGP uses position index based on Einhorn's equation in order to cover the scene above and below the fixed line of sight. This glare metric which has shown better correlation with subjective assessments, is dependent on the visual adaptation level measured by illuminance at the eye level  $E_v$  and less dependent on the glare source specifications.

The gaze point and direction is, however, a pre-requisite to any glare evaluation. A field of view is shaped with respect to the line of gaze and the photometric variations that define our comfort or discomfort sensation are quantified within the FOV.

## II.2 Discomfort Glare Models

The existing discomfort glare models were developed for making visual discomfort predictions with electrical light, e.g. VCP, UGR, BGI, CGI, DGR, DGI, DGI<sub>N</sub> [51, 52, 53, 54] (Table II.1). More recently, models have focused on daylight [55, 56, 5, 57] such as DGP [45]. Among the different available models there are at least two that aim to make daylight glare predictions DGI (equation VII.1), and DGP (equation VII.2):

$$DGI = 10 \cdot \log\left(0.5 \sum_{i=1}^n \frac{L_{s,ii}^{1.6} \cdot \Omega_s^{0.8}}{L_b + .07\omega_{s,i}^{0.5} \cdot L_s}\right) \quad (II.3)$$

$L_s$	Luminance of a glare source
$L_{s,i}$	Luminance of a glare source $i$
$\omega_{s,i}$	Solid angle of glare source $i$ subtend at the eye
$\Omega_s$	Solid angle of source modified for position factor
$L_b$	Luminance of the background

DGI is based on the modification of an earlier model: the British Glare Index. The development was made with experiments conducted with less than 10 participants and under uniform large glares sources using electrical light sources [58, 59]. Validation studies on this equation show that the correlation between predictions and observations is not as strong for windows as it is for electrical light [32, 60]. The best correlation exists when there is diffuse light from the sky with no direct sunlight inside [5]. Moreover, some of the validations on DGI show over-prediction of the glare situations [28] which could be due to cultural differences amongst participants in the validation experimental set up [5] or due to the pleasantness of the content of the view outside the window [46, 61].

DGP (Daylight Glare Probability) is a model which was developed based on subjective assessment studies conducted in an office situation and under real daylit clear sky conditions. The DGP describes the probability that a person is disturbed by daylight [62]. The DGP equation (Eq.VII.2) includes vertical illuminance at the vertical level ( $E_v$ ) [63, 22] in addition to the common glare equation variables. This model, which is being validated for real life situations [64, 65], correlates better under direct sun conditions while not taking into account the contrast-induced glare [66]. Contrast-induced glare refers to conditions where there is a discomforting luminance difference between the central vision region and the background. The validation studies suggest that DGP outperforms DGI [65].

$$DGP = 5.87 \cdot 10^{-5} \cdot E_v + 9.18 \cdot 10^{-2} \times \log\left(1 + \sum_i \frac{L_{s,i}^2 \cdot \omega_{s,i}}{E_v^{1.87} \cdot P_i^2}\right) + 0.16 \quad (\text{II.4})$$

$L_{s,i}$	Luminance of a glare source $i$
$\omega_{s,i}$	Solid angle of glare source $i$ subtend at the eye
$E_v$	illuminance at the vertical level

Other studies take different approaches by using quantifiable photometric measures of luminance or illuminance to evaluate and understand the relations between perception of luminous space and visual comfort. Some of these approaches include different luminance ratios in the visual scene [67, 68], luminance differences [69], J index [70], predetermined absolute luminance values, mean luminance values or standard deviation of scene luminance [71, 65], average, min or max luminance values in different parts of the FOV [72], uniformity of luminance distributions [73], per luminance pixel analysis from high dynamic range (HDR) images [74] or illuminance values on the horizontal levels in the visual

## **Chapter II. Discomfort Glare and Gaze: State of the Art**

---

scene such as the desk. The mentioned approaches are not as commonly used for visual discomfort evaluations and they are not implemented in any computational tool. In this study to investigate the difference between the gaze-driven and the fixed-gaze approach, we compared illuminance at the vertical level and at the eye level  $E_v$ , a luminance measure of the central vision, DGI and DGP.

Acronym	Index	Model reference	Light source used at experiment	Light source to evaluate	Facts (based on literature survey)	Basic form: $G \approx \sum \frac{L_s \omega_s^2}{L_b P^{0.4}}$
BGI	British glare index	Hopkinson, Petherbridge, 1950	Small artificial	Artificial	<ul style="list-style-type: none"> <li>It is limited to small light sources (<math>L_s &lt; \omega_s</math>)</li> <li>Does not take the adaptation effect into account-</li> </ul>	$BGI = 10 \log_{10} 0.478 \sum_{i=1}^n \frac{L_{s,i}^{1.5} \omega_{s,i}^{0.8}}{L_b P_i^{1.6}}$
DGI	Daylight glare index	Hopkinson, Chauvel, 1972	Large artificial	Daylight	<ul style="list-style-type: none"> <li>Developed for daylight glare predictions</li> <li>Modification of BGI based on less than 10 participants</li> <li>Correlates better with artificial light situations</li> <li>Not acceptable when window is parallel to the participant's view</li> <li>The values are higher than what is perceived</li> </ul>	$DGI = 10 \log_{10} 0.48 \sum_{i=1}^n \frac{L_{s,i}^{1.6} \omega_{s,i}^{0.8}}{L_b + 0.07 \omega_{s,i}^{0.5} P_i}$
CGI	CIE Glare Index	Einhorn, 1969,1979	Small artificial	Artificial	<ul style="list-style-type: none"> <li>Developed based on BGI to correct its inconsistency for multiple glare sources</li> <li>Mainly applicable for artificial light sources</li> </ul>	$CGI = 8 \log_{10} 2 \frac{\left[ 1 + \frac{E_d}{500} \right] \sum_{i=1}^n \frac{L_{s,i}^2 \omega_{s,i}}{E_d + E_i}}{L_b P_i^2}$
UGR	CIE's unified glare rating system	CIE, 1992	Small artificial	Artificial	<ul style="list-style-type: none"> <li>Developed based on CGI and BGI to evaluate glare for artificial lighting</li> </ul>	$UGR = 8 \log_{10} \frac{0.25 \sum_{i=1}^n \frac{L_{s,i}^2 \omega_{s,i}}{L_b P_i^2}}{L_b}$
VCP	Visual Comfort Probability	IESNA, 1993	Small artificial	Artificial	<ul style="list-style-type: none"> <li>VCP cannot be applied to very small, to very large or very non-uniform glare source</li> </ul>	$VCP = 279 - 110 \left[ \log_{10} \left( \sum_{i=1}^n \frac{(0.5 L_{s,i} (20.4 \omega_{s,i} + 1.52 \omega_{s,i}^{0.2} - 0.075))}{P_i E_{d,avg}^{0.44}} \right) \right]^{n-0.0914}$
DGI <sub>N</sub>	New daylight glare index	Nazzari, 2005	-	Daylight	<ul style="list-style-type: none"> <li>Mathematical prediction based on DGI</li> <li>Geometrical information of the room is needed</li> </ul>	$DGI_N = 8 \log_{10} 0.25 \left[ \frac{\sum_{i=1}^n L_{s,i}^2 \Omega_{p,N}}{L_{adapt} + 0.07 \left( \sum_{i=1}^n L_{s,i}^2 \Omega_{window} \omega_{N,i} \right)^{0.5}} \right]$
DGP		Wienold & Christoffersen, 2006	Daylight	Daylight	<ul style="list-style-type: none"> <li>Probability of being disturbed</li> <li>Based on the vertical illuminance at the eye</li> <li>Use of CCD cameras &amp; HDR imaging</li> <li>Gaze direction is always center of picture</li> <li>It does not take into account the contrast-based glare</li> </ul>	$DGP = 5.87 \times E_v + 0.18 \times 10^{-2} \times \log \left( 1 + \sum_i \frac{L_{s,i}^2 \times \omega_{s,i}}{E_{p,i}^{1.87} \times P_{t,i}^2} \right) + 0.16$

Common variables  
 $L_s$ : Luminance of source [cd/m<sup>2</sup>]  
 $\omega_s$ : Solid angle of source  
 $L_b$ : Luminance of the background (adaptation luminance)  
 $P_i$ : Position index

Specific variables

$\Omega_s$  = Solid angle of the source modified to include Guth's position index [Str]  
 $L_w$  = window (avg. luminance of the sky, added by Chauval 1982 to account for daylight tolerance) [cd.m<sup>-2</sup>]  
 $L_f$  = luminance window,  $L_c$  = ceiling,  $L_e$  = source [cd.m<sup>-2</sup>]  
 $\omega_w$  = Luminance window,  $\omega_c$  = ceiling,  $\omega_s$  = source [Str]  
 $E_v$ : Illuminance at the vertical eye level [lux]  
 $\Omega_{p,N}$  = Solid angle of the source modified to include window configuration and observation position in relation to the window [Str]

The most cited and used for discomfort glare assessment in daylight conditions  
 The most used for discomfort glare assessments under artificial light  
 The most recent based developed based on real daylight situations and with HDR imaging technics

Table II.1 – Commonly known discomfort glare models

### **II.3 Gaze and Natural Behaviour in Relation to Glare**

The interest in the relation between gaze and natural behaviour in real life scenarios dates back at least to the early 20th century. In the early studies the focus was mainly on eye movements alone.

Eye movements can be volitional or reflexive; as a result, they may serve to scan the visual environment or to stabilise gaze during self-movement or on a moving object. For these movements, a number of distinct classes are known and their neural control is reasonably well understood [75]. These movements are typically studied in terms of fixations (periods of pause) and saccades (rapid movements between fixations) with respect to temporal and spatial characteristics such as duration or dispersion [76].

So-called *saccades* constitute a prominent class of human eye movements; they are extremely rapid shifts (up to about  $\frac{500^\circ}{s}$ ) that occur about 3 times each second. Other types of eye movement include smooth pursuits to follow isolated moving objects, the vestibular ocular reflex (VOR) to stabilise gaze during self-motion, the optokinetic nystagmus (OKN) to stabilise gaze during movement of the scene, vergence movements to allocate gaze in depth as well as several classes of tiny movements (drift, micro-saccades and tremor) that occur while the eye is fixating.

During natural perception the eye-movement classes coexist and interact with head and body movement to direct our gaze. Therefore, eye movements alone do not tell us enough about actual gaze control during real-life behaviour [77, 78]. Thus, understanding the natural behaviour of gaze in relation to real world conditions such as glare requires accounting for all these coexisting movements.

The early studies, which focused only on eye-movements, pointed out that –besides visual input – cognitive factors such as task, experience and memory play a key role in driving eye movements [79, 80]. In contrast, most computational modelling for understanding natural gaze allocation behaviour has focused on stimulus-driven factors [81], largely using static images of natural scenes and assigning a probability of attracting ("saliency") attention to the stimulus regions.

Task can override such factors entirely [82, 83] and immediately [84], as can context [85, 86]. Quantitative models that include the task typically focus on visual search [87, 88, 83], which is of high theoretical interest, but a situation that rarely occurs in real life. Other task oriented approaches have either used much reduced stimuli, or focused on restrained settings, such as driving [89], food preparation [90, 91] or sports [92, 93, 78].

On the other hand, there are several hypotheses on how parameters relate to our visual system relate to glare perception. For example extensive discomfort glare could make the gaze direction stray away from glare sources to rest on a comfortable region with a mechanism similar to photophobic situations [38]. Another theory is that the human eye has a penchant for light and thus the eyes are attracted to the bright glare source [37]. Recent eye-tracking studies with static images of natural scenes have in turn shown a tendency of observers to avoid bright and dark stimulus regions and to direct gaze to

regions of medium luminance instead [15, 16]. Glare is also a source distraction that demands higher attention for the eye, which would be seen in a decreased gaze distribution, and an increase of pupil size on average [42]. Also, gaze movements cause temporary re-adaptation, which if repeated could cause reduced performance [18].

### II.4 View Outside the Window and Glare

Daylight is commonly provided in workplaces through an opening in façade or in a more familiar word, windows [94]. As much appreciated as daylight is, the daylight variation in the FOV can also be a source of discomfort.

While most studies on light-induced discomfort have mainly focused on eliminating the discomforting periods that daylight can create in workplaces, the moderating influence of view on glare perception has been addressed by only few studies. View from windows influences the office workers physical [95] and psychological well-being [96]. More interestingly, the sensation of light-induced discomfort [46, 58, 97] is different in presence of view from the window.

What we know is that in presence of an interesting view the perception of glare decreases in comparison to a neutral screen or poor view [46]. An interesting view refers to a view to a natural scene and a poor view is defined as a dull urban context. View types and their visual quality have been studied and categorised ranging from natural and distant views as the mostly appreciated view-types to dull and grey view types with minimum complexity in the view composition as the least appreciated view types [61, 98]. The confounding effect of the daylight access and view on glare perception is not negligible. In order to understand the glare and gaze relation from windows, the view outside of the window have to be considered as an affecting variable.





# III Methodology

In this chapter a background and description of methods employed in this study and their integration are presented. Following the steps of the schematic map (Figure III.1), the experimental set up and measurements general to all performed experiments are listed. Design and adaptation of the subjective assessments and visual task that were implemented in the experimental phases are described. Additionally, HDR imaging techniques and eye-tracking methods integrated in this study are explained. Finally, the analysis methods used most frequently in the study are presented. The Gaze-driven method is described in the following chapter IV.

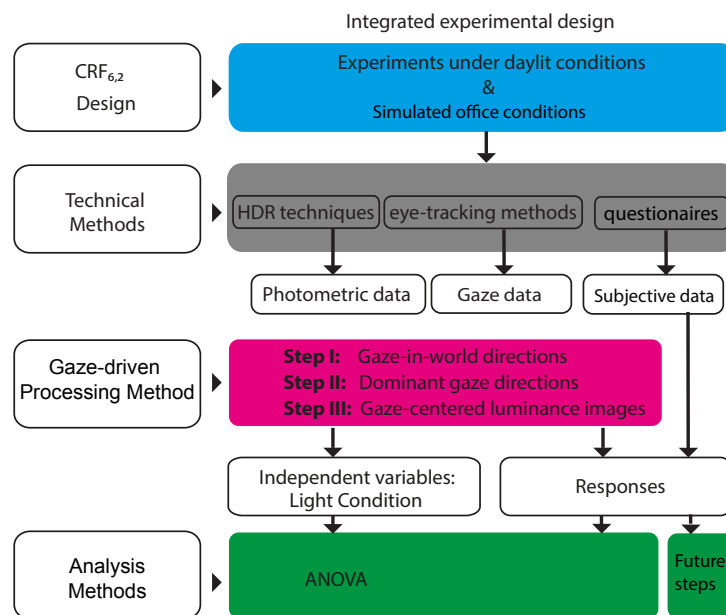


Figure III.1 – Schematic map of methods.

### III.1 Experimental Strategy

To address the natural behaviour in the office related tasks, only little constraint over the participants' task setup and visual environment was imposed. A sufficient control, however, was considered and maintained over the relevant photometric parameters. A mobile eye-tracker (EyeSeeCam) was adopted to monitor gaze and head movements. The EyeSeeCam is a state-of-the-art light-weight head-mount eye tracker [99] that records the pupil position of each eye with two high speed video cameras. Additionally, there is a camera fixed to the head, known as "head or scene camera", with a wide angled lens that is referred to as "head-in-world signals". Wearable eye-tracking technology makes recording of natural gaze behaviour in real-life scenarios with little constraints possible. Therefore this technology was adopted in our experimental setup. We hypothesise that spatial distribution of fixations (dominant gaze directions) and gaze horizontal, vertical and/or radial orientation variances are discomfort glare indicators. The experiments were performed in a parameterised daylit office-like test room where we asked the participants to perform a standardised sequence of office tasks.

Out of the four experiments, the first two served as to prepare, design and optimise the experimental set up while focusing on eye-tracking parameters, façade settings and tasks effects. In the final set of experiments the three technical methods were integrated for extensive data collection: the photometric data was recorded with two calibrated CCD cameras and later possessed using high dynamic range (HDR) imaging techniques. Mobile eye tracking enables us to record gaze movements during the experimental trial, thus giving us better estimates of the luminance values actually received at the participants eye. Additionally, subjective assessments were made using different measurement scales based on multi-criterion glare-rating methods.

The following parameters were extracted for each participant, task and phase of the experiment:

- HDR luminance images for a 270° record of luminance values
- The gaze direction parameters from the eye-tracking records
- The subjective assessment data

The experiments were designed based on a complete randomised factorial design for two independent variables, lighting condition with 6 levels of treatment and task-support with two levels of treatment (CRF<sub>6,2</sub>). Several details concerning the experimental strategy including the use of a laboratory setting, measurement tools in the set up, the design and development of the office task sequence and the standardised introduction to the experiments are explained in this chapter. Moreover, the technical methods of HDR imaging, mobile eye-tracking, and subjective assessment are explained.

For statistical analysis we used ANOVA in order to test the effects of the dependent variables on the response variables. This relation can be explained as a shift in gaze direction that is expressed as a function of the lighting condition. In this chapter, methods and tools employed for the analysis are

also described.

The development of a gaze-driven approach for discomfort glare assessments was based on experiments with a total of 142 participants. The dominant gaze directions for each case were then determined based on the gaze direction parameters. In this approach we take into account the most influencing parameters to visual comfort *a priori*. Deriving the relevant photometric parameters for integrated discomfort glare and gaze direction evaluations constitutes extensive data preparation in and of itself. Several algorithms and binning methods used to calculate the dominant gaze direction were tested in order to derive the corresponding luminance field. This created the basis for further analysis on dynamics of gaze direction in a day lit environment. The details of the gaze-driven approach are explained in a separate (Chapter IV).

### III.2 Experimental Set up

Boyce [19] categorises studies concerning light and work into two major user assessment groups: real task studies (based on actually performed tasks) and abstract studies (based on simple visual tasks, e.g. Landolt rings or d2 test).

The real task studies refer to experiments where the measurements are gathered either in a field study with less control or in a simulated setting (daylight laboratory) with higher control over the influencing parameters. In field studies, the measurements and experiments are done in offices with participants as they are on a normal office day. However, field study measurements are time consuming for the data collection phase and they do not allow for much control of influencing variables, e.g. room temperature, noise, performed tasks, different condition (treatment) arrangements, etc. In this study we used the real task method in a simulated setting.

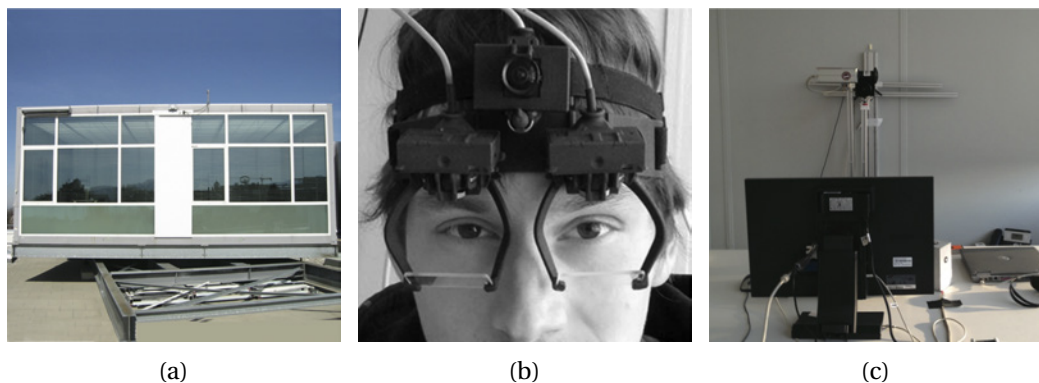


Figure III.2 – **Main facility and tools in the general set up:** a) the daylight laboratory which is an office like test facilities, b) the ESC worn by a subject, b) the two CCD cameras used in the experiments installed so as to be positioned above the participants head.

## Chapter III. Methodology

---

All the experiments were conducted in an office-like daylight laboratory (Figure: III.2a) described in more detail in section III.2.1. The objective of this study was to understand the natural gaze behaviour in caused by light and glare, for office spaces. It was important to impose little constraint over the participant's task set up and over the visual environment while maintaining sufficient control over the relevant photometric parameters. Thus, a simulated office task setting with higher control over the affecting variables proved to be ideal for the purpose of the study.

A standardised office task activity was designed and developed to simulate a short period of office task work. In each experimental trial the gaze directions were monitored using a state-of-the-art wearable mobile eye tracker (EyeSeeCam, [www.eyesecam.com](http://www.eyesecam.com)) (Figure III.2c). The HDR images were captured every 30 second (Figure III.2b). The general set up shared by all the conducted experiments are described here. The specific modifications made to this set up are mentioned in each experiment's respective section.

### III.2.1 Daylight Laboratory

The daylight laboratory used in these experiments is located on top of a four-story building (Fraunhofer ISE main office building at latitude 48.01°N and longitude 7.84°E) Figure III.2a. This laboratory consists of a container refurbished to make two side-lit office rooms Figure III.2a. This construct is installed on a structure that allows for full rotation. This flexibility is crucial in order to adjust the orientation of the daylight laboratory to a pre-defined sun azimuth angle so as to keep daylighting conditions under experimental control over the duration of the experiments. This also allows for reasonably repeatable experiments for varying sun positions. The rooms are of typical single office size (3.5 m wide × 3 m high × 4.5 m deep) with the following photometric properties:  $\rho_{wall} = 0.62$ ,  $\rho_{ceiling} = 0.88$ ,  $\rho_{floor} = 0.11$ , and include one glazed façade (colour-neutral, double glazing:  $\tau_{\perp} = 72\%$ , U-value = 1.1 W/m<sup>2</sup>K, g-value = 0.29). The distance between the desk and the window and the wall behind it were set to the architectural standard for single office rooms [100] shown in Figure VI.1. The computer screen used in for the experiments was a Samsung LED screen with a 19" screen size (S19A450MW Series 4 LED) (except in the first pilot study). The tilt angle of the computer screen was set to 10° from vertical. The distance between the centre of the screen plane to the edge of the desk was set to 550 [mm] to allow for readability of the characters on the screen [101]. The office chair used in the experiment was a padded, wheeled chair of adjustable seat height with no armrest. The room temperature in the daylight lab was kept constant with the help of an air conditioner installed in the room. Figure VI.1 shows the layout of the test rooms, the measurement devices and their positions and all the other objects used during the experimental trial or that were present in the scene.

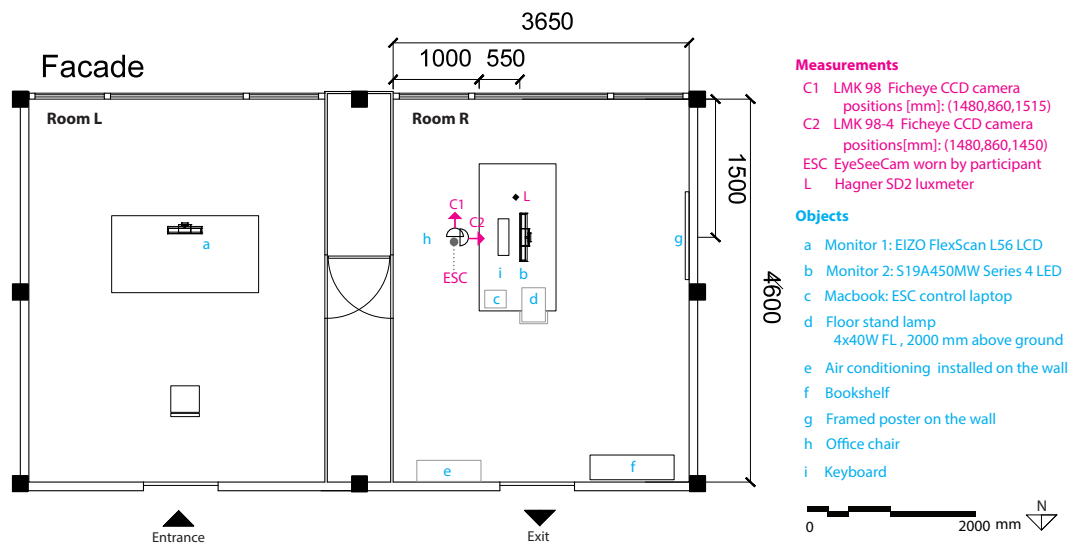


Figure III.3 – **Plan of the daylight laboratory:** the layout of the rooms, the position of the measurement devices and all the objects that were used in the experiment or were in the scene.

### III.2.2 Photometric Measurements

To relate gaze direction patterns and subjective comfort votes to objective properties of the luminous environment, the following variables were measured:

**Illuminance measurements** (Type: Hagner SD2 luxmeters) on work-plane illuminance [lux] , illuminance [lux] on the computer screen surface plane. This data was not used in the study, but served as a backup.

**A meteorological station** on the roof of the test rooms recorded the global and diffuse irradiance [ $W/m^2$ ]. This data was not used in the study, but served as a backup in case of inconsistency in recorded sky conditions and lighting condition categorisations.

**Luminance measurements** was recorded every 30 second using a pair of calibrated CCD cameras from TechnoTeam (LMK 98 Luminance Video Photometer, LMK 98-4 colour) equipped with a fish-eye lens (Nikon FCE8 lens, FOV 183°). The cameras' sensor positions had a small difference in location (Figure III.5a). Each captured image has 786 pixels in both the horizontal and vertical level. The pixel values in an image from a digital camera are proportional to the luminance in the original scene. The CCD cameras used in this study produce a specific data format which was converted to *Radiance* HDR format. The cameras were mounted on a simple structure so as to be positioned above the participants' head with 90° of rotation from each other in order to capture the 270° span of the scene (cf. Figure III.5b). The illuminance measurements at the eye level and the vertical level in this study were derived from the luminance images.

To check and compare the two cameras, under stable artificial lighting condition, we captured two images with the cameras and made sure the images were giving the same output (cf. Figure V.2 a-c &

Table III.1). The mean luminance values in the predefined areas with 7830 number of pixels have 1.57% of difference which is not considerable in light measurements.

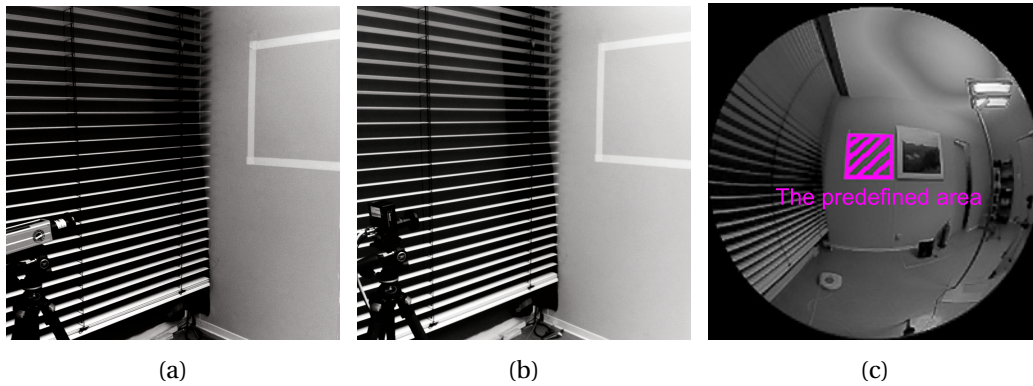


Figure III.4 – **Cameras comparison method:** by capturing images with each camera, a) C1: LMK 98 and, b) C2: LMK 98-4, c) the photometric output of the predefined region was then compared.

Table III.1 – Comparison of the two CCD cameras C1: LMK98 & C2: LMK98-4

	image type	class.	Unit	Number of pixels	Mean	$\sigma$	Min	Max
C1	Black & White (HDR)	Standard	[cd/m <sup>2</sup> ]	7830	50.91	4.514	40.8	64.35
C2	Black & White (HDR)	Standard	[cd/m <sup>2</sup> ]	7830	50.11	4.505	41.03	62

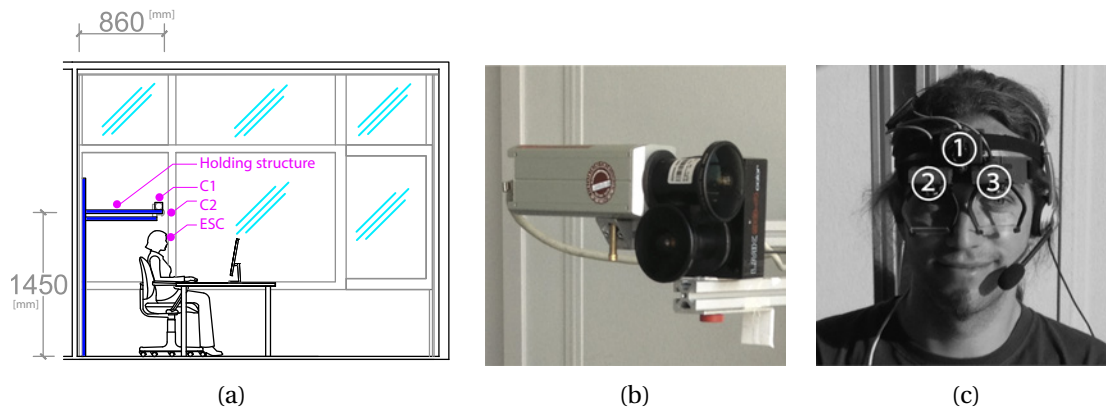


Figure III.5 – **Cameras positions:** a) the section showing the position of the CCD cameras and the approximate position of the EyeSeeCam mounted on the participants head, b) the two CCD cameras are installed above the participants head position with 90° of rotation from each other, c) the EyeSeeCam is equipped with three cameras, (1) Head-fixed scene camera, (2) & (3) Eye-tracking cameras.

### III.2.3 Visual Office Task: Development & Design

Gaze real-world scenarios depends on the task at hand [102] which can override both discomfort sensation [103] and gaze behaviour [104, 105]. Therefore a well-defined task that encourages a realistic office task sequence plays an important role in this type of study.

Task is defined as a required activity to achieve a goal by human-system interaction ergonomics (ISO9241-303-2011) [106]. In office environments, which is the focus of this study, these activities can be cognitive or physical. Office tasks such as reading and hearing (on the phone) are cognitive, while tasks such as speaking and typing are physical tasks [101]. Also, Boyce defines the office work components as visual (input of information), cognitive (interpretation and determination of an action) and motor component (interacting with the stimuli or input information) [19]. Having this in mind, in order to address natural gaze behaviour in the offices, we designed an office task sequence that would include visual, cognitive and motor components of an everyday office task with explicit instructions while leaving enough room for unconstrained visual exploration.

The general design of the office task activity and its specifications, which was developed and modified through the study, is described here. The details specific to each experiment are further described in each experiment respective section.

### Task Activities

Each trial was divided into different "task activities" where the participant performed a standardised office task using different task-supports (Figure:III.6). Task-support refers to a medium device that is used to assist the participant to perform the task.

In the first pilot study a computer screen was used as the task-support. In the second pilot study the adopted task-supports were a computer screen, paper and a phone. In the final two sets of experiments, only a monitor and a phone equipped with a headset were used as task-supports. A headset was employed in the last set of experiments in order to avoid any biases caused by the physical object of the phone present in the scene and in the participant's field of view. The order of use of the task-supports was randomised for each participant.

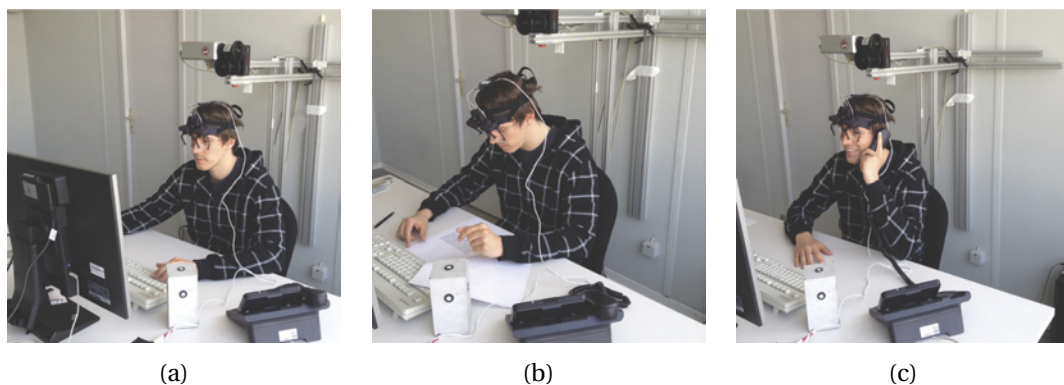


Figure III.6 – **Task-supports:** a) screen, b) paper, c) phone.

Table III.2 – Office task sequence specifications

Activity	Task description	Task-support	Task interaction	Visually focused	Visually explorative	Cognitive	Motor	Time [sec]
1) <i>Input</i>	getting input information.	✓	✓	✓	✗	✗	✗	60
2) <i>Thinking</i>	thinking about the input information.	✗	✗	✗	✓	✓	✗	120
3) <i>Response</i>	responding to a question on input info.	✓	✓	✓	✓	✓	✓	60
4) <i>Interaction</i>	giving one's opinion about the input info.	✓	✓	✗	✗	✓	✓	≈ 180

Table III.3 – On-screen specifications

font type	Calibri,Sans serif
character size on-screen	16' [arcmin]
between character size	11.3 pt
between letter spacing	1 pt
between word spacing	2 pt
between line spacing	2 pt

### Standardised Task Sequence

In the final design each task activity consisted of four main phases: *Input*, *Thinking*, *Response* and *Interaction* (Table: III.2) (In the first pilot study the last phase was *Pause*). The flow of phases for on-screen tasks was as follows: During the *Input* phase of the on-screen task event, the participant would read a text from the computer screen which is visually a highly demanding office task. This phase was followed by the *Thinking* phase. For this phase the participant was asked to think about the information he/she received during the previous phase. The monitor was turned off so as to minimise the interaction with the task-support, thus allowing for non-task orientated eye movements. During this phase, the average luminance value on the screen was on average decreasing from 128 to 58 [cd/m<sup>2</sup>] (Figure III.8a). In the *Response* phase, the participant responds to a multi-choice question about the input phase topic. The last phase of this trial was *Interaction* during which the participant was asked to process and produce an opinion about the *Input* information (see Appendix B for an on-paper example & Figure III.7 for an onscreen example). Then the participant conveyed this opinion through interaction with the task support by typing it on the screen in the designated area. The last two phases encourage a realistic flow of office task where both visual and cognitive performance is required. In the case where paper was used as a task-support the trial followed the same procedure except that all the tasks were performed on-paper. This also applies to the on-phone task activity where the four phases were carried out on the phone. The trial duration was standardised so that each block took seven minutes: 1 minute for the input phase (the texts were tested to be read in 1 minute), 2 minutes for the thinking phase, 1 minute for the response phase and 3 minutes for the interaction phase. There was a small variation in time during the on phone interaction phase. There was a small variation in time during the on phone interaction phase as it was harder to encourage longer or shorter conversations. To avoid task difficulty [47, 48] and content [107] biases, the texts used at the *Input* phase were selected carefully from 12 main articles of easy reading level in German, and provided information about a



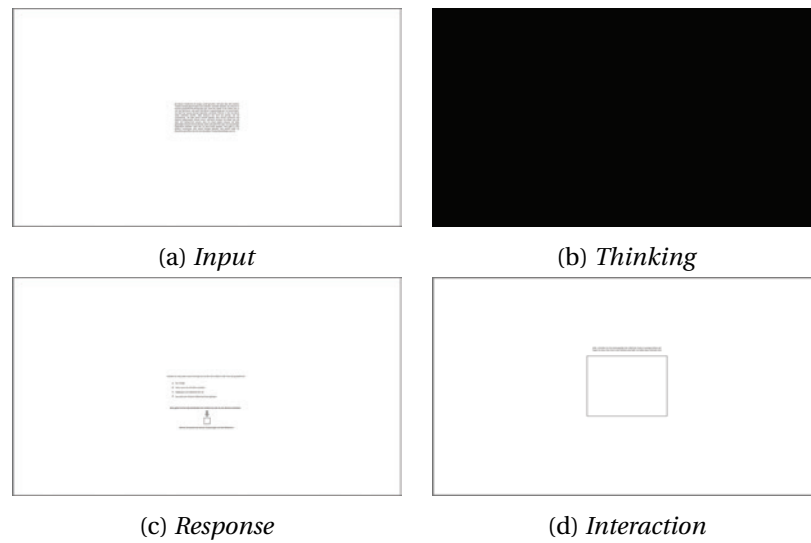


Figure III.7 – **Task sequence on screen:** a) input text justified in the screen centre; b) thinking phase with an off screen; c) the multi-choice question based on the content of the input text; d) a designated area was presented for typing.

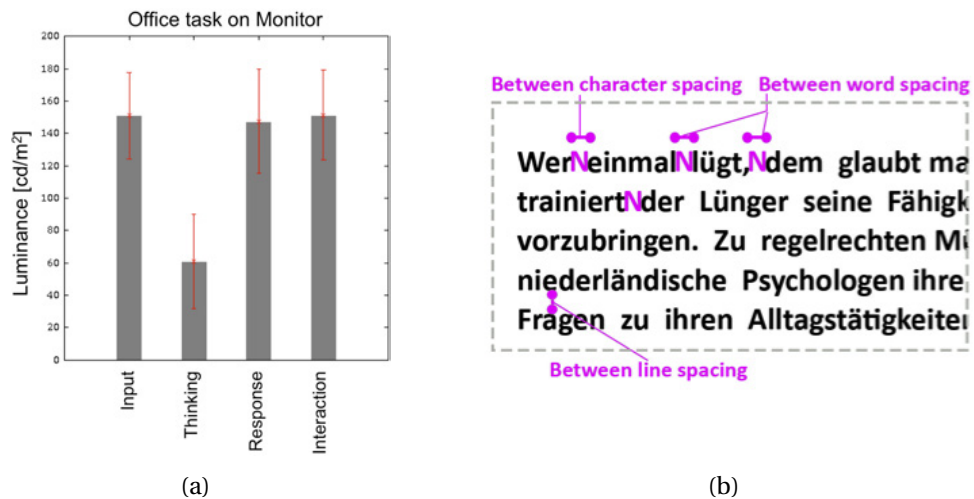


Figure III.8 – **On-screen specification:** a) computer screen luminance variations during the on-screen task, b) the figure shows an upper corner section of one of the texts as displayed on the computer screen. Measures such as word, character and between line spacing as well as font size and font type was taken into consideration for a standardised visual task representation. These measures, shown in table III.8a, were set in the Adobe Flash software.

familiar topic. The paragraphs were adjusted so as to be read/listened to in about one minute. During each experimental trial, the text was selected randomly from these 12 articles for each task activity using a bash script.

When using the computer screen as the task-support, the visual consistency of the reading task for all participants was ensured by standardising its appearance on the computer screen, i.e. character size,

font type, between line can character spacing, etc. [108, 109], Figure III.8b & Table: III.3. The minimum character height recommended by [106] is 16' [arcmin]. In order to avoid uncontrolled skimming or skipping that occurs naturally when reading a continuous paragraph [107], the text was adjusted and set to the centre of the computer screen and paper during each respective task block. This task sequence for the on-screen phase was programmed in Actionscript 3.0. During the paper session, all phases were done on the paper. During the phone session the sequence was prepared by reading aloud and recording each phase, e.g. the input text, the glare rating question, etc.

### III.2.4 Standardised Introduction

The introduction to the experiment was standardised so to leave no bias in participants' understanding of the experiment. The observer (here the term "observer" is used as the experiment operator) repeated the following steps for each participant:

#### **Step 1:** Visual & Thermal adaptation 1

In this step the concept of the test is was introduced to the participants:

*Observer: "The test is about lighting and daylighting in the offices and it concerns visual comfort. I will make an eye sight check here in this room and then we will go to the next room and you will wear and eye-tracker and do some office work."* The data sheet including date, time, time of the day category, orientation of the test-room, name of the observer, name of the subject, sky type and lighting condition category was filled.

#### **Step 2:** Performing the visual acuity and contrast sensitivity test

In this step the participant was asked to sit on the designated seat. The distance between the monitor and the participant's eye is set to 2000 mm (Figure III.9a). The participant is introduced to the response box (Figure III.9b) and how it functions. The following introduction was given:

*Observer: "You are going to see these Landolt ring optotypes coming up on the screen (the C shaped symbols are shown to the subject on the response key). Press the corresponding key to the symbol that you will see."*

The following clarification was also given about the test:

- If you don't see it, make your best guess.
- It's ok if you don't see it - the computer always tries "too difficult" optotypes too.
- It does not help to ponder long on the stimulus - one doesn't get better after a few seconds.

Visual acuity and Contrast Sensitivity were measured twice.

*Observer: "Now we go to the next room."*

The participant guided to Room R and was seated in the position allocated for the eye-tracking calibration. At this stage the questionnaire was placed on the desk. The observer's data gathering sheet was placed on the desk by the window.

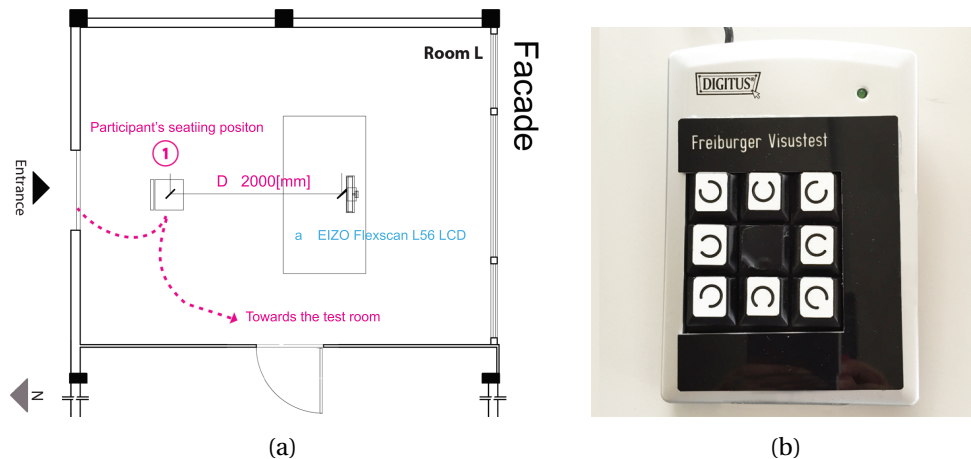


Figure III.9 – **Introductory phase:** a) the participants entered Room L and took position at seat 1. b) the response box

### Step 3: Eye-tracker Calibration

Eye-tracking calibration procedure was done in the experiment room which also allowed for participant's visual adaptation to the room's lighting condition. The calibration procedure took about 5 to 10 minutes.

### Step 4: Filling up the questionnaire

After the calibration session, the participant was asked to take place behind the desk and then asked to fill out the four first pages of the questionnaire (Appendix A). The observer left the room while the participant was filling up the questionnaire. After the questionnaire was finished (which can be seen by the observer from the control room), the observer goes back to the test room to give the final instructions for the remaining parts of the experiment including the task activities.

### Step 5: Performing the office task activities

The next remaining parts consist of office tasks using a task-support. The use of the task supports are randomised for each participants. Depending on which task-support the participant would work with the task activity is described as follows:

On-screen phase:

*Observer: "There is going to be a text that appears on the screen which you will read and then answer some questions. You will be instructed on the screen for each phase."*

On-paper phase:

*"You will be notified on the screen that the session is starting. You will be instructed to pick up these*

## Chapter III. Methodology

---

*papers (the pre-printed papers with the four phases placed on the desk were shown to the participant.). Please read the text and follow the instructions."*

On-phone phase:

*Observer: "For this part you will be using a headset (the head set is adjusted). You will be notified on the screen that you will receive a call. When you receive the call, to answer you press this button (the respective button is shown to the subject). You will listen to a text that is read to you and then answer some questions. When you are asked to hang up you press this button, (the respective button is shown to the participant)."*

At the end of the this step and before starting the task activities, the head position of the participant from the wall behind, the parallel window and from the floor is made was made. The following description was given to the participant:

*Observer: "I will make a measure of your head position. This is just for me to have a reference point. You don't need to keep this position and can change your head position. I will leave now and the test will start."*

### III.2.5 Subjective Assessments: Development & Design

A subjective assessment questionnaire was developed to record the participant's self-evaluated measure of the discomfort glare. This questionnaire was prepared in German. These assessments were done using two different measurement scales. A Likert glare rating scale was used after each phase of the trial. Additionally, before starting the trial and at the end of the trial a glare rating was made using a printed questionnaire with continuous scales. The questionnaire included socio-demographic related questions, standard questions about mood, a context recognition part and finally a glare rating section that included an introspective value judgment measure on the glare magnitude (Appendix A). The combination of Likert and continues scales gives a better understanding of the magnitude of perceived brightness that is being judged as glare. The context recognition section was meant to give the participants training about the context of the study and bring them to a same level of understanding without additional explanation from the observer in order to avoid any cognitive biases.

#### Subjective Assessments & Glare Ratings

The subjective assessment methods take two distinct approaches in their discomfort glare assessments. One method is based on recording subjective reactions through questionnaires. The second method consists of measuring visual sensitivity/acuity under glare conditions or measurements of visibility. The visibility measurements have used different visual test objects (optotype), such as character size, for appraising the luminous intensity necessary to reveal the test object to the participant's vision

([63]). The first method is the main approach for glare assessment that has been used to scale the human preference towards different light conditions. Eventually prediction models were derived from this method and they are currently used to evaluate light settings in an indoor environment. The most common method used so far in subjective glare assessment measurements is the Hopkinson multi-criterion system as a one-item scale, which is based on introspective judgment [110, 111] (Figure III.10a). This scale allows for evaluation of the lighting condition based on four criteria:

- just perceptible
- just acceptable
- just uncomfortable
- just intolerable.

The expressions used in this method creates confusion for the participants and it has been shown that it does not meet the main requirements for such assessments, which are simplicity and unambiguity. Moreover, the ranking of acceptance and comfort of glare is under debate. In recent studies on glare the Hopkinson glare scale has been transformed into a Likert glare scale. The advantage with this type of scale is that it has clear selection borders and it disregards neutral judgment by making the participants choose between the four options (Figure III.10b). In this study the glare rating is created based on a combination of measurement scales.

*Likert scale.* To evaluate the magnitude of glare we use a Likert glare scale after each phase of the trial, meaning that the participants were asked about the glare rating 4 times during the on-screen task (Figure: III.10b) and 4 times during the on-phone task. A Likert scale is a symmetric itemised 4 category scale with no neutral tendency. The adopted is a modification of the Hopkinsop's scale [111] used in the study that led to development of DGP. This scale also allows for evaluation of the lighting condition based on four criteria:

- imperceptible
- perceptible
- disturbing
- intolerable

he advantage with this type of scale is that it has clear selection borders and it disregards the neutral judgment. Moreover, the gathered data is comparable to that from the previous studies on discomfort glare [5, 45]. *Continuous scale.* To avoid limiting the survey to only a one-item scale, the participants were also asked about the glare magnitude before and after the trial using a continuous scale (Figure III.11a). These scales were presented to the participant on a paper questionnaire. A continuous scale is a vertical line representing a symmetry of categories from a midpoint, and bounded between two

### Chapter III. Methodology

---

extreme poles. The continuous scale has several advantages: it offers advantages in terms of subject's discrimination ability due to its large number of points [112], it produces scores that are normally distributed( which is important for statistical analysis) [113] and it may force the respondent to think about what the question really means [114, 115]. In attitude research, respondents have indicated that the continuous format may show their judgment more accurately [116]. The use of the continuous scale means that the respondent indicates his/her response by placing a check at a point on a line that is bounded by two poles of the response category and represents his/her judgment of the situation. This line can be horizontal or vertical [114].The questions asked were as follows:

- The question before the start of the trial:

How do you rate the glare that you are experiencing at this moment?

- The question after the start of the trial:

How do you rate the glare that you perceived during the task?

To make an introspective value judgment on the glare magnitude measure, we included a scale in terms of both comfort and acceptance [110, 51, 117, 118] (Figure:III.11b).

- The question was:

How would you rate the light level in the room,  
if you had to do your daily office work under this lighting condition?

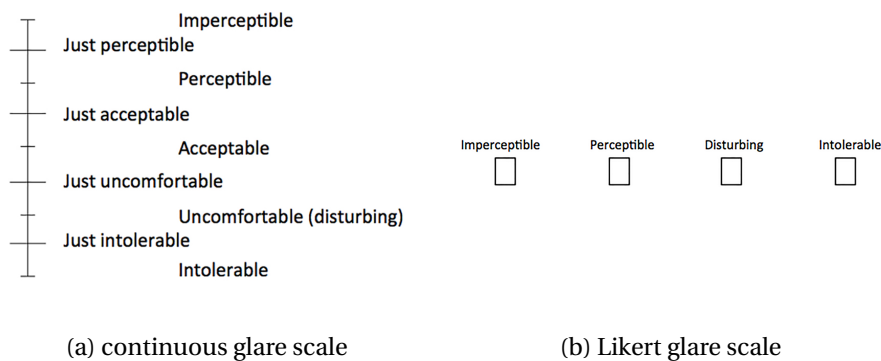


Figure III.10 – **Glare ratings:** a) Hopkinson's glare scale, b) participants were asked to rate glare with the Likert scale after each phase.

### Context Recognition

It was intended that the context recognition part would train the participants to have a sense of their level of glare sensation. This allowed the participants to have the same understanding of the context

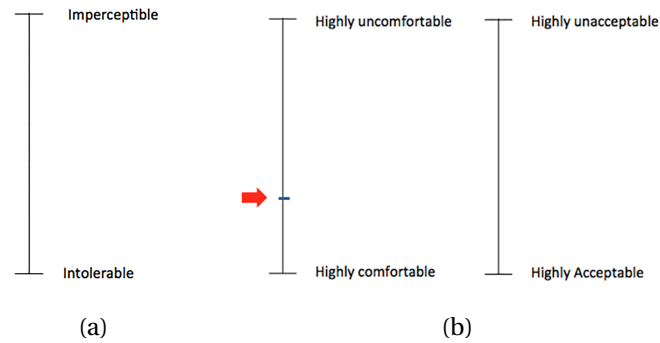


Figure III.11 – **Continuous scale:** a) participants were asked to rate glare on a continuous glare scale with vertical representation before and after the experiment, b) the purpose fitness scale using a continuous itemised scale with vertical representation. The participants were instructed on how to use the scale.

of the text and their own perception of lighting in offices. For this reason two exercises inspired from previous studies [117] were designed. The first exercise asked the participants to mark the areas in the room that they found glary on a printed image of the room (Questionnaire page 3, question 13, Appendix A). The second exercise asked the participants to describe their impression of the lighting of the room by selecting among a few descriptive words: Dull, Dim, Comfortable, Bright, Glary (Questionnaire page 3, question 14, Appendix A).

### III.3 HDR Imaging Techniques for Discomfort Glare Evaluations

The most recent methods for glare-free daylighting design rely on analyses of high dynamic (HDR) range images. HDR images are an accumulation of luminance values from a fixed point of view, which creates a basis for luminance-based metric analysis. These type of images allow for a larger difference between the brightest and the darkest areas of the registered image, thus representing a range of intensity levels that is similar to the real scene. This provides accurate, quick and inexpensive lighting analysis [119].

HDR images are created either by advanced physically-based renderings (used in daylighting design phase) (Figure: III.12a) or by multiple-exposure image capture (taken from the real situations)(Figure: III.12b).In the former's case an advanced lighting renderings of simulated 3D model of the architectural space is achieved by using tools such as *Radiance* [120]. using tools such as *Radiance* [120].The latter also known as HDR photometry techniques [121] with correct validations [122, 123] and image processing methods [45] have proven to be a perfect method for evaluation of luminance distribution for the FOV measurements. Normally, a fisheye image for large FOV is considered to cover the whole FOV of human eye. Figure (Figure: III.12b) shows an 180° angular fisheye projection captured with a CCD camera with an HDR imaging set up. This type of which has been used in this study for capturing the luminance distributions through the experiments. Each pixel is defined by three coordinates in the camera coordination system and an RGB value (Figure: III.12c). These image can then be processed using *Radiance*-based tools (*Findglare* [120] or *Evalglare* [45]) for deriving relevant photometric quantities to glare evaluation. Amongst others, vertical illuminance ( $E_v$ ) and average luminance ( $L_m$ ) that are used in several analysis part of this study are calculated using respectively equation III.1 and III.2.

$$E_v = \sum_j L_j \cdot \omega_j \cdot \cos \theta_j \quad (III.1)$$

$$L_m = \frac{1}{2\pi} \sum_j L_j \cdot \omega_j \quad (III.2)$$

$L_j$	Luminance of one pixel $j$ [ $\text{cd}/\text{m}^2$ ]
$\omega_j$	Solid angle of the pixel $j$ subtended at the eye [sr]
$\theta_j$	angle between the pixel $j$ and the optic axis [rad]

As convenient as this approach seems, it has complexities in attempts to define different components of the visual comfort metrics. One of these complexities is detecting the glare image pixels and deriving glare zones, as they are perceived by human eye. The existing glare source detection methods consider any image pixel of luminance value that is larger than a threshold luminance. This threshold luminance



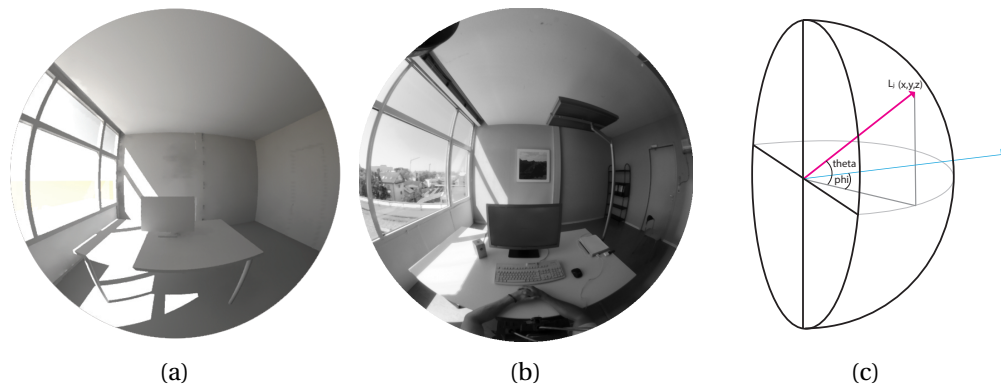


Figure III.12 – **HDR luminance images:** a) physically-based renderings, b) an HDR image captured by a CCD camera equipped with fisheye lens, c) luminance value of pixel  $L_j$  is calculated based on the recorded RGB values and its position is defined by three coordinates.

can be determined by different algorithms. One of them, implemented in *Evalglare*, uses the average luminance of a visual adaptation region and uses a multiplier  $x$  to derive the threshold luminance. The visual adaptation region is the fovea region of the eye for a presumed point of fixation in the space, e.g. the monitor screen. The method then searches the image for "glare pixels". Once one found, it starts searching around this pixel within a predefined search radius in order to find and combine glare pixels to a glare zone. In this method, the default values of the threshold multiplier  $x$  (default value =5) and the search radius (default value =0.2 rad) are set intuitively based on the luminous environment of the underlying images of the *Evalglare* development. Another method to derive the threshold luminance is the usage of a multiplier  $x$  on the average luminance of the entire image. This algorithm is implemented in *Evalglare* (default value =5) and in *findglare* (default value =7). For both algorithms and their default values exist so far no study about their accuracy or sensitivity. In this study we have made a sensitivity analysis on the threshold multiplier and search radius parameters for glare source detection. In two series of experiments we took HDR images under different sky and lighting conditions and with different façade systems. We then made measurements for 15 different combinations of the two parameters (Threshold multiplier with 5 levels and search radius with 3 levels of treatment) on each image using the *Evalglare* tool. The idea was to investigate if the different combinations of threshold multiplier and search radius make a significant difference on the resulting detected glare sources.

#### Glare detection parameters

For the image evaluation the Radiance-based tool *Evalglare* is used. The *Evalglare* is a tool to evaluate HDR images in order to derive the physical quantities relevant to five more commonly applied existing glare metrics DGP, DGI, UGR, CGI and VCP. The core algorithm of *Evalglare* is dealing with the detection of the "glare sources". The algorithm implemented in this tool goes through the image column by column in  $x$  and  $y$  direction and it checks every pixel luminance value and compares it with a luminance

threshold  $L_t$  (Figure: III.13a).  $L_r$  (marked in figure III.13b) with a blue circle over the monitor screen) is

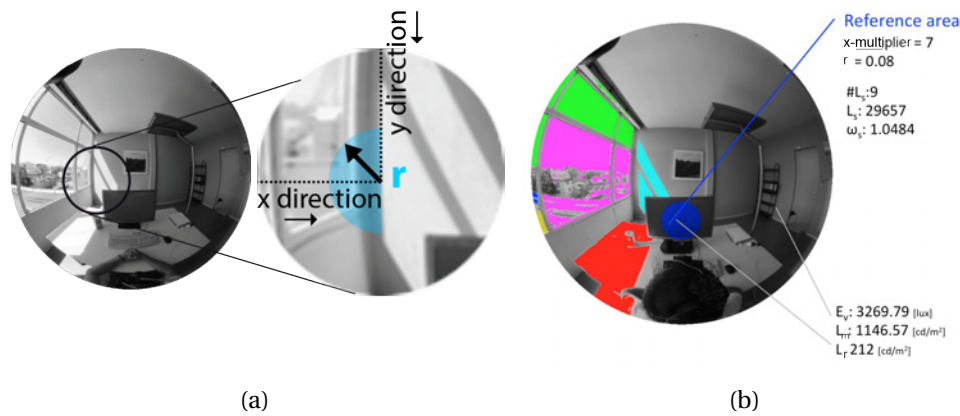
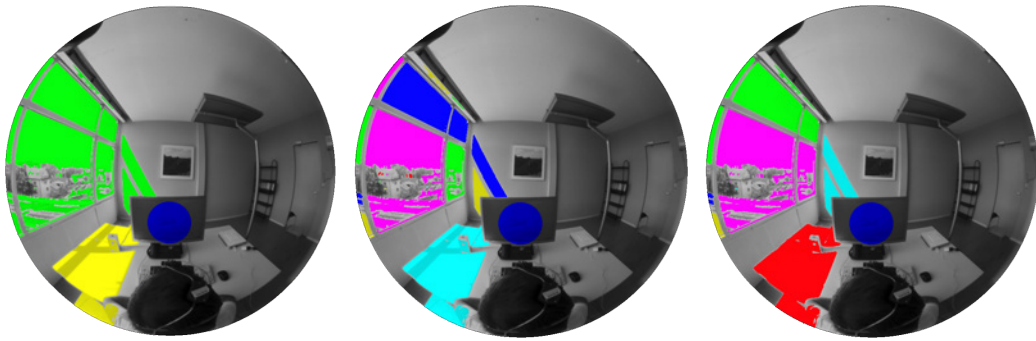


Figure III.13 – **Image processing for glare evaluation:** a) the algorithm searches the pixels column by column, b)

determined by the product of the luminance of a reference area in the image and a threshold multiplier  $x$ . Both of  $L_r$  and the threshold multiplier are defined by the user. When a glare pixel luminance value exceeds a  $L_r$ , the algorithm starts searching for similar pixels in the vicinity of the detected pixel. This search is done within a search radius  $r$  also pre-defined by the user. The detected pixels within the search radius are combined and defined as one glare source. The algorithm then continues to the next pixels. Ultimately, all the glare source patches within the image are detected based on this method. For each glare source the luminance of the glare source  $L_s$ , the solid angle of the glare source  $\omega_s$  and the angular position of each glare source to the optical axis of the image. The latter is used to calculate the  $P_i$  value. The default threshold multiplier  $x$  and search radius  $r$  values recommended for this tool are respectively 5 and 0.2 rad. Figure III.12 the influence of different settings of the luminance threshold multiplier  $x$  and search radius  $r$  on the size and amount of glare sources is visualised for one example image. The smaller  $x$  and the larger  $r$  is, the larger and fewer glare sources are detected. For a larger  $x$  and smaller  $r$  more glare sources of smaller size are detected.

### Glare detection parameters settings

A sensitivity analysis of the threshold and search radius parameters for glare source pixels detection showed a significant effect of threshold and search radius on most visual comfort metrics [124]. The sensitivity study was based on the HDR images which were captured under different sky and lighting conditions. Using *Evalglare* measurements for 15 different combinations of the two parameters (Threshold with 5 levels and search radius with 3 levels of treatment) (Figure: III.14) were made on each image. We tested these combinations for five different visual comfort metrics including Daylight Glare Index (DGI), CIE Glare Index (CGI), Unified Glare Rating (UGR), Visual comfort probability



(a) Threshold 7, Radius 0.2 rad (b) Threshold 7, Radius 0.4 rad (c) Threshold 7, Radius 0.8 rad

Figure III.14 – **Image processing for glare evaluation:** Using *Evalglare* we measured 5 different thresholds and 3 different search radii to calculate the visual comfort models. a, b and c show three examples, where the glare sources found with 3 different combinations are highlighted. The colours don't have a meaning.

(VCP), and Daylight Glare Probability (DGP). By comparing the prediction output to the subjective assessments, we can also conclude if a certain combination is more suitable for a specific lighting condition and visual comfort metric. The sensitivity to threshold and search radius selection means that if not correctly selected, the output result could lead to over- predictions of the visual comfort condition. Therefore, a more comprehensive study that includes several lighting conditions and facade configurations is necessary. In the current study the threshold and search radius parameters were respectively set to 10 and 0.2 rad after skimming through processed images with the 15 different combinations. The selected values were chosen to best fit all the lighting conditions in the experiment.

### III.4 Mobile Eye-tracking Method & Measurements

The EyeSeeCam is a state-of-the-art lightweight head mounted eye tracker [99] equipped with three cameras. This eye-tracker measures both eyes' pupil positions with two IR-sensitive cameras (Figure: III.5c, camera (2) & (3)), i.e. video-oculography (VOG). The EyeSeeCam software transforms these pupil detection data in real-time into head-referenced eye positions, which are referred to as "eye-in-head coordinates" in this paper. Additionally, an integrated inertia measurement unit (IMU) records head movements, i.e. rotation velocities and translative accelerations. A camera located on the forehead records point of view (POV) videos in an AVI format (Figure: III.5c, camera (1)). All data streams are synchronized with the POV video so that their information is mutually combinable. The mobile EyeSeeCam minimally limits the participant's movements and allows for natural exploration of the scene. Essentially, we processed the following raw data:

- Eye-in-head positions from VOG at a frame rate of 221[Hz] which rely on a prior calibration with a 5 point laser diffraction pattern that was performed successfully for each participant.

## Chapter III. Methodology

---

- A scene video recorded with a wide-angle POV camera that is configured to a resolution of 366x216 pixels at a sampling rate of 25 [Hz]. A camera calibration [125] and the image pixel where the centre point of the 5-point calibration pattern was projected to connect the eye-in-head data to the scene POV.
- Angle velocities and translative accelerations from the IMU deliver relative head rotations and up to a certain limit relative head translations, both at synchronised 221 [Hz]. These are applied to interpolate between absolute head orientations and positions, that we extracted approximately every 2nd second from a 3D pose estimation made by the POV camera [125].

Based on these data, a conversion to room referenced coordinates for head and gaze direction was realised (cf. Section IV.1).

### Calibration procedure

In the calibration session (Figure: III.15a) , participants had to fixate subsequently and repeatedly about one second on five dots that were projected on the wall at a 100 cm distance to the eye (Figure III.15b). The order was arbitrary. In this process the pupil positions are detected and described in the coordinate system of the camera image in units of pixel. After this procedure, the participant was asked to take place behind the desk (Figure III.15c) and the mentioned raw data was recorded from this position.

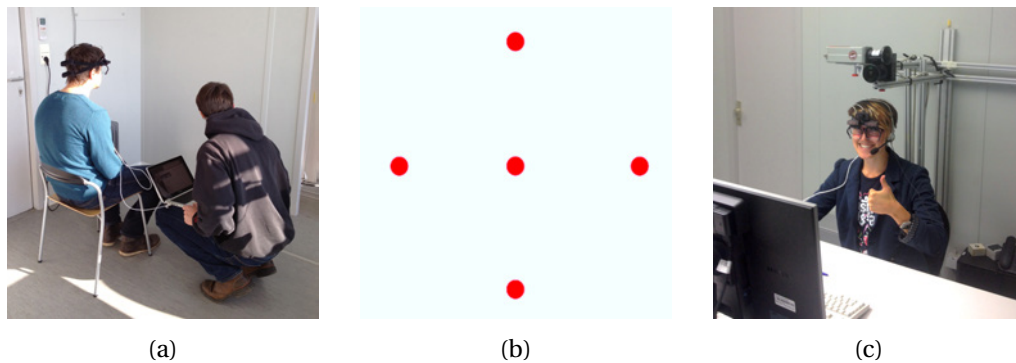


Figure III.15 – **EyeSeeCam calibration:** a) The seating position 100 [cm] from the opposite wall, b) five dots that are projected on the wall from the ESC, c) Participant wearing the eye-tracker and a headset at the desk position.

### III.5 Analysis Methods

The findings are based on statistical analysis using an analysis of variance (ANOVA) which allows for analysis of the differences between group means. This statistical test is a useful method for comparing (testing) three or more means (groups or variables) for statistical significance. For a homogeneity of

variance check Levene's test was used. The analyses were performed using MATLAB (R2014a) statistical tool. In order to assess the practical significance of the findings, the effect size  $f$  is measured by equation III.3. The Effect size is a function of differences among means [126], i.e.  $k$  population mean.

$$f = \frac{\sigma_m}{\sigma} \quad (III.3)$$

where for equal sample size in factorial and other complex designs,

$$\sigma_m = \sqrt{\frac{\sum_{i=1}^k (m_i - m)}{k}} \quad (III.4)$$

The final results presented in this study considered the illuminance at the vertical level (equation III.1) as the eye adaptation level and average luminance values (equation III.2) in FOV or central vision as an independent variable of light. The dependent variables were derived from the luminance images captured with two CCD-cameras.

The dependent variables were the horizontal and vertical gaze orientations, the gaze distributions and dominant gaze fixation durations. The gaze directions are unit vector elements in a 3D space represented in spherical coordinates that in turn represent the direction towards a fixation point and two polar angles. The polar angles were with the radius of 0 point in between both eyes with direction  $(0^\circ, 0^\circ)$  straight ahead from the participant. In this coordinate system the gaze orientations are noted analogously to Euler angles with the spherical angle  $\phi$  between  $-180^\circ$  and  $180^\circ$  for head rotations around the vertical z-axis (horizontal orientation) and the azimuth angle  $\theta$  between  $-90^\circ$  and  $90^\circ$  for down and upward directions (vertical orientation). The horizontal and vertical gaze variance are the gaze response (dependent) variables.

$$Radialstd = \sqrt{\frac{1}{n} \left( \sum_i^n (\phi_g - \bar{m})^2 + \sum_i^n (\theta_g - \bar{m})^2 \right)} \quad (III.5)$$

$\phi_g$	Horizontal orientation, a polar angle between $-180^\circ$ and $180^\circ$ [deg]
$\theta_g$	Vertical orientation, a polar angle between $-90^\circ$ and $90^\circ$ [deg]
$\bar{m}$	The centre of distribution

As the gaze direction is spatially distributed and two-dimensional, one of the gaze responses the radial standard deviation from the centre of the distribution is a liable measure to give distinct descriptions of the effect of each of these factors as opposed to the standard deviation. Radial standard deviation is fundamentally a quantity defined as the square root of the total sum of squares of the deviations in the horizontal and vertical directions from their respective sample distribution centres, divided by

### **Chapter III. Methodology**

---

the number of points of impact (equation III.5). The radial standard deviation of each task activity's gaze distribution is marked with a dashed circle whose radius corresponds to the standard deviation and whose centre corresponds to the mean value of the distribution. The independent and dependent variables are introduced in each result report. Finally, the spatial intensity of the dominant gaze was used to measure the duration of the fixations.

## IV A Novel Gaze-driven Approach

In this chapter, the development of a novel gaze-driven approach for estimating luminance values in the FOV is explained. This method which was developed for observing the relations between glare and gaze for discomfort glare assessments, was achieved based on three major steps. The developed processing method serves as a mean for deriving actual luminance fields perceived by the participants with respect to their gaze direction. Knowing the 3-dimensional (3D) properties of the test room geometry and the experimental set up including the position of the cameras and the participants' initial head position, the gathered eye-tracking data (eye-in-head and head-in-world movements) were transferred into world coordinates for computing the actual gaze-in-world directions.

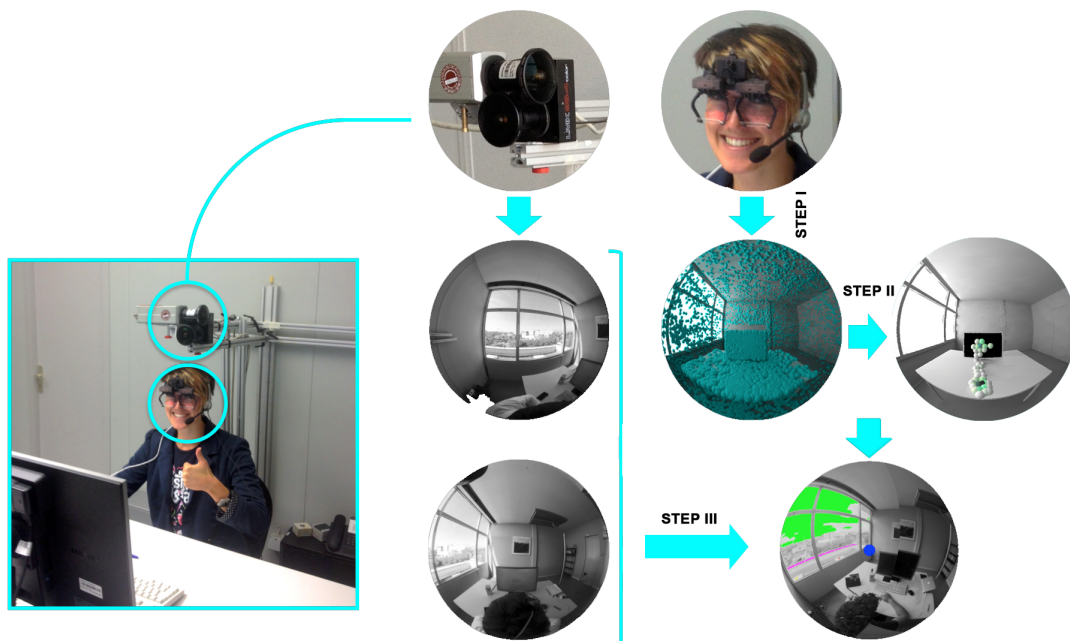


Figure IV.1 – Generating a gaze-centered luminance image.

As the first step towards a gaze-driven luminance image, the dominant gaze directions were identified using a spatial dispersion protocol. The gaze directions were then translated to the luminance camera coordinate system after camera position corrections and after considering misalignments, e.g. through slipping of the eye-tracker on the participant's head. A tool was developed to extract the luminance pixels from two captured luminance HDR images corresponding to 180° of the FOV with respect to the direction of the actual gaze. As a result, for each individual dominant gaze direction a new luminance image was produced that showed the luminance distribution in the FOV as experienced by the participant. In summary the following major steps in terms of processing were taken to derive luminance-fields relative to each dominant gaze direction:

- **STEP I:** Gaze-in-world orientations were measured
- **STEP II:** Dominant gaze directions were identified
- **STEP III:** Gaze-centred luminance images were derived

### IV.1 Step I: Gaze-in-world Directions

The EyeSeeCam has to deal with two coordinate systems: the eye orientation relative to the head ("eye-in-head") and the head relative to the setup ("head-in-room"). The eye-in-head data, which is a head referenced eye coordinate, is obtained directly from the device using its intrinsic calibration. The recorded eye-in-head data rely on a prior calibration with a 5-point laser diffraction pattern that was performed successfully for each participant. The "head-in-room" data is obtained by combining two sources: coarsely sampled coordinate transformations are first computed from the scene-camera video and then interpolated at high temporal resolution using the IMU acceleration data.

The eye-in-head records are then related to the room coordinates of the measurement set-up to derive the "gaze-in world" coordinate. Gaze-in-world is simply referred to as gaze direction in this study is where the participants have directed their gaze by shifting eye and head and body. The process of obtaining room referenced gaze directions consists of several stages. The first stage was to derive the 3-dimensional position and orientations of the head in world coordinates from the POV videos described in the following sections. Several processing steps are done to obtain the eye-in-head and head-in-room from the same rotation axes which are described here. The superposition of the two data is done to obtain gaze-in-world vectors ( $\hat{g}$ ) (Figure: IV.2(a-c)).

#### EyeSeeCam Coordinate System

Eye-in-head coordinates are represented in spherical coordinates with a radius representing the fixation distance and two polar angles, where a radius of 0 would point in between both eye balls and the origin direction (0, 0) is set initially by the projection direction of the central dot in the calibration pattern



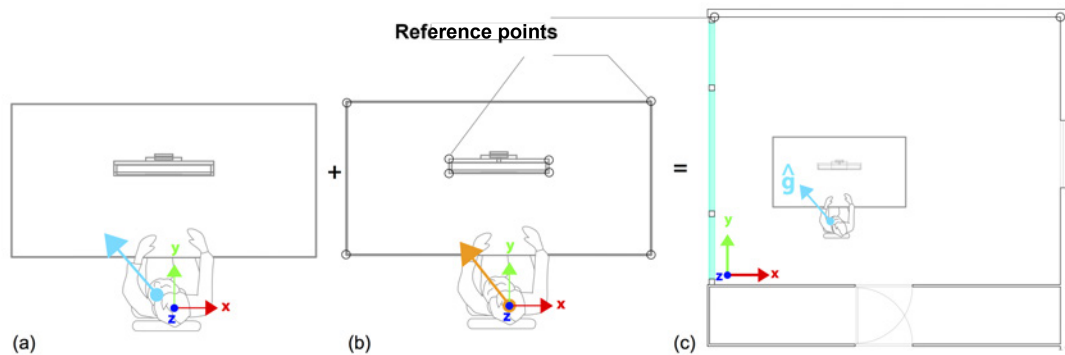


Figure IV.2 – **The gaze-in-world coordinates are derived from:** a) the eye-in-head coordinates superimposition with the, b) head-in-room coordinates to derive, c) the gaze-in-world coordinates.

(c.f section III.4). Thus the gaze origin directs straight ahead from the participant along the  $y$ -axis as represented in figure IV.3a.

The obtained head-in-room coordinates (from the scene camera and the IMU data) are aligned with the setup such that a head orientation straight ahead when sitting at the desk with the POV camera's optical axis parallel to the  $y$  room reference axis represents the original direction (Figure: IV.3a). Head orientations are notated analogously to Euler angles with the azimuth angle  $\phi$  between  $-180^\circ$  and  $180^\circ$  for head rotations around the vertical room axis, the elevation angle  $\theta$  between  $-90^\circ$  and  $90^\circ$  for down and upward directing, (Figure: IV.3a), and the angle  $\beta$  for sideways head tilts (Figure: IV.3b). Thus, for example while setting each other angle to zero,  $\alpha$  maps rotations around the  $z$  room reference axis,  $\gamma$  around the  $x$ -axis and  $\beta$  around the  $y$ -axis (Figure: IV.3b).

Eye-in-head coordinates are represented in spherical coordinates with a radius representing the fixation distance and two polar angles. A radius of 0 would point in between both eye balls and the origin direction  $(0^\circ, 0^\circ)$  is set by the projection direction of the central dot in the calibration pattern (Figure: III.15b). Thus the gaze origin points straight ahead from the participant and deviates only little but well controlled from the POV camera's optical axis, since we localised the central dot in the video from each participant's calibration and evaluated the offset angle between both. The offset angle is added to the eye-in-head angles for further gaze-in-world processing.

### Absolute Head Orientation and Position Determined by Video Analysis

In order to map coordinates from the scene-camera image to room-fixed coordinates, we defined 12 locations in room-fixed coordinates that are known from the computer aided design CAD model of the set-up, covered well within the  $270^\circ$  field of the CCD cameras which were not too eccentric in the scene (in order to minimise errors by camera calibration, which increases with eccentricity): the four corners of the screen, the corners of the window, corners of the desk and corners of the door. For each analysed

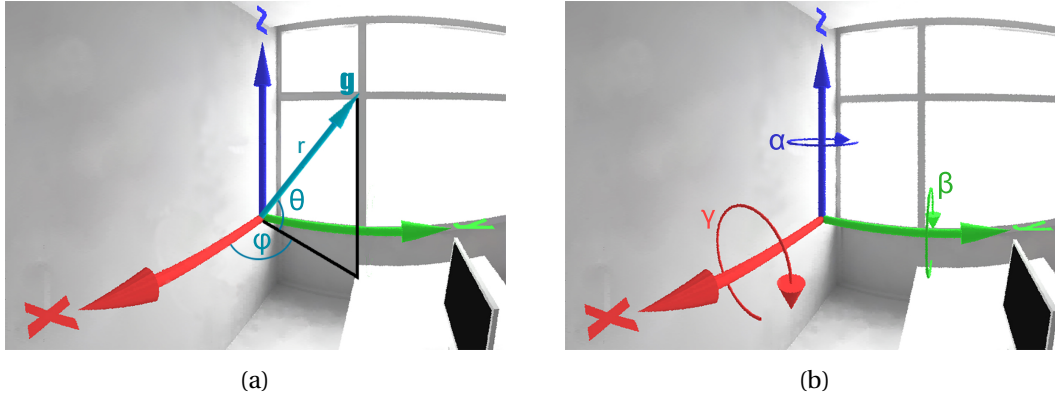


Figure IV.3 – **EyeSeeCam coordinate system**: a) EyeSeeCam coordinate system in the room and the rotation IMU, b) the spherical coordinates representing the horizontal and vertical angular definitions of the gaze vectors in the 3D space.

frame, we manually selected the 4 key points most central to scene-camera image (Figure: IV.2 (a-c)). Mapping the 2D image coordinates to 3D room coordinates requires solving a perspective n-point problem (PnP), which we accomplished using the camera calibration toolbox [125]. This procedure returns the translation vectors  $t_{Head}$  and the rotation matrix  $R_{Head}$  of the coordinate transformation from camera-centred to room-centred coordinates, with  $R_{Head}$  and  $t_{Head}$  defining the head position in the room.

### Relative Head Orientation Through Integrated Angle Velocities

The head orientations resulting from the scene video analysis are essential for determining absolute head and gaze directions, but they are only produced for a few time points, relative to the number of data points recorded by the EyeSeeCam. For a continuous time series of head orientations, the angle velocities given by the IMU were integrated over time. The sampling rate is adjusted to match the high rate sampling of the VOG cameras, which allows a direct bin-wise synchronisation of head and eye data. The IMU acceleration data are represented in a head-referenced 3D coordinate system, and provide angular velocities relative to head-fixed axes ( $\vec{w}$ ). To transform those to room-fixed coordinates, we use a quaternion rotation operator  $\mathbf{Q}$  [127]:

$$\mathbf{Q} = (\cos(|\vec{w}|/2), \frac{\vec{w}}{|\vec{w}|} \cdot \sin(|\vec{w}|/2)) \quad (IV.1)$$

Transforming back to angular coordinates, we obtain IMU velocity data in a room-referenced frame. By determining the line of gravity from the sensor data and integrating the velocities starting at the point inferred from scene-camera data, we obtain an estimate of the head-in-room position. The quaternions are multiplied incrementally by using the *Matlab* function `quatmultiply()` with absolute head orientations. Absolute head orientations are transformed between the EyeSeeCam coordinates

## IV.2. Step II: Identifying the Dominant Gaze Directions

---

and the quaternion formalism by using the *Matlab* functions `angle2quat()` or `quat2angle()` respectively. Finally, the time series of quaternions was transformed back into angles using the *Matlab* function `quat2angle()`. The key-frame selection was done every 30s (750 frames) or in case of a gaze shift (resulting in a new scene frame). This procedure ensured that we obtain head-coordinates had a high resolution to be synchronised to the IMU sensors, and later on matched to the eye-tracker's sampling rate, and at the same time avoid the accumulation of errors due to integration of the acceleration signal.

### Gaze-in-world coordinates

As a final step, we mapped the eye-in-head data to the head-in-room data. To do so, the head tilt needs to be considered for the eye-in-head directions, since the head fixed cardinal axes are tilted with respect to room-referenced horizontal and vertical axes. For compensation we applied a rotation around the zero eye-in-head direction with the negative tilt angle  $-\beta$  on the eye-in-head data whereas eye-in-head angles were mapped before into a Cartesian norm vector and transformed back afterwards into angles,  $\phi_{Eye}$  and  $\theta_{Eye}$  (Figure: IV.3b). The tangent from eye-in-head data gives Cartesian coordinates, which are transformed to polar coordinates their resulting polar angles and the head tilts are summed together for each time point. Then the inverse transformation was applied. These resulting eye-in-head angles have the same rotation axes as the head-in-room angles  $\phi$  and  $\theta$  and are superposed together to obtain gaze-in-world vectors ( $\hat{\mathbf{g}}$ ).

## IV.2 Step II: Identifying the Dominant Gaze Directions

Gaze allocations are typically studied in terms of fixations (periods of pause) and saccades (rapid movements between fixations) with respect to temporal and spatial characteristics such as duration or dispersion [76]. It is generally agreed upon that visual and cognitive processing occurs during fixations when the retinal image from the visual environment is stabilised.

The spatial distribution of the fixation points were measured based on a spatial dispersion method [76]. This method focuses on the probability density of the fixation points over the visual space. The angular positions of the highest frequency of gaze encounter were then considered as the dominant gaze directions (Figure:IV.5). The gaze directions were binned with a  $5^\circ$  width, which encompasses foveal ((up to  $1.5^\circ$ ) and para-foveal components ( $1.5^\circ$  up to  $5^\circ$ ) of the central vision (Figure:IV.4a & IV.4b).

With this method we minimised the risk of selecting a pre-assumed gaze position present in other methods, e.g. averaging, clustering, weighted averaging, etc. The binned data was computed for each individual and the dominant gaze directions were selected (Figure: IV.10 ( a-d) & IV.10 ( a-d)). In these 3D visualisations the size of the spheres in each image represents the number of gaze encounters on

that point. As the data is represented in 3D space, the further the spheres fall, the smaller they look. To avoid this effect we rescaled the spheres based on the distance of the allocation point to the viewpoint. The dominant gaze directions were used to calculate the adaptation luminance in the FOV by deriving gaze-centred luminance images.

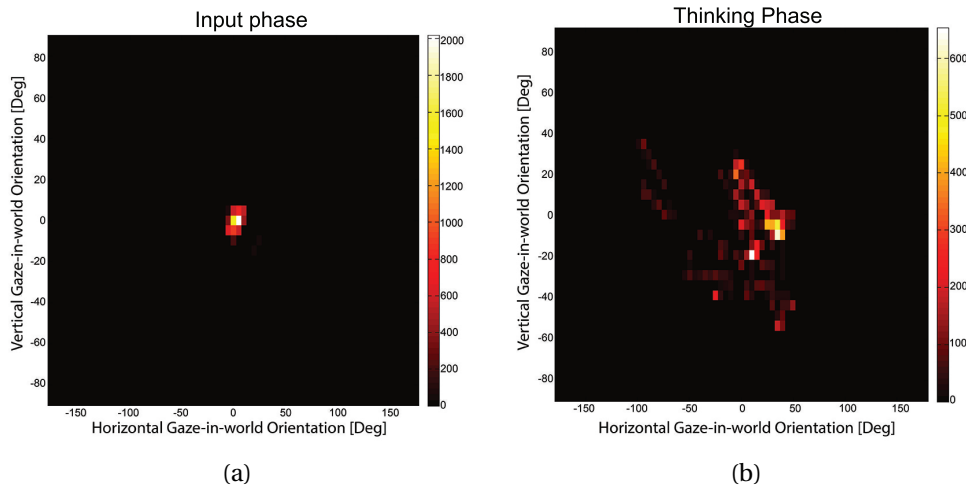


Figure IV.4 – **Gaze-in-world distributions:** a,b) a participant’s gaze distribution binned during on-screen *Input* phase and *Thinking* phase; the x-axis and y-axis respectively correspond respectively to 180° horizontal gaze orientation and 90° vertical gaze orientation.

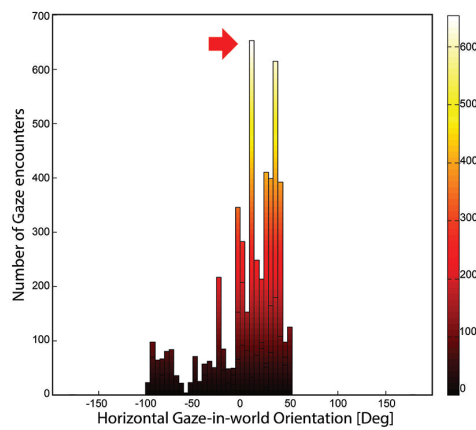


Figure IV.5 – **Gaze-in-world distributions:** a histogram of gaze-in-world distribution; the x-axis corresponds to 180° horizontal gaze orientation; the y-axis and the colour bar shows the number of gaze encounters at each point in space; the dominant gaze direction with the highest number of encounters is shown with an arrow.

### IV.2.1 Secondary and Tertiary Dominant Gaze Directions

In most cases there were situations with more than one prominent gaze direction (Figure: IV.6). We considered a filtering algorithm to include and evaluate all the relevant dominant gaze directions that created a new luminance field. The filter detects all the gaze points with high frequency that do not fall in the same region and do not exceed a sensitivity threshold of 70% of the highest detected frequency. This threshold is arbitrary.

The regions were defined with a span of  $20^\circ$  angular deference to cover the central fixation span [128]. In scenarios where gaze is directed outside the window, we hypothesise that the process of re-adaptation occurs with each gaze shift and thus the gaze shifts have a higher visual impact. Thus, in such cases the sensitivity threshold was disabled. The filtering resulted in one to five dominant gaze directions per experimental phase for each participant.

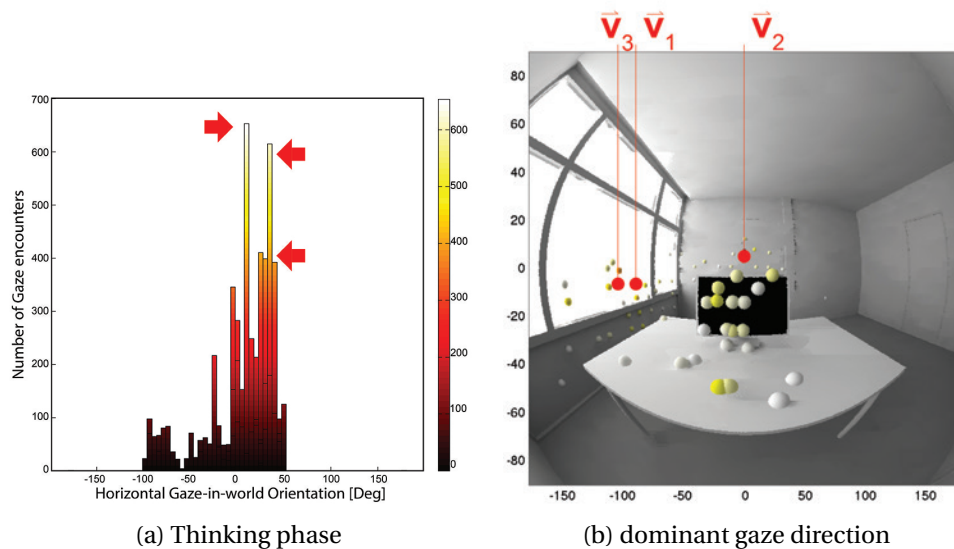


Figure IV.6 – **Primary, secondary & tertiary gaze:** a) a participant's gaze allocations during a *Thinking* phase. Three dominant gaze directions are identified. b) 3D visualisation of the gaze allocations.

### IV.2.2 Analysis of Secondary and Tertiary Dominant Gaze

The dominant gaze directions represent the direction that the participant looked at the most during the task phase. Using a filtering algorithm described in section IV.2.1, we included all the relevant dominant gaze directions that created a new and unique luminance field. The filtering resulted in one to five dominant gaze directions per experimental trial for each participant. A gaze-centred luminance image was developed with respect to each gaze direction: primary ( $\vec{v}_1$ ), secondary ( $\vec{v}_2$ ) and tertiary

( $\vec{v}_3$ ) (Figure: IV.7a-c).

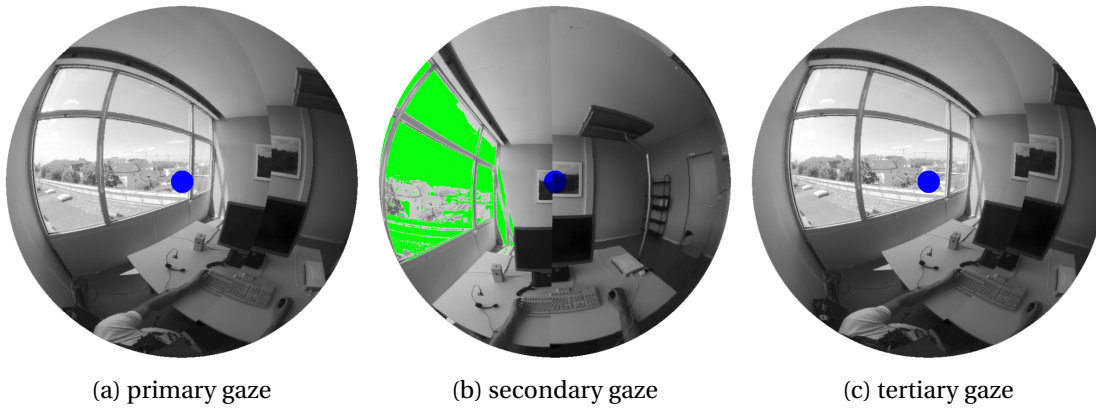


Figure IV.7 – **Primary, secondary and tertiary gaze:** a gaze-centred luminance image was developed with respect to each identified dominant gaze and processed, a) the primary dominant gaze, b) the secondary dominant gaze, c) and the tertiary dominant gaze.

The number of cases with fourth or fifth dominant gaze directions was very minimal (Figure: IV.8a). The boxplot (Figure:IV.8b) displays the distribution for each group with the median value highlighted in red. A one-way ANOVA was made on the illuminance at the vertical level ( $E_v$ ), which is the dependent variable, and the three ranked dominant gazes are the independent variables. Our one-way ANOVA results ( $F(2, 771) = 0.47, P=0.58$ ), that analyse the effect of the three ranked dominant gaze measurements, show no significant effect of neither the secondary nor the tertiary gaze directions. Therefore, the dominant gaze directions were used for evaluations.

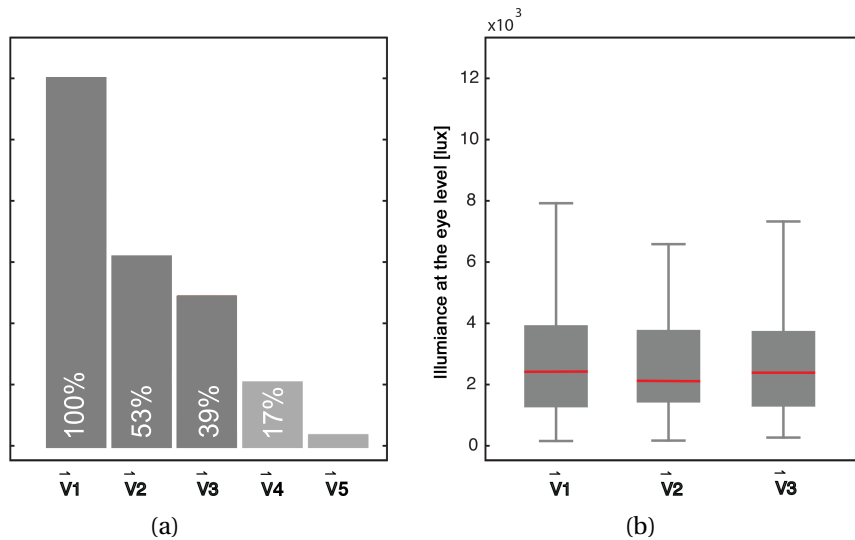


Figure IV.8 – **Primary, secondary and tertiary gaze:** a) percentage of all cases of identified dominant gaze encounters ion comparison to the primary gaze, b) a boxplot showing the distribution of the vertical illuminance for primary , secondary and tertiary dominant gaze directions.

## IV.2. Step II: Identifying the Dominant Gaze Directions

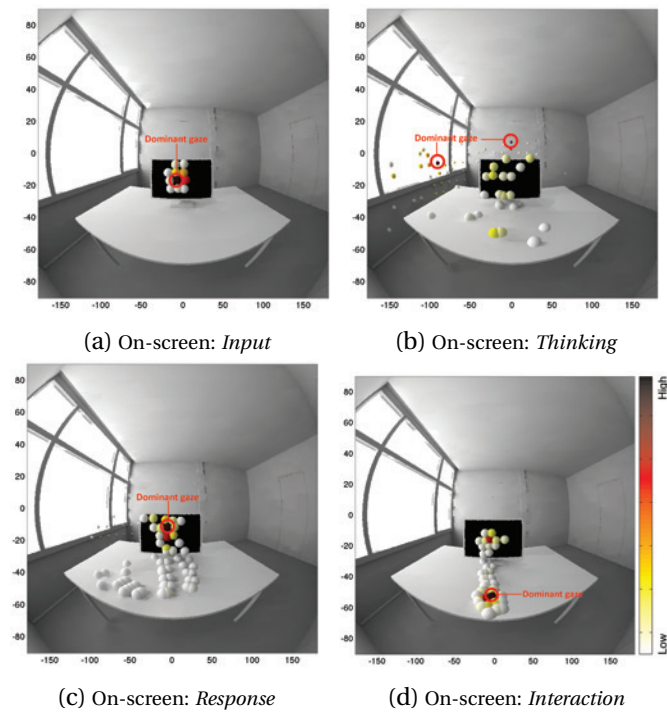


Figure IV.9 – **3D visualisation:** one participant's gaze allocations for each task phase using computer.

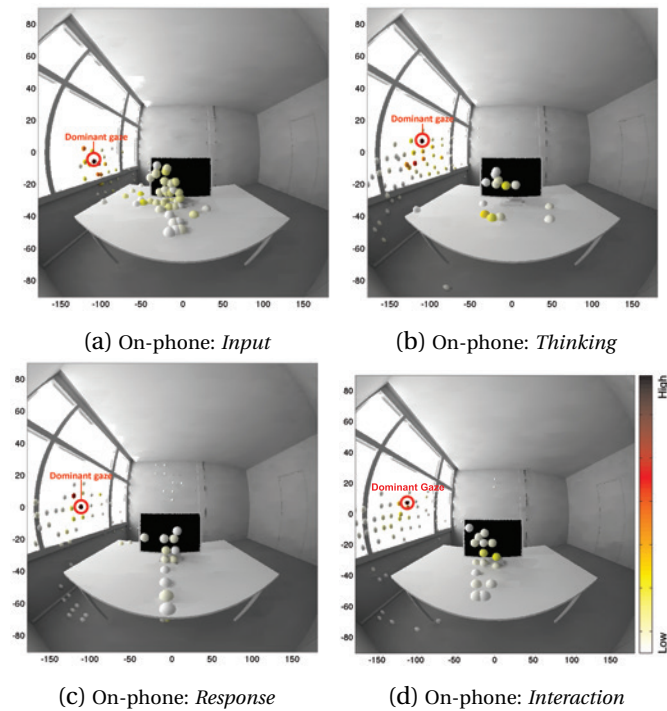


Figure IV.10 – **3D visualisation:** One participant's gaze allocations during each task phase using a headset.

### IV.3 Step III: Deriving Gaze-centered Luminance Images

What the human eye can see is the luminance distribution in the FOV. Luminance is technically defined as the luminous flux per unit area of light travelling in a specific direction and the solid angle containing that direction. It is perceived by a viewer as the brightness of a light source measured in candela per square meter. The luminance measurements of all the areas across the FOV and the relationships between them contribute favourably or unfavourably to visual comfort perception. While the luminance perception inside the central part of the FOV contributes more to the visibility of the observed scene, the peripheral luminance distribution has more impact on the visual comfort sensation [26]. Therefore it is sensitised to have a comprehensive understanding of the relation between the luminance distributions in the FOV perceived by the eye. HDR photometry techniques [121] with correct validations [122, 123] and image processing methods [45] have proven to be a perfect method for evaluating luminance distribution for the FOV measurements. An HDR luminance image is an accumulation of luminance values from a fixed point of view. The coordinates of the optical system centre correspond to the assumed fixed-gaze direction and all the luminance measurements are evaluated with respect to this axis.

In order to translate the gaze direction vectors to the wide-angle HDR images, we employed methods that use the lighting simulation tool *Radiance* [120] and the CAD 3D geometrical model of the test room in order to transfer the gaze vectors from the eye-tracker to the camera position. Having the actual gaze direction vector properties in the luminance camera coordinate system (origin: camera position), we were able to extract luminance images corresponding to each vector from the two captured images. For this a new tool was developed which takes the two luminance images and the vector coordinates as input and generates one wide-angle luminance image with respect to the input vector as the centre of the image. The final output luminance image was evaluated using *Evalglare* [45] to calculate the relevant photometric measurements for visual comfort models.

#### Translating the Gaze Directions to the Camera Coordinates

Correction for the different positions of the luminance camera and the eye tracker (participant's head position) was necessary to derive the gaze-centred luminance images. This correction was done by a redefinition of the EyeSeeCam coordinate system and the coordinates of the 3D geometry of the space as defined in *Radiance*. The *Radiance* coordinate system is defined in such a way that the  $y$  axis points towards the north direction (Figure:IV.11 a). The coordinate systems redefinition had to be done in several steps of the data processing phase. To obtain the coordinates of the intersection point of each gaze direction vector  $\hat{\mathbf{g}}$  with the 3D geometry of the space, the normalised vectors were transformed to the *Radiance* coordinate system. Using *rtrace*, which is a *Radiance* command, we are able to trace a line on the vectors trajectory in the space. The point where this line reaches a surface in the 3D geometry of



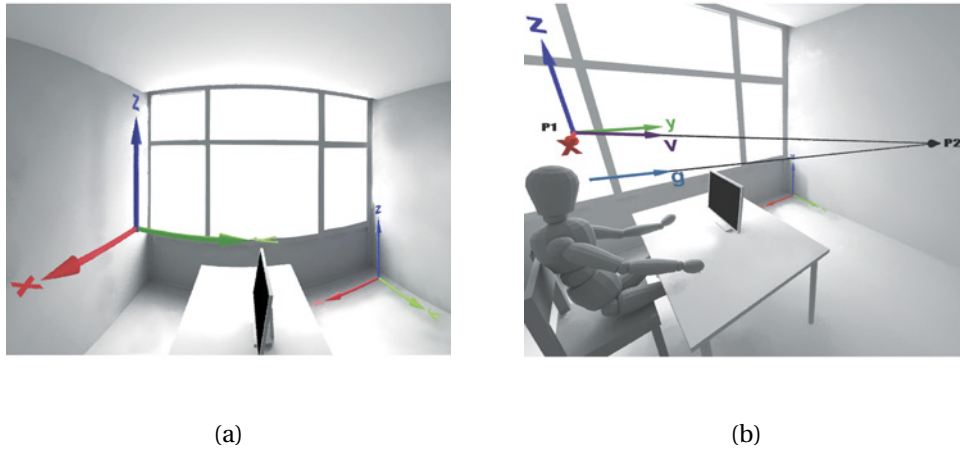


Figure IV.11 – **Translating the gaze directions to the camera coordinates:** a) the coordinate system of the EyeSeeCam and *Radiance* is shown, b) vector  $\hat{\mathbf{v}}$  is a gaze direction from the camera position that is looking in the same direction as  $\hat{\mathbf{g}}$ .

the space is the intersection point. The output is the 3D coordinates of the intersection point in the *Radiance* coordinate system  $P_2 (x_2, y_2, z_2)$  (Figure:IV.11b).

Figure IV.12 illustrates all the intersection points that represent raw gaze allocations data over the space for one subject during a one minute reading task. The scene is viewed from the luminance camera's point of view which is located above the participant's head position. Knowing the intersection point, we can calculate the vector between the camera point  $P_1 (x_1, y_1, z_1)$  and the intersection point ( $P_2$ ) (equation IV.2). The resulting gaze vector  $\hat{\mathbf{v}}$  within the camera coordinate system is a unit vector from the camera position  $P_1$ .

$$\mathbf{v} = P_1 \vec{P}_2 = (x_2 - x_1, y_2 - y_1, z_2 - z_1) \quad (\text{IV.2})$$

#### Merging the Gaze-centred Luminance Images

A tool was developed to extract the luminance pixels corresponding to 180° of the FOV with respect to the gaze directions  $\hat{\mathbf{v}}$  from the two captured luminance HDR images Figure (Figure: IV.13a, IV.13b). As a result, a new gaze-centred image was produced for each gaze direction that corresponds to the actual luminance distribution experienced by the participant (Figure:IV.13c). The tool merges the two images in a four-step procedure. In a first step, the overlapping pixels at the border of the lens within a 2° range were removed before merging the images to get rid of the vignetting problem (Figure: IV.14a). To minimise the effect of camera displacement, the pixels from the window-facing camera

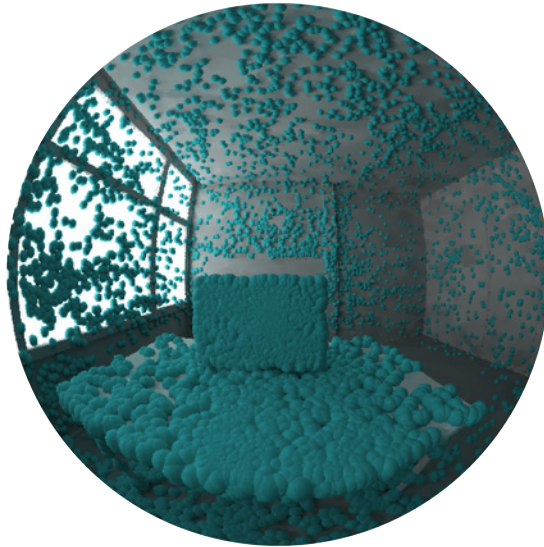


Figure IV.12 – **Gaze intersection with the 3D geometry:** a) the resulting 3D representation of all gaze points from one participant over a minute of *Input* phase recorded with 221Hz sampling rate.

were chosen in order to have the "displacement-line" far inside the room, where no glare sources were expected. Each image's view direction property was then rotated, so that it pointed to the centre of the image. The result is shown in Figure IV.14b & IV.14c. In the next step, these two images were merged into one image. The un-captured areas were filled up with the last captured values from the last row of available pixel data. Figure IV.14d highlights this region with red on the example image. Ultimately, the resulting gaze-centred image, Figure IV.13c, could be further processed to derive the relevant photometric parameter.

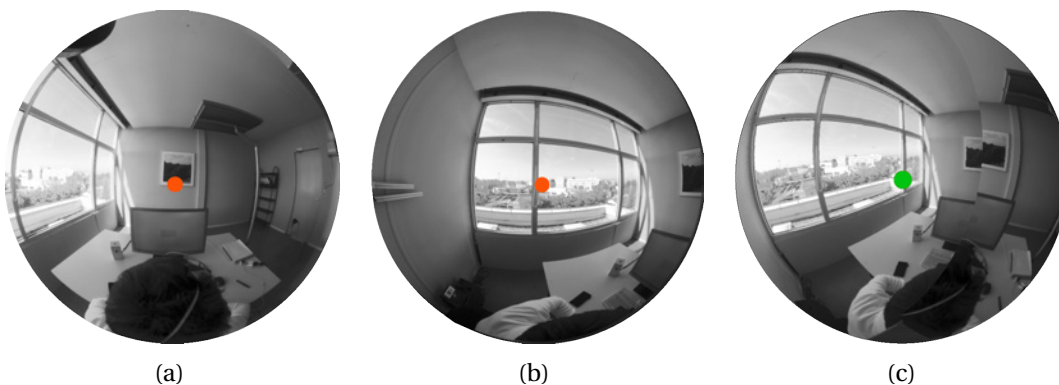


Figure IV.13 – **Luminance images:** a) participant's view, and b) window's view, c) resulting image for a dominant gaze direction.

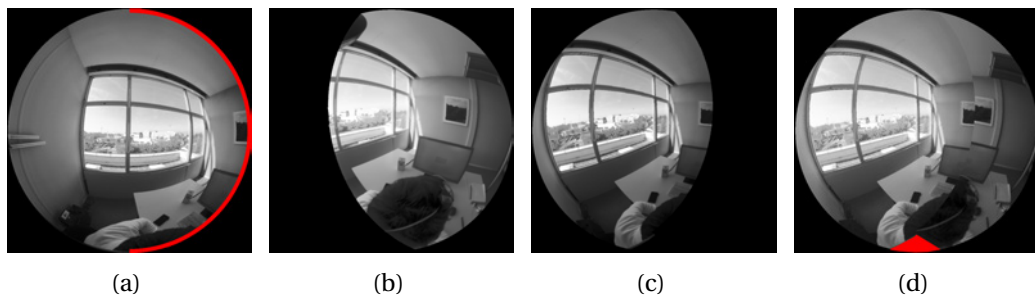


Figure IV.14 – **Merging the two luminance images:** a) the overlapping Pixels at the border of the lens within a  $2^\circ$  range, here highlighted in red, were removed, b, c) each single image is rotated, so that the image's view direction property is pointed to the centre of the image, the black areas are the regions that were not captured by either camera, d) The areas that were not captured by any camera are highlighted in red.

## IV.4 Summary

Gaze-centred luminance images were derived in three major steps. The first step to this approach was to compute the gaze directions in the real scene (gaze-in-world) from the data recorded by an eye-tracker. The second step was to identify the dominant gaze directions, i.e. fixation points over the scene, hence determining the dominant field(s) of view for each task phase and participant. The final step was to derive gaze-centred luminance images based on the dominant gaze directions.



# V Experimental Phase: Pilot Studies

To identify which eye-tracking parameters could serve as the most robust predictors of visual comfort and optimise the experimental set up, we performed two pilot studies. Integrated eye-tracking and luminance mapping and a user assessment experimental procedure was developed through these pilot studies prior to the final extensive data collection (cf. section V.1 & V.2). The first set of experiments served as proof of concept [129] with 5 participants (**Experiment I**, section V.1). The second served as a pilot study for variable characterisation and optimisation of the experimental set-up with 23 participants [130, 104] (**Experiment II**, section V.2) .

## V.1 Experiment I: Integrating Eye-tracking Methods

As a first step, we conducted a pilot study, whose objective it was to investigate the possible relations between eye-movement patterns and light distribution in the room

### V.1.1 Set up

#### Layout & Test Procedure

Each trial started with the participant coming in from the outside, first to the neighbour module and then to the test scene (Room R) so that each participant would have a similar visual and thermal adaptation process to indoor light (Figure: V.1). Participants wore the EyeSeeCam (Figure:V.2c), and performed one trial per façade condition. The office task activity consisted of four task phases: 1) *Input* phase, 2) *Thinking* phase, 3) *Response* phase, 4) *Pause* phase (table V.1). Each phase lasted a one-minute. The reading text of the *Input* phase was chosen randomly among 12 articles and displayed on the monitor at the beginning of each trail. For the on-screen task , an LCD monitor was used in this first study.

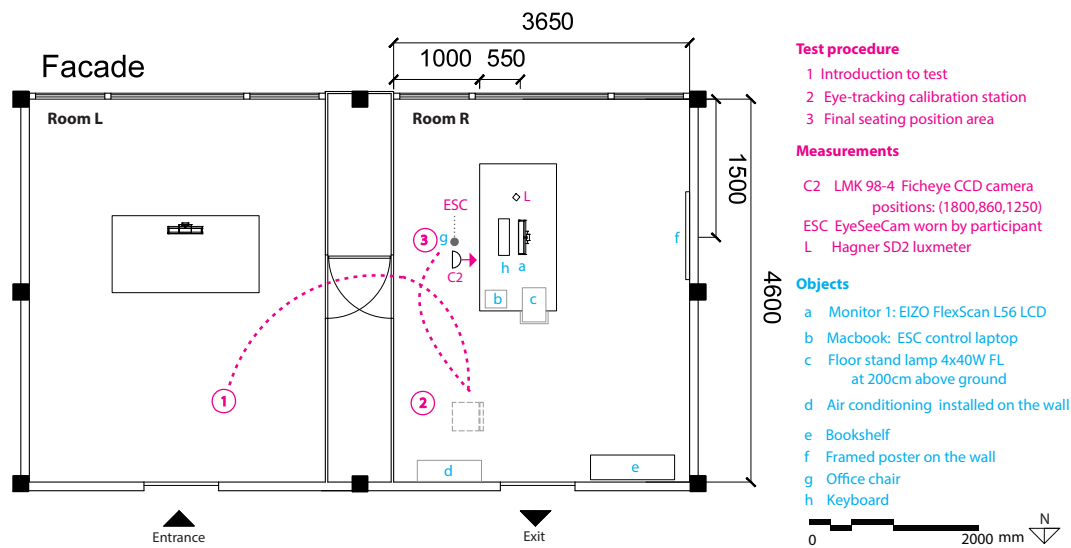


Figure V.1 – Plan of the daylight laboratory for experiment I: the layout of the rooms, location of the participant during the test procedure, the position of the measurement devices and all the objects that were used or were in the scene in the first pilot study.

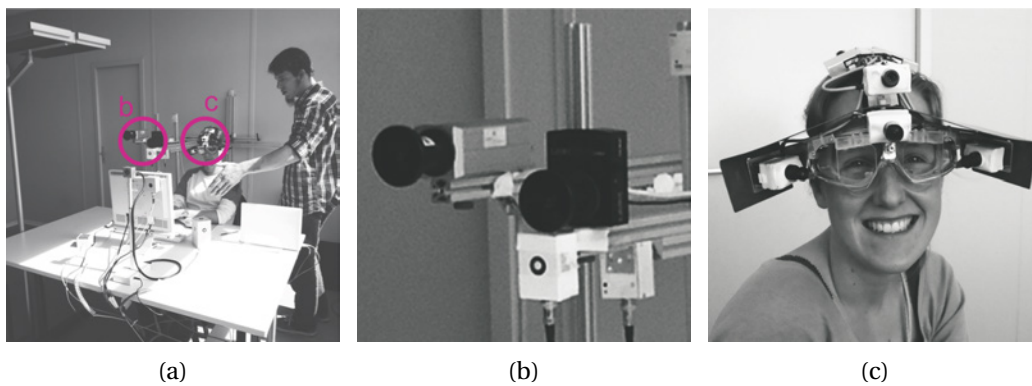


Figure V.2 – Set up and main measurements: a) a participant being introduced to the experiment. b) the two cameras were installed side by side, here the possibility of getting a 360° image by rotating one of the cameras by 180° was tested, c) earlier version of ESC used in these experiments.

Table V.1 – Office task sequence specifications

Activity	Task description	Task-support	Task interaction	Visually focused	Visually explorative	Cognitive	Motor	Time [sec]
on-screen								
1) <i>Input</i>	reading a text	screen	screen	✓	✗	✗	✗	60
2) <i>Thinking</i>	thinking about the text	screen	screen off	✗	✓	✓	✗	60
3) <i>Response</i>	responding to a question	screen	screen/mouse	✓	✓	✓	✓	60
4) <i>Pause</i>	waiting	screen	✗	✗	✓	✗	✗	60

### Façade Configuration

The sequence of light conditions ranging from dark and low contrast to bright and extreme contrast was determined through initial testing with different façade configurations compared in simulation

## V.1. Experiment I: Integrating Eye-tracking Methods

using *Radiance* [131] and in the real space with the help of HDR imaging techniques [119]. The main concern was to have different significant lighting conditions and glare situations in the room while maintaining the view contact to the outside and ensuring an easy flow of the measurement procedure. Four daylight conditions were considered for the experiment (Figure V.3). These lighting conditions were created by rotating the test facility or by changing the facade by blocking a part of the window. The rotation of the test room resulted in different views outside of the window. As result, the view outside of the window and lighting conditions are confounding in this pilot study and we refer to this variable as façade configuration . The four façade configurations are namely:

FC1: clear sky condition with no direct sunlight in the room (dark and Low contrast)

FC2: clear sky condition with venetian blind half way down (dark and high contrast)

FC3: clear sky condition with direct sunlight in the room (bright and high contrast)

FC4: clear sky condition with the sun in the FOV (bright and extreme contrast)

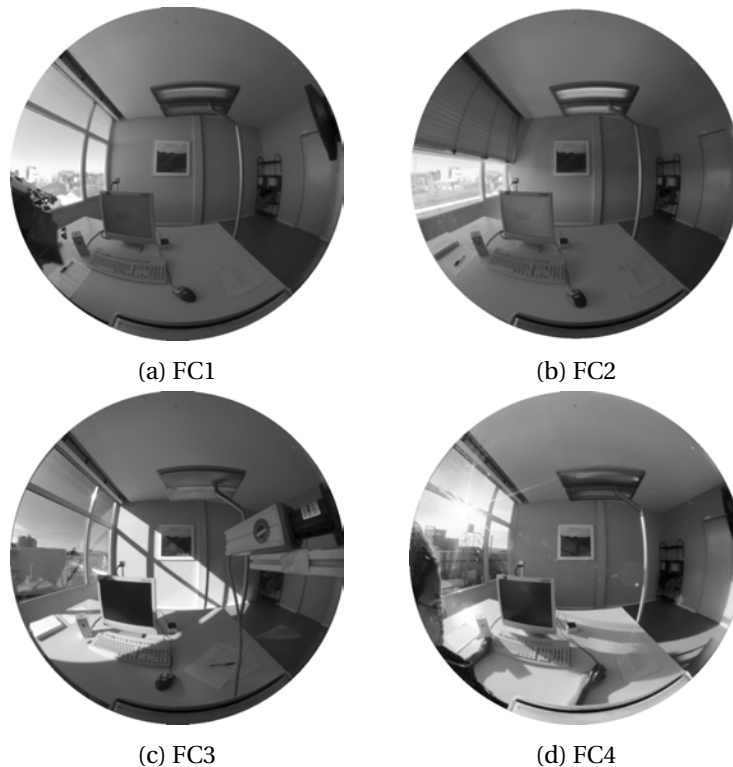


Figure V.3 – **Façades considered in the pilot study:** a) FS1: clear sky condition with no direct sunlight in the room, b) FC2: clear sky condition with venetian blind half way down, c) FC3: clear sky condition with direct sunlight in the room, d) FC4: clear sky condition with the sun in the FOV.

Table V.2 – Façade & lighting condition specifications

	Window	Sky	Direct sun	Contrast	$DGP$
FC1	-	clear	-	Low	0.2327
FC2	cover on	clear	-	High	0.2321
FC3	-	clear	x	High	0.3339
FC4	-	clear	x	Extreme	0.4345

### Participants

Five native German speaker (to avoid biases caused by understanding the Input texts) volunteers between the ages of 20 and 30 were recruited amongst the Fraunhofer-ISE staff.

### Measurements

Indoor light distribution was monitored by lux-meters and calibrated HDR cameras (Figure: V.2b) equipped with fish-eye lenses as described in section: III.2.2. The configuration of the CCD cameras' placements was different in this first pilot study. Here the possibility of recording 360° of photometric data by rotating one of the cameras by 180° at the beginning and end of each trial (Figure: V.2b) was checked. Due to highly uncorrectable uncertainties caused by the disposition of the two cameras and lack of recorded data, this method was not further used in the experiments. An HDR image was captured every 30 second and one image per task phase was selected to observe the lighting condition variations. The images were processed to derive the photometric quantities using *Evalglare* (Figure: V.4). Eye-movements were recorded by means of the EyeSeeCam (cf. section: III.4). The EyeSeeCam version used in this set of experiments were an older prototype as can be seen in Figure V.2c. This version has a fourth camera, the "gaze camera", which is a pivotable camera that is continuously aligned with the participant's gaze (eye-in-head movements) and verifies the eye-in-world measurements from which the distribution of gaze and gaze-in-world parameters can be derived. No glare rating data was gathered in this experiment.

### View Outside the Window

The effect of façade configuration and task was addressed in a preliminary analysis of the eye movement data. The view outside the window changed from a view towards containers on the rooftop to one of mixed vegetation and buildings at a distance in different settings.

#### V.1.2 Proof of Concept

The effect of façade configuration and task was addressed in a preliminary analysis of the eye movement data. This analysis was restricted to the two extreme façade configurations for glare, namely the dark



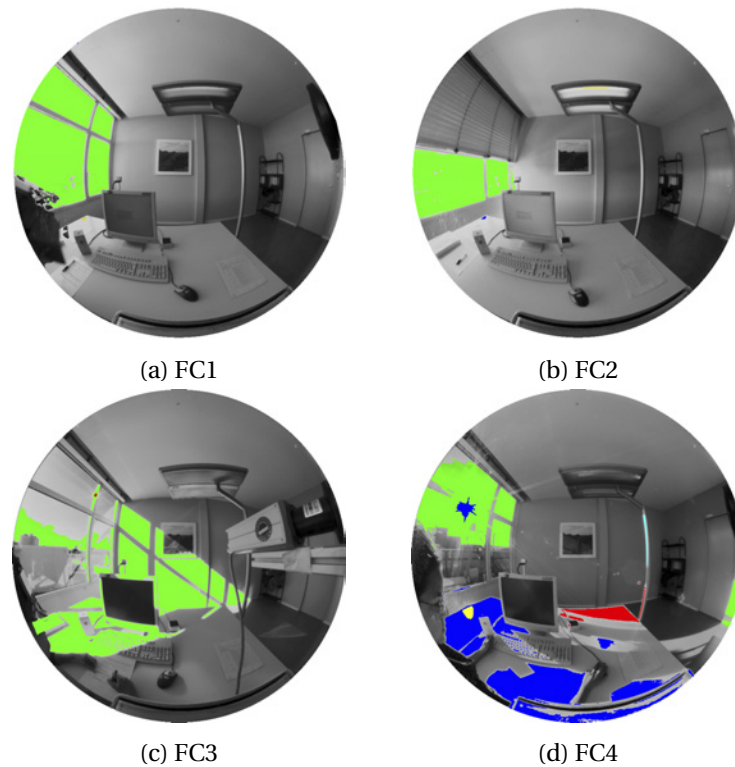


Figure V.4 – **Processed images:** To evaluate each condition one image per task phase was processed, a-b) coloured patches show the identified glare sources.

and high contrast and the bright and extreme contrast. Variance over the horizontal eye-in-head position signal ("horizontal variance") was likely to measure behaviour with more sensitivity than radial variance or vertical variance since the window was always to left. Horizontal variance increased in the tasks that invited participants to explore the surroundings, *Thinking* and *Pause*, as compared to the two tasks where gaze is restricted to the monitor (*Input* and *question*) (cf. Figure: V.6a & V.6b). During the *Thinking* phase of the trials this increase is lower for the bright and extreme contrast façade. This suggests that horizontal variance of eye-in-head orientation is sensitive to the effects of light conditions on comfort. To quantify this, a three-way ANOVA was performed on horizontal variance. The factors used were façade ("2: dark and high contrast", "4: bright and extreme contrast"), task (*Input*, *Thinking*, *Response* or *Pause*) and eye ("left" or "right").

There are main effects of façade ( $F(1, 40) = 34.49, P < .001$ ) and task ( $F(3, 40) = 70.94, P < .001$ ). There is no main effect of eye ( $F(1, 40) = 3.04, P = .088$ ). There is no other two-way or three-way interactions (all  $p > .643$ ). Interaction between façade and task ( $F(12) = 17.99, P < .001$ ). There were no other two- or three-way interactions (all  $P > .643$ ) (Table: V.3). The effect of the façade means that eye-orientation varies depending on which system is used. Glare evaluations were made by *Evalglare*, a *Radiance*-based tool (Figure V.3). Graph V.5 demonstrates the light variations produced by each façade system in terms of illuminance at the vertical camera C2 level [lux] and the average luminance [ $\text{cd}/\text{m}^2$ ]. These

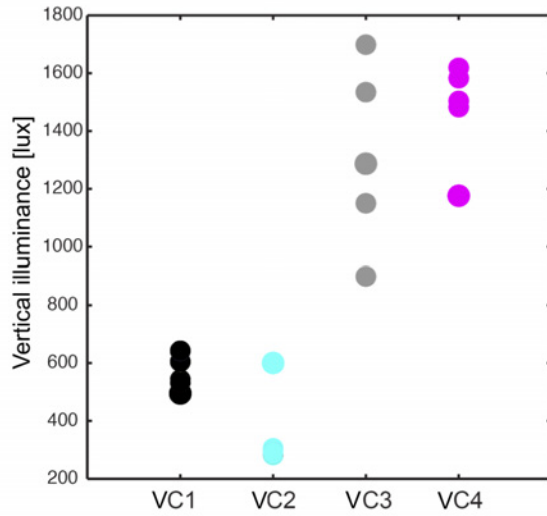


Figure V.5 – **Results:** illuminance at the vertical level [lux] of each participant (at the assumed eye position at camera C2 position) measure per each façade configuration are shown.

photometric light measures of each façade configuration, have created a good diversity of perceived light and have kept a reasonable homogeneity in each façade configuration. Table: V.2 shows the specifications of each façade configuration and its average DGP measure.

The results also indicate that façade effect is different for different tasks. For example, when participants are reading, the variation of eye-orientation is mainly determined by the task, but when they are thinking or making a pause variation of eye-orientation is mainly determined by the façade.

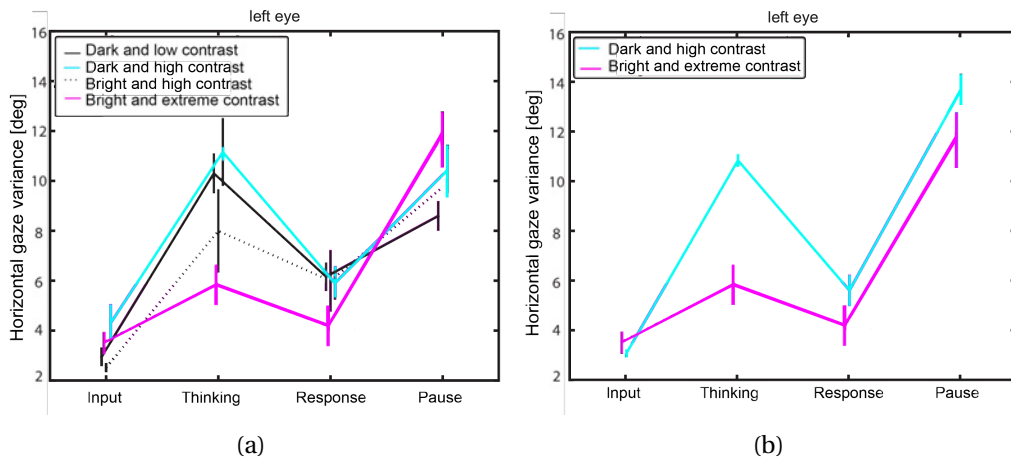


Figure V.6 – **Results:** a) horizontal variance between all four façades b) horizontal variance between two façade configurations: "2: dark and high contrast" "4: bright and extreme contrast".

Table V.3 – Three-way ANOVA results

Source	SS	df	MS	F	<i>P</i>
x1:façad	53.1	1	53.1	34.4	$7.13 \times 10^{-7}$
x2:task	327.8	3	109.2	70.9	$4.56 \times 10^{-16}$
x3:eye	4.7	1	4.6	3.0	0.088
x1.x2	83.2	3	27.7	17.9	$1.5 \times 10^{-7}$
x1.x3	0.22	1	0.2	0.14	0.70
x2.x3	2.6	3	0.86	0.56	0.64
x1.x2.x3	1.09	3	0.36	0.23	0.87
Error	61.6	40	1.5		

Table V.4 – Two-way ANOVA results: left eye

Source	SS	df	MS	F	<i>P</i>
x1:façad	30.129	1	30.129	21.53	0.00015
x2:task	194.010	3	64.670	46.22	$3.52 \times 10^{-9}$
x3:eye	41.397	3	13.799	9.8	0.00033
Error	27.98	20	1.39		

### V.1.3 Conclusions of Experiment I

This study, which served as a pre-experimental planning phase, was the first step in the integration of the eye-tracking method into the experiments by determining what the influential variables on gaze direction distributions are. Four different façade configurations producing four light conditions (ranging from dim and low contrast to bright and high contrast) were created in an office-like test room for this initial study which resulted in four different levels of visual comfort experienced by the participants while they were performing an office task. The results indicated that the effect of different light conditions were different for different office tasks, meaning that while the participants were not focused on a certain task such as reading from a monitor screen, the gaze direction distributions were mainly affected by the light conditions in the room. A new set of experiments was performed with more participants and a refined design for higher statistical relevance. Also, subjective glare ratings were considered in order to have self-evaluations of glare in each situation. The view outside the window, which is a confounding variable for both the lighting condition and the gaze variables, was considered in the new set up.

## V.2 Experiment II

Based on the first pilot study, where a clear effect of the four daylight conditions on gaze distributions [129] was shown, a new series of experiments were set up as a second pilot study to further investigate this effect. These experiments were **first** conducted with a focus on "office task activity" and "view outside the window" (a confounding variable) [104]. This first part had two outcomes:

- **Outcome I:** gaze behaviour with a focus on "office task-activity" in glare-free overcast sky daylight conditions.
- **Outcome II:** gaze behaviour and possible biases towards "view outside the window" for three different task-supports (monitor, paper and phone) in glare-free, overcast sky daylight condition for two slightly shifted view orientations (West vs. South-West).

The **second** focus of this set of experiments was to investigate the effect on gaze directions of being exposed to two very different lighting conditions for the same tasks [130] on gaze directions, which led to:

- **Outcome III:** gaze behaviour with focus on two lighting conditions (no direct sun in the room) and (direct sun in the room).

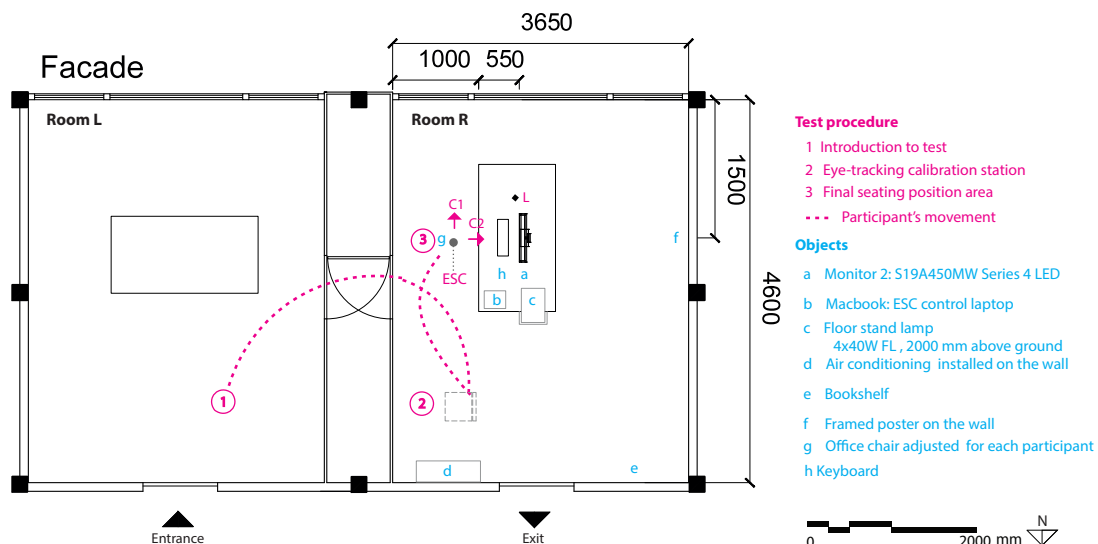


Figure V.7 – **Plan of the daylight laboratory for experiment II:** the layout of the rooms, location of the participant during the test procedure, the position of the measurement devices and all the objects that were in the scene during these experiments.

## V.2.1 Set up

### Layout & Test Procedure

The participants worked on a standardised task activity (Table: V.5) in the office-like daylight laboratory (cf. section III.2.1) while their gaze and the room's photometric data were recorded. The cameras were situated above the participant's head and were adjusted according to each participant's height while seated. The office task activity here refers to a standardised sequence of tasks used to simulate a flow of daily office tasks, and was composed of visual, cognitive and motor components while accounting for task difficulty biases (resulting in lower glare tolerance) (cf. section III.2.3). The tasks ranged from visually demanding phases such as reading on the monitor and typing to contemplation and reflection phases using three different task-supports (monitor, paper and phone). Each trial started with the participant entering from the outside, first through the neighbouring module, and then to the test scene so that each participant would have a similar visual and thermal adaptation processes to indoors light. Before the start of the trial, the eye-tracker was calibrated for each participant (Figure V.7 & V.8).

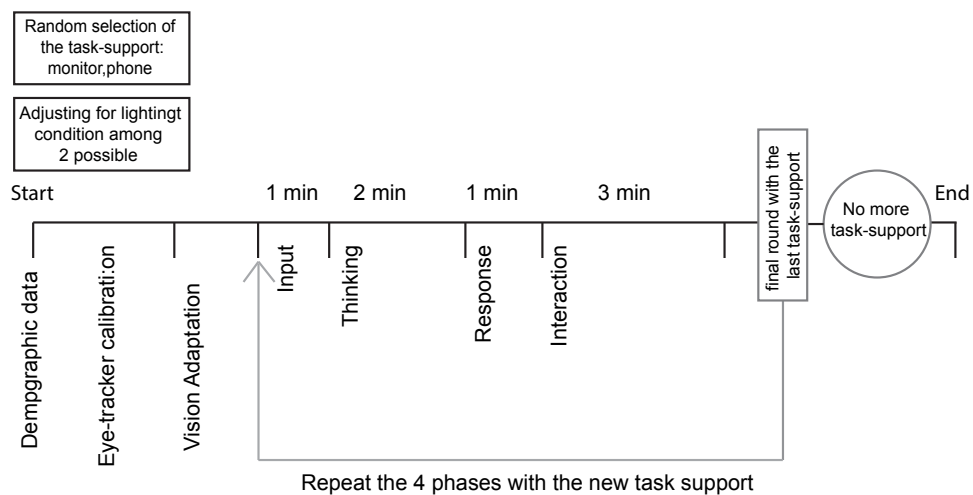


Figure V.8 – **Test procedure:** a schematic representation of the test procedure of the experiment

### Lighting Conditions

In the first part of the study where the main concern was to observe the effect of task activities and the view outside the window, it was necessary to have minimum light variations over the course of the experiment to minimise the effect of light. The luminance contrast of the scene was evaluated based on luminance measurements made every 30 seconds. The luminance values that exceeded 5 times the average luminance of the task area (Figure: V.9 a-c) were determined using *Evalglare* [45]. The average luminance of these peak luminance regions was then divided by the average luminance of the scene to

## Chapter V. Experimental Phase: Pilot Studies

Table V.5 – Office task sequence specifications

Activity	Task description	Task-support	Task interaction	Visually focused	Visually explorative	Cognitive	Motor	Time [sec]
on-screen								
1) <i>Input</i>	reading a text	screen	screen	✓	✗	✗	✗	60
2) <i>Thinking</i>	thinking about the text	screen	screen off	✗	✓	✓	✗	120
3) <i>Response</i>	responding to a question	screen	screen/mouse	✓	✗	✓	✓	120
4) <i>Interaction</i>	typing ones opinion	screen	screen/keyboard	✓	✗	✓	✓	180
on-paper								
1) <i>Input</i>	reading a text	paper	paper	✓	✓	✗	✗	60
2) <i>Thinking</i>	thinking about the text	paper	paper at hand	✗	✗	✓	✗	120
3) <i>Response</i>	responding to a question	paper	paper	✓	✓	✓	✓	60
4) <i>Interaction</i>	writing about one's opinion	paper	paper	✓	✓	✓	✓	180
on-phone								
1) <i>Input</i>	listening to a recorded text	phone	phone	✗	✓	✗	✗	≈60
2) <i>Thinking</i>	thinking about the text	phone	phone	✗	✗	✓	✗	120
3) <i>Response</i>	responding to a question	phone	phone	✗	✓	✓	✓	≈ 40
4) <i>Interaction</i>	talking about one's opinion	phone	phone	✗	✓	✓	✓	≈ 180

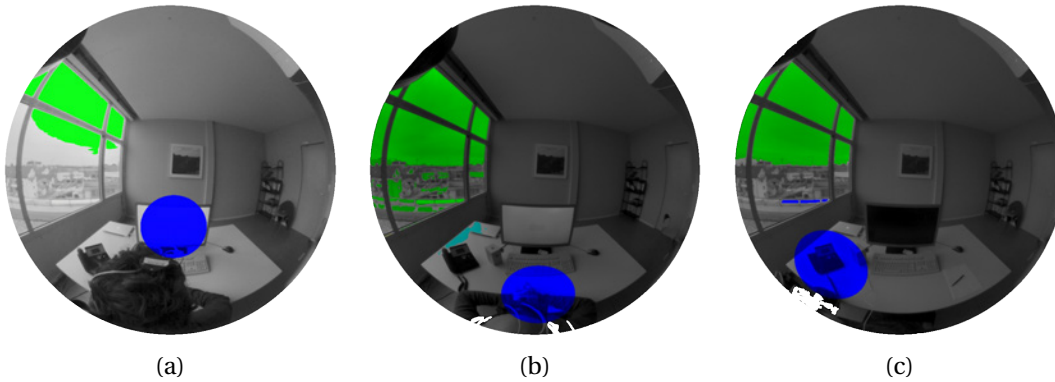


Figure V.9 – **Luminance images processed:** a) on-screen task, b) on-paper task, c) on phone task. The reference task area is marked in blue and the detected glare sources are highlighted.

account for small changes in contrast (equation V.1 & III.2).

$$C_l = \sum_{j=1} \frac{L_{s,j} \cdot \omega_{s,j}}{L_m} \quad (V.1)$$

$C_l$  Luminance contrast with the assumption that gaze is fixed on the task area

$L_{s,j}$  Luminance of detected glare source  $i$  [ $\text{cd}/\text{m}^2$ ]

$\omega_{s,j}$  Solid angle of glare source  $i$  subtended at the eye [sr]

$L_m$  Average luminance of the scene, equation III.2

The results demonstrate that consistency is a requisite for the participant grouping under the clear or overcast sky for lower contrast lighting conditions. The luminance contrast variations over the whole trial for 50% of the participants lie between 0.6 and 0.8 while all are below 1, staying at consistent and low luminance contrast variations. There are certain changes in variation due to events such as the monitor screen turning off during the on-monitor task block (Figure: V.10a) or possible position changes by the participant while writing on the paper during the on-paper task block (Figure: V.10b). In both

cases the decrease in the luminance of the task area results in the detection of lower peak luminance values which consequently lowers calculated luminance contrast. The detection algorithm thus needs to be refined for a fixed luminance value of the task area in order to avoid these inconsistencies.

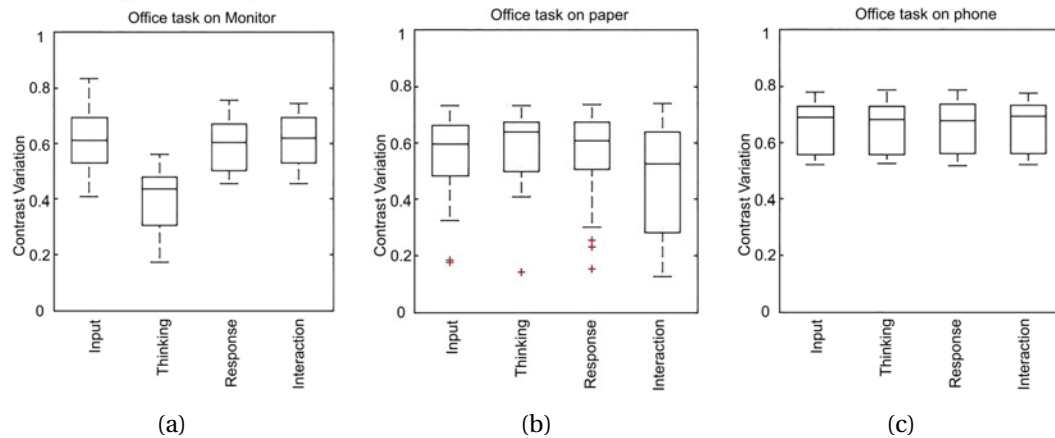


Figure V.10 – **Luminance contrast during different task activities:** box-plot representation of the contrast and its variation. The box represents 50% of the data and the outer borderlines 95% of the data. a) During the on-screen activity's *Thinking* phase, the screen turns off which significantly lowers the general luminance contrast. b) Certain large variations of contrast can be seen due to participants' position changes while working with paper. c) The inconsistencies seen in the previous task activities are not visible in this phase. The screen is off and the participant holds a stable position.

## Participants

23 participants, 17 males and 6 females, between the ages of 20 to 50 were recruited under consent from the Fraunhofer-ISE staff to participate in the experiment. All the participants were German speakers in order to avoid any bias due to a lack of comprehension of the text in the input phase. The participant's head position was then measured in the room and they were asked to keep the correct distance from the monitor screen during the trial. Demographic data were gathered for each person. Among the 23 participants, 8 had corrected eyesight and only 2 considered themselves sensitive to brightness. T

## View Outside the Window

The two views from the window were selected among the range of possible views towards the south. The two selected views extended to a far distance and included a varying mixture of artefacts and natural elements and were both high in diversity. Both views fall into the category that is most appreciated by office workers [46, 61] and there were only minor differences between the two. The two selected view orientations were separated by a 45° angular difference, oriented towards southwest or west, with an overlap of 47% at the participant's eye position (Figure: V.11a & V.11b).



Figure V.11 – **The two view outside the window:** a) southwest orientation b) west orientation.

### Experimental design

The participants were randomly allocated to each lighting condition and were exposed to either southwest orientation or west view orientation. This type of experimental design known as completely randomised factorial design [126] allows for more flexibility in participant recruitment by recruiting more participants for each condition. Here we based the design of the experiment on completely randomised factorial design with two treatments (lighting condition or view and office task activity). Each participant experienced only one lighting condition (and only one view) and an office task activity with three task supports (namely three levels of treatment : screen, paper and phone).

### Dominant Gaze Direction

The dominant gaze directions (fixations) were determined by organising the gaze direction data in 73 bins on the horizontal axis and 37 bins on the vertical with a 5° spread. The angular position of the longest fixations was then considered as the dominant gaze direction of the task phase.

### V.2.2 Outcome I

Gaze behaviour in relation to different office task activities was investigated as a first focus. Figure V.12 (a-d) shows the dominant gaze of each participant coloured in red, black and gray when using different respective screen, paper and phone task-supports. Each data point is a participant's dominant gaze direction. The  $x$ -axis shows the angular horizontal orientation of the gaze directions ( $\phi_g$  [deg]) and the  $y$ -axis shows the vertical orientations ( $\theta_g$  [deg]). As the gaze direction is spatially distributed and two-dimensional, the radial standard deviation from the centre of the distribution is a liable measure to give distinct descriptions of the effect of each of these factors as oppose to standard deviation.



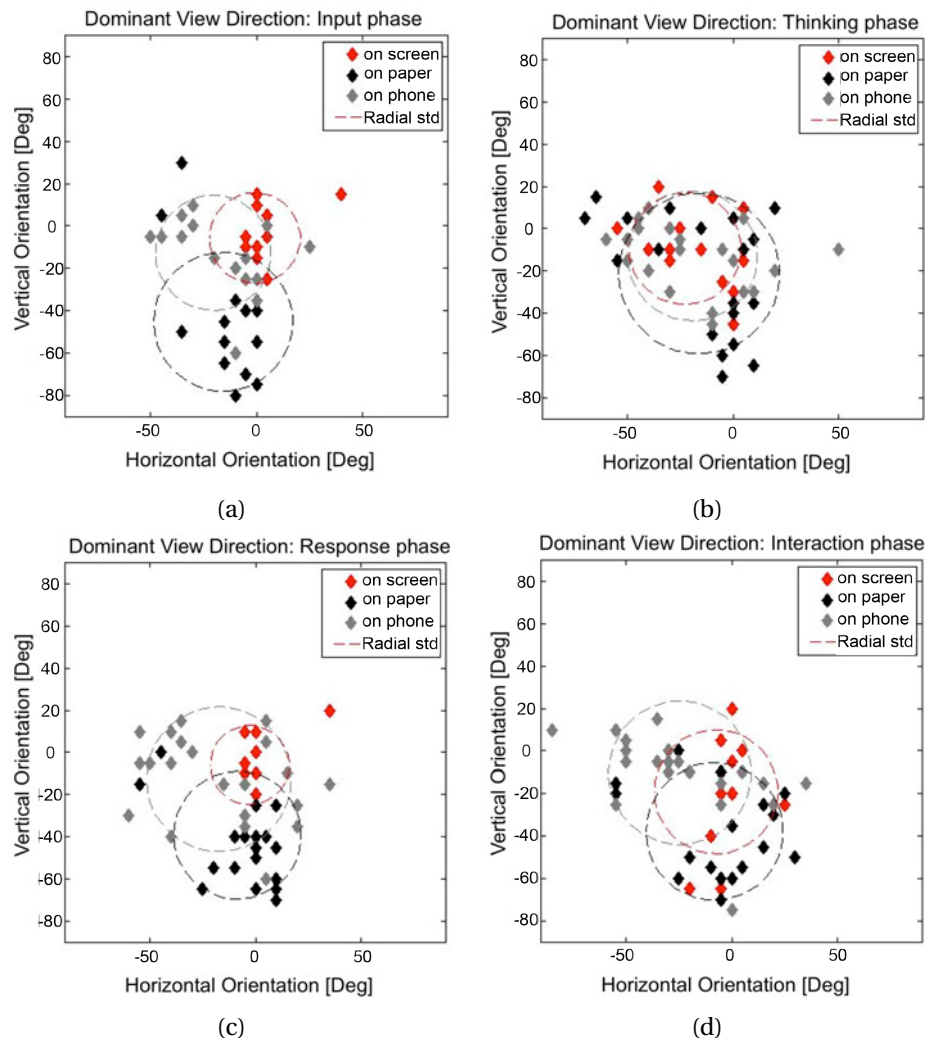


Figure V.12 – **Results overview:** a) *Input* phase b) *Thinking* phase, c) *Response* phase, d) *Interaction* phase

The explorative analysis of the graphs in Figure: V.12a & V.12c shows that if the participants were not focusing on the task, the gaze directions were oriented towards the view outside the window. The comparison between the two distinct phases of input and thinking, respectively the task-focused phase and the visual exploration phase, shows this observation clearly. This behaviour is similar when using the three different task-supports, indicating that the three task-supports had no effect on gaze direction distributions.

To quantify the effects of the independent factors a three way ANOVA was performed on the radial standard deviation of the gaze directions. The factors were view outside the window (south-west & west), task-support (monitor screen, paper work, call on phone), and office task phase (input, exploration, response, interaction). There was an effect of office task ( $F= 14.17, P<0.001$ ) and task support ( $F=7.96, P<0.005$ ). The effect of the two views outside the window was not significant ( $F=4.6, P>0.05$ ), which

means that the participants looked at the two different views in a similar manner.

The small interaction between task-support and task phases indicates a probable difference of gaze direction distributions while having the on-phone task-support. As the ANOVA results suggest, the gaze direction distributions were mainly determined by the office task and the task-support that was used to perform the task. Otherwise, if the participants were not focusing on the task, the gaze directions were oriented towards the view outside the window. Another possible interpretation is that during cognitive parts of the task, while the participant was thinking about the answer or the opinion, they would direct their gaze direction to the view outside the window.

### V.2.3 Outcome II

The dominant gaze direction distributions show little significance for either view. Figure: V.13a & V.13b compare the gaze distributions for the two distinct phases of *Input* and *Thinking* respectively the task-focused phase and the visual exploration phase. As in previous graphs the x-axis shows the angular horizontal orientation of the gaze directions ( $\phi_g$  [deg]) and the y-axis shows the vertical orientations ( $\theta_g$  [deg]). The radial standard deviation is marked by a dashed line. Figure: V.13c illustrated all the dominant gaze directions and the two views are shown with two different colours. As the graph illustrate, the differences between gaze distribution under SW view and W view is not significant.

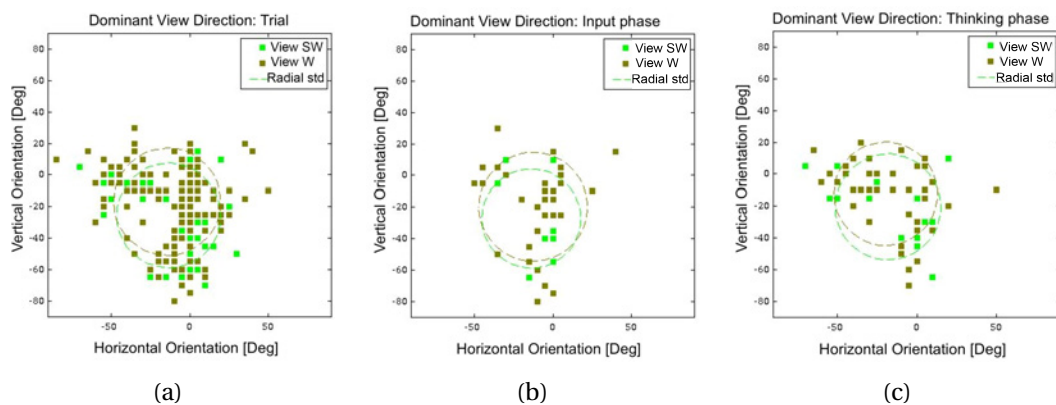


Figure V.13 – **Results overview:** a) dominant gaze distribution for all participants and for the four phases of the trial; view southwest and west are shown with two colours , b, c) the gaze direction distribution behaves independently of view outside the window for different ranges of visual engagement in the office task

### V.2.4 Outcome III

Two different daylight conditions were evaluated and analysed for their effects on the radial distribution of the gaze directions and the dominant gaze directions. The low contrast condition was defined as a situation where there was no direct sunlight coming into the room and the sky condition was either overcast or clear. The high contrast condition was defined as a situation where there was direct sunlight coming into the room and the sky condition was clear. Each measurement set was categorised based on observations made at the time of the experiment. Thereafter, based on the photometric measurement evaluations using *Evalglare*, the data was regrouped into the correct lighting condition group. Figure V.14 shows the two lighting conditions and the illuminance at the vertical level [lux] (at assumed eye level at the camera Camera 2’s position) variations over all the trials for each task activity. The radial standard deviation of the gaze distributions, which is an appropriate measure to demonstrate the general spatial tendencies, was used in the analysis (equation :III.5). To quantify the effects of the independent factors we made an ANOVA test on the radial standard deviation of the gaze directions

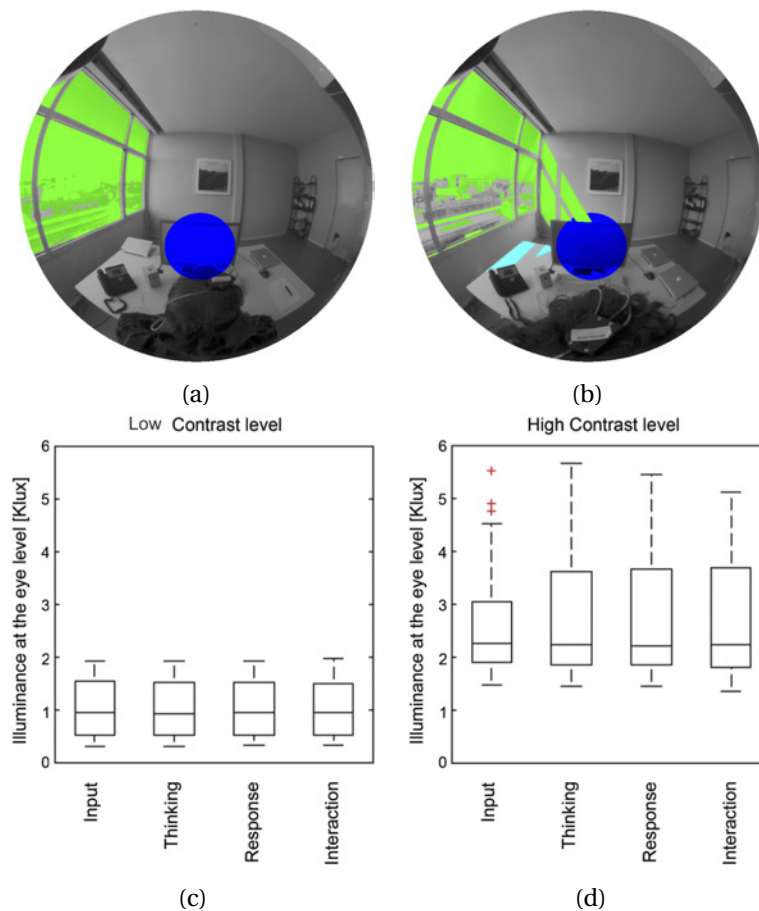


Figure V.14 – **Daylight conditions:** glare evaluations were used for refining the groupings: a) low contrast, b) high contrast; c, d) the box-plot shows illuminance variations reaching the eye at a vertical level.

for each task phase. The factors were the lighting conditions (low contrast, high contrast) and the task supports (monitor screen, paper, phone). During the *Input* phase the effect of lighting condition was small ( $F=0.76$ ,  $P < 0.05$ ), though the task-supports' effect was apparent ( $F=17.16$ ,  $P < 0.00001$ ). There was an effect of lighting condition under the *Thinking* phase ( $F= 4.58$ ,  $P < 0.05$ ). There was neither an effect of lighting conditions nor of the task support during the response phase. The last phase was the interaction phase where we found an effect of task-support ( $F=8.66$ ,  $P < 0.001$ ). By comparing the two distinct *Input* and *Thinking* we see that they were respectively the most and the least visually demanding phases. As shown in the ANOVA results, the gaze directions were mainly determined by the task-support during the *Input* phase under both light conditions (Figure: V.15a). The gaze directions during the *Thinking* phase were more dispersed (Figure: V.15b). The results also show that the focus on the task area was less apparent for the telephone call. Even though the phone was situated to the participant's left, participants tended to direct their gaze towards the inside of the room (right) under the high contrast lighting conditions (Figure: V.16a & V.16b). This result does not apply to the paper task

activity. We speculate that this is due to the presence and availability of the task support at all times.

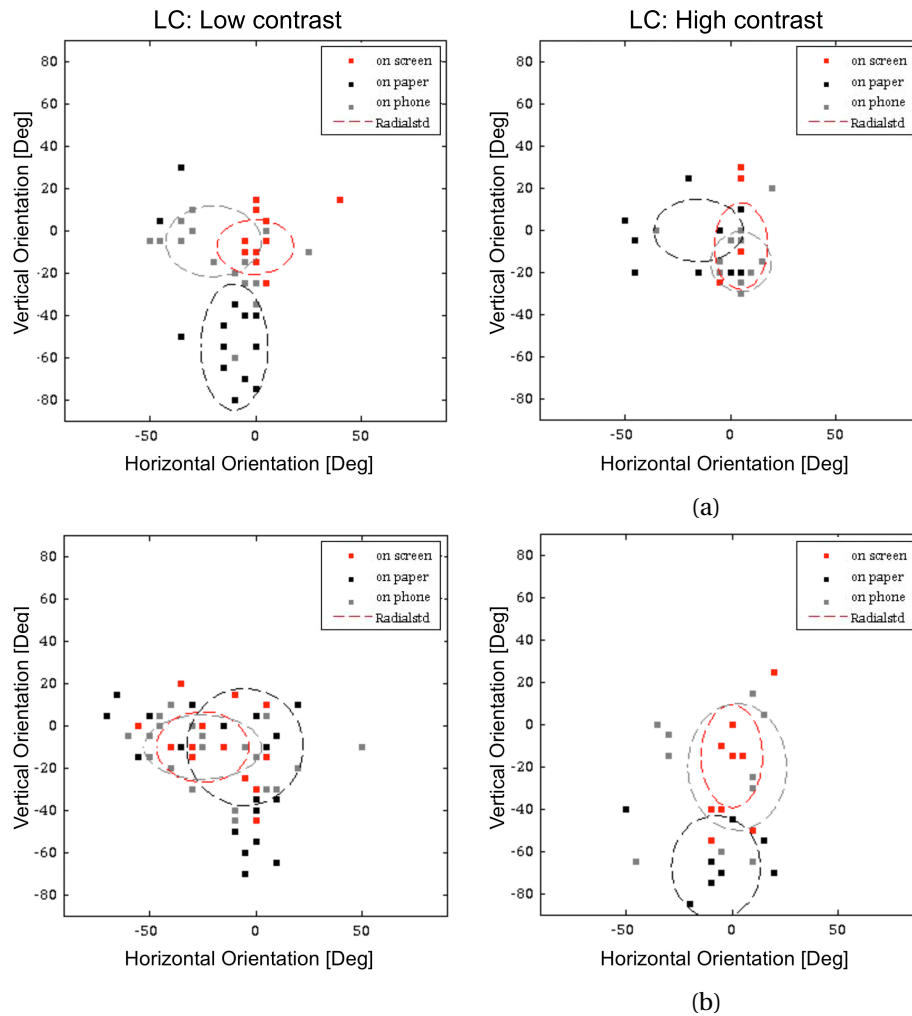


Figure V.15 – **Results overview:** during the a) *Input* phase the gaze directions are more focused on the task area under both light conditions, whereas during the b) *Thinking* phase the gaze direction is more dispersed over the space.

### V.2.5 Conclusions of Experiment II

The two pilot studies were designed to establish a foothold for the use of eye-tracking methods in order to have a better understanding of the gaze direction in the room as a function of luminance variations. The results from the two pilot studies thus allowed us to make a qualified selection of tasks and settings for the initial experiment as well as establish precise control of light conditions. The results also provided a proof of concept about the relation between lighting and gaze direction. The results from these two studies showed that when the participants were not engaged in any visually focused task and the presence of the task support was minimal, the gaze directions were systematically

biased towards the view outside the window under low contrast lighting conditions [104]. On the other hand, the results regarding the two lighting conditions (Figure: V.14) showed that the gaze direction distributions acted differently in different lighting conditions [130]. The tendency to direct the gaze outside the window was less apparent and the gaze directions were more inclined towards the inside of the room under highly contrasted lighting conditions.

### V.3 Summary & Discussion

The results from the two pilot studies provided a basis for an optimised experimental set up which would allow us to record all the relevant and necessary variables to answer the main questions of the study. In summary the most prominent outcomes to consider in the final experiments were:

- Development and design of an experimental strategy
- Thorough study of view and office task
- Development of an refined office task sequence

The developed experimental strategy a standardised office task sequence was considered as described in section III.2.3 to be performed in less than 30 minutes. The task sequence was designed to include main components of an office task including a range from visually focused tasks to free explorations. The two extreme end of the range being an *Input* phase and *Thinking* phase prove to give an understanding of the gaze behaviour in relation to light and view. Therefore, these two phases were considered in the analysis parts. Also several conclusive decisions were made based on the two pilot studies. The task-supports were limited to screen and phone. Paper task-support was eliminated since it did not produce reliable data. This was due to presence of the task-support at all time which minimised the observers control of the experimental sequence. Consequently, the photometric and gaze data were unreliable. Also, the phone was equipped with a head set to eliminate a presence of a phone object in the field of view. The façade configuration which a combination of lighting and view has to be studied to see the effect of the two variables on gaze in separate experiments. Two view were tested so far which had minor differences from each other. The gaze behaviour were almost similar for these two orientation. Therefore, it was decided to rotate the test facilities only towards southwest or west view to avoid any biases caused by view when observing the lighting condition effects on gaze orientations. Additionally, inclusion of a new view type in the final experiments was considered to further investigate the effect of view outside on gaze behaviour. Building upon these findings, an extensive series of experiments were performed with a refined experimental strategy to include gaze, lighting exposure and subjective assessment measures. Six different lighting conditions and two types of views outside of the window were considered in these experiments. These experiments are explained in detail in the following section.

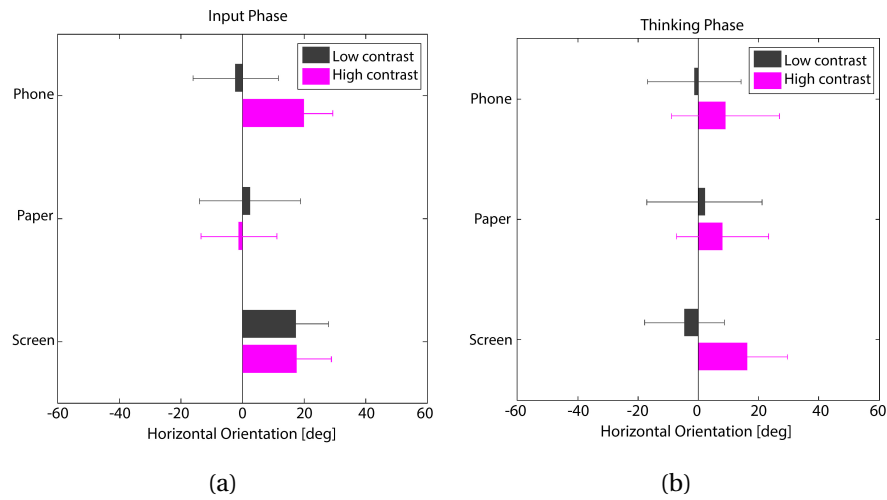


Figure V.16 – **Results overview:** the mean and radial standard deviations of the gaze orientations are compared for the three task-supports under the two lighting conditions during: a) the *Input* phase, b) the *Thinking* phase. The origin is at the border of inside and outside at the corner of the room (Figure: V.17b).

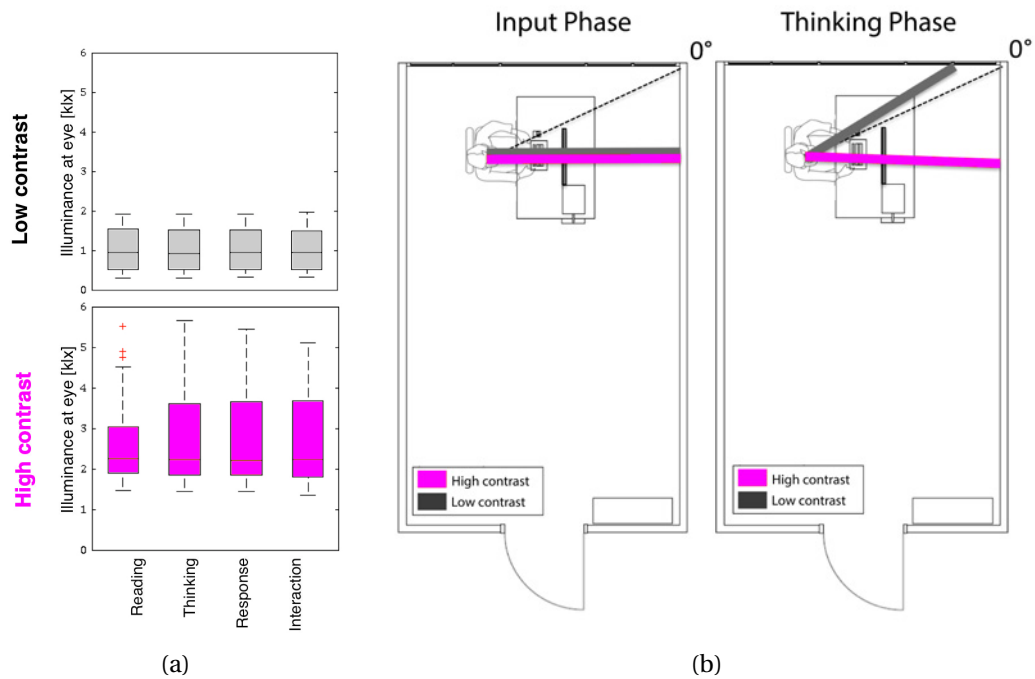


Figure V.17 – **Results overview:** a)  $E_v$  for the two lighting conditions, b) the mean gaze orientation is illustrated: when the participants are not engaged in visually demanding task and the presence of the task-support is minimal, the gaze orients towards the view outside, but this tendency is less in high contrast lighting conditions.





## VI Experimental Phase: Full Study

The development of a gaze-driven discomfort glare assessment method was based on experiments conducted under day lit conditions with a total of 142 participants, of which 28 participated in pilot studies, and 97 participated in the study on dynamics of gaze as a function of light. 17 participants were included in a combined experimental design to evaluate the effect of view outside the window on gaze dynamics.

Building upon the findings and outcome of the two pilot studies, a new and extensive series of experiments were performed. In these experiments we considered five different daylight conditions and one artificial lighting condition to further our understanding of natural gaze behaviour in relation to light (**Experiment III**, section VI.1).

The fourth set of experiments were designed in combination with Experiment III in order to further observe the effect of the view outside the window on view directions (**Experiment IV**, section VI.2). Previously, our investigations on the effect of the view outside the window on two views with minor differences from each other showed no effect on the gaze distributions. In this last set of experiment we investigated the view outside the window for two very different categories.

## VI.1 Experiment III: Investigating Gaze in Relation to Glare

The experiments were performed from July to mid-October in the daylight laboratory specifically designed for these type of studies at the Fraunhofer Institute for Solar Energy Systems (ISE) in Freiburg (southwestern part of Germany) (cf. section III.2.1).

### VI.1.1 Set up

Participants were asked to perform a sequence of standardised office tasks while their subjective responses of the glare situation were assessed using a questionnaire that employed different measurement scales (designed mainly based on multi-criteria glare rating methods) [110].

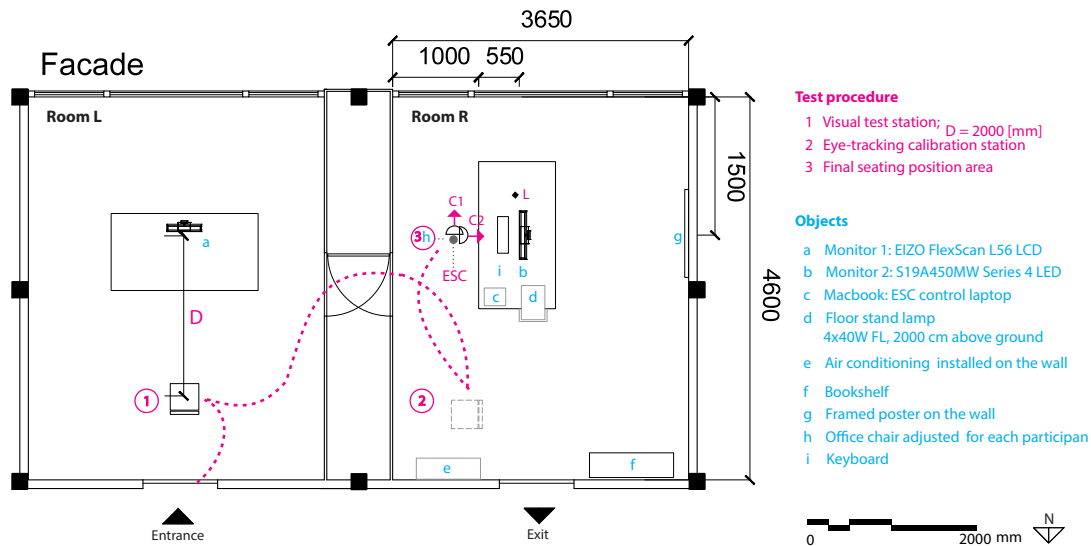


Figure VI.1 – Plan of the daylight laboratory for final experiments: the layout of the rooms, location of the participant during the test procedure, the position of the measurement devices and all the objects that were used in the experiment or were in the scene.

Table VI.1 – Office task sequence specifications

Activity	Task description	Task-support	Task interaction	Visually focused	Visually explorative	Cognitive	Motor	Time [sec]
<b>on-screen</b>								
1) <i>Input</i>	reading a text	screen	screen	✓	✗	✗	✗	60
2) <i>Thinking</i>	thinking about the text	screen	screen off	✗	✓	✓	✗	120
3) <i>Response</i>	responding to a question	screen	screen/mouse	✓	✓	✓	✓	60
4) <i>Interaction</i>	typing one's opinion	screen	screen/keyboard	✓	✓	✓	✓	120
<b>on-phone</b>								
1) <i>Input</i>	listening to a recorded text	headset	✗	✗	✓	✗	✗	60
2) <i>Thinking</i>	thinking about the text	headset	✗	✗	✓	✓	✗	120
3) <i>Response</i>	responding to a question	headset	✗	✗	✓	✓	✓	≈ 40
4) <i>Interaction</i>	talking about one's opinion	headset	✗	✗	✓	✓	✓	≈ 180

### Test Procedure

The test procedure (Figure: VI.2) started with the participants entering from the outside, first through the neighbouring room (Room L), and then to the test scene (Room R) so that they would have similar adaptations to the indoor environment (see Figure:III.2).

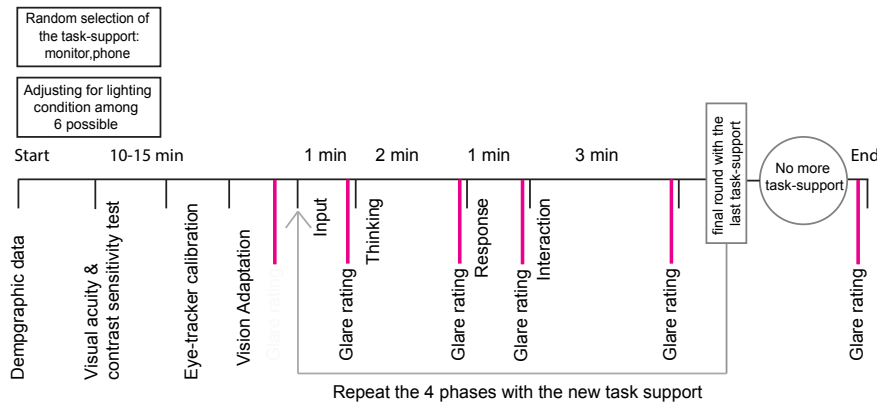


Figure VI.2 – **Test Procedure:** a diagram showing the flow of the test procedure with different data collection and experimental trial phases for each participant

When entering the (Room L), the participant went through several introductory steps (section III.2.4). One of the first steps was a test of visual acuity and contrast sensitivity which was conducted by a computer-based visual test under standard lighting conditions for such a test [132]. The luminance of the visual display (a) used for this test was  $105 \text{ cd/m}^2$  ( $125 \text{ cd/m}^2$  at the centre and  $100 \text{ cd/m}^2$  at the margins). Considering the size of the screen ( $8^\circ$  at the participant's eye level in 2000 mm distance) the luminance of the surroundings were adjusted to comply with the standards (not darker than 1% of the screen average luminance) [132]. After entering the test scene (Room R), the eye-tracker was calibrated to the participant's pupil. A socio-demographic questionnaire (on paper) was filled in as well as the first lighting condition assessment questionnaire before starting the task activities. As explained in section III.2.3, each task activity consisted of four phases. To evaluate the magnitude of glare with subjective judgment, the participants were asked one question after each phase of the task activity and was gathered this data using a Likert glare scale. This glare rating was assessed 4 times during the on-screen task and 4 times during the on-phone task. The glare scale was based on four criteria: 1) imperceptible, 2) perceptible, 3) disturbing, and 4) intolerable [110, 5, 45]. After performing the task activities with each task-support and before the end of the trial, a final lighting condition assessment was done. To make an introspective value judgment on the glare magnitude measurement, we included a scale in terms of both comfort and acceptance [117, 118].

### Glare Ratings

After performing the four-phased task with each task-support, a final lighting condition assessment question was conducted. To evaluate the magnitude of glare we used a Likert glare scale after each phase of the trial, meaning that the glare rating was assessed 4 times during the on-screen task and 4 times during the on-phone task. This scale allowed participants to evaluate the lighting conditions based on four criteria: 1) imperceptible, 2) perceptible, 3) disturbing, and 4) intolerable. Additionally, the glare magnitude was also measured before and after the trial using an itemised continuous scale. The combination of Likert and continuous scales gives us a better understanding of the magnitude of perceived brightness that is being judged as glare. To make an introspective value judgment on the glare magnitude measurement, we included a measurement scale in terms of both comfort and acceptance (Questionnaire cf. Appendix A , section III.2.5).

### VI.1.2 Experimental Design

The experiments were designed based on a randomised factorial design [126], which is shown in Table VI.2, and includes the average number of participants in each condition. The unequal sample size for each condition was an inevitable consequence of weather conditions and not fully under our control. As shown in the experimental design scheme, the between group effects are six lighting conditions and the within group effects are two task-supports (computer screen and phone). The participants were randomly assigned to the lighting conditions. The order of useage of the task-supports was randomised for each participant. This design allowed for more flexibility in participant allocations to the groups.

Table VI.2 – Experimental protocol with achieved sample sizes for all conditions

Within Groups Design:	Task-support 1: Task-support 2:	Computer screen Phone
Between Groups Design: Lighting conditions	LC1: Clear sky, no sun inside	N= 23
	LC2: Clear sky, sun on the wall	N= 16
	LC3: Clear sky, sun on the desk	N= 11
	LC4: Clear sky, sun in the scene	N= 15
	LC5: Overcast sky, diffuse light	N= 15
	LC6: Artificial light	N= 17
		Total number of subjects = 97

### Participants

Participants, 63 males and 34 females, between the ages of 20 to 60 were recruited from the Fraunhofer ISE staff to participate in the experiment. The relevant body at Fraunhofer ISE approved the procedure and each participant volunteered to participate and gave informed consent. All participants were German speakers in order to avoid any bias due to a lack of comprehension of the text in the input

## VI.1. Experiment III: Investigating Gaze in Relation to Glare

phase. Among the 97 participants, more than half had uncorrected-normal vision and the remainder corrected-to-normal vision. On a continuous scale from "not at all sensitive" to "very much sensitive", 65% of the participants considered themselves sensitive to brightness (rating > 1/2 of the scale line). The subjects were randomly allocated to different experimental conditions.

### VI.1.3 Lighting Conditions

Daylight is a dynamic variable. Therefore, to be able to have a range of lighting conditions that were repeatable through the experiments for all participants, a thorough study was done to make a selection that fits this purpose. The possible lighting conditions were determined in advance by making simulations for the foreseen period of the experiments for two orientations (southwest and west). These two orientations were tested so as not to have any bias caused by the content of the view outside the window [130]. We considered a criterion based on three main components of the daylight dynamics in the space that is relevant to visual comfort: glare, visible sun-patch inside the room and sun-patch luminance variations. Based on these evaluations, we were first able to categorise the

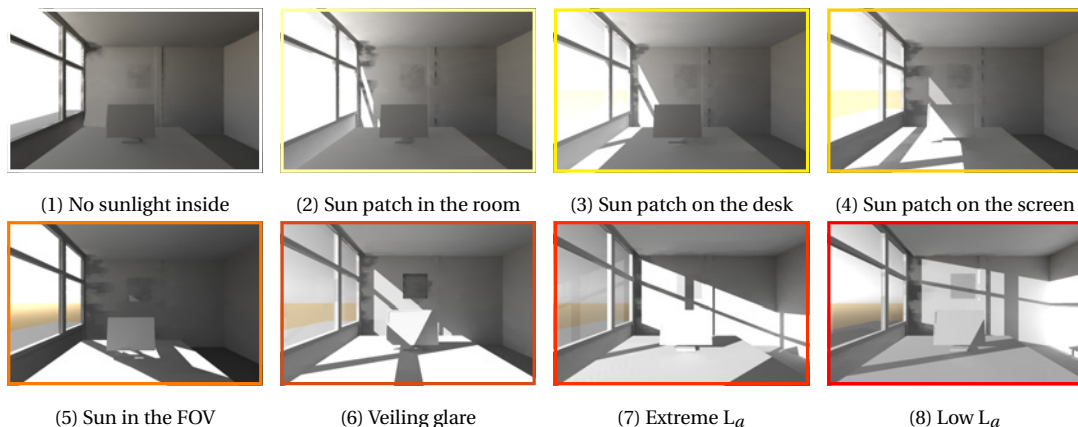


Figure VI.3 – **Simulations for the foreseen experimental:** daylight condition categorisation based on the direct sunlight geometry

potential lighting conditions over the course of the experimental period first into 8 clear sky conditions (Figure: VI.3) and then, after checking for the highest possible probability of reoccurrence during the foreseen experimental period (Figure: VI.4 & VI.5), a selection of five daylight conditions and one electrical lighting condition was made (Figure: VI.7).

The five daylit conditions were achieved by adjusting the position of the daylight test-room between the two orientation at different times of the day under a clear sky. Figure VI.6a & VI.6b show the resulting  $E_v$  and  $L_m$  distributions of each lighting condition over all experiments. Each lighting condition has different lighting characteristics (Table VI.3). These lighting conditions vary in luminance distribution, presence of sun-patches and glare perception based on DGP.

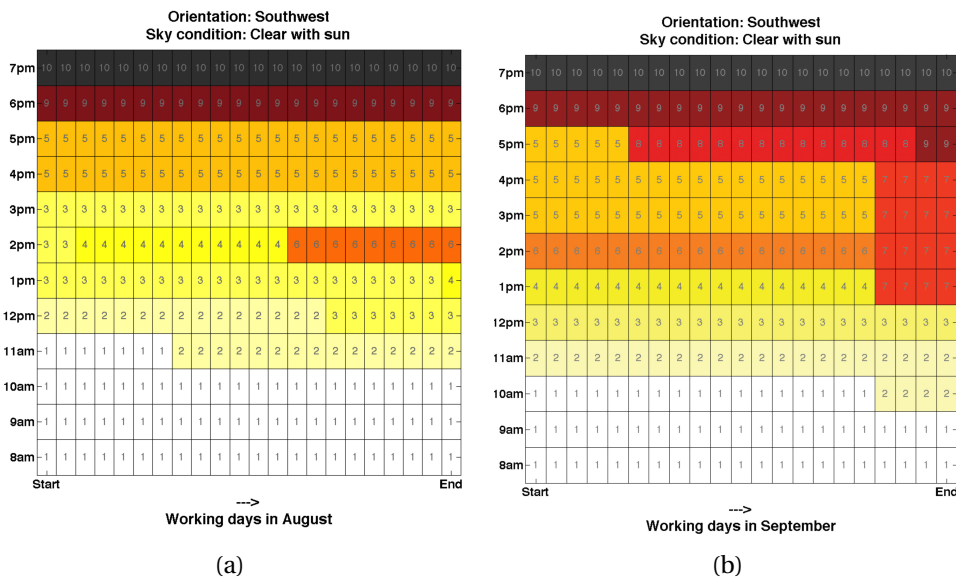


Figure VI.4 – **Daylight conditions:** based on the sun-patch geometry variations for southwest orientation, a) August, b) September; Daylight saving time has not been considered. Numbers 1-8 corresponds to number shown in figure VI.3. Number (9) is the sunset and (10) is after sunset conditions.

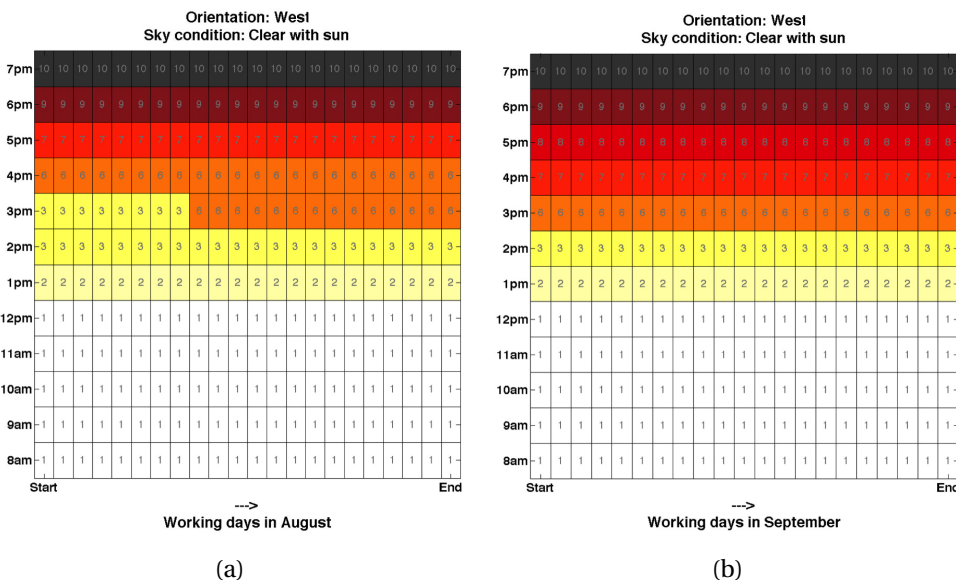
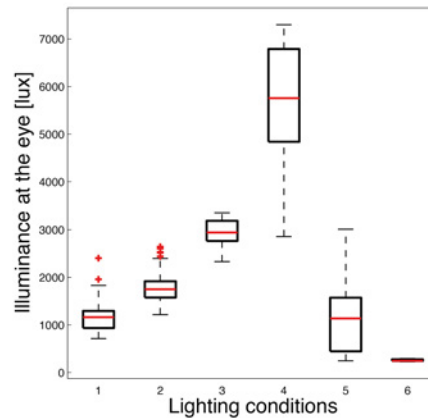
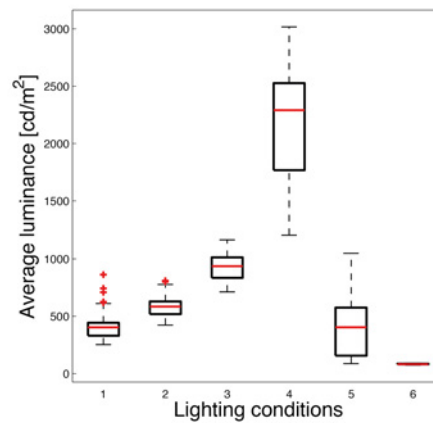


Figure VI.5 – **Daylight conditions:** based on the sun-patch geometry variations for west orientation, a) August, b) September; Daylight saving time has not been considered. Numbers 1-8 corresponds to number shown in figure VI.3. Number (9) is the sunset and (10) is after sunset conditions.

## VI.1. Experiment III: Investigating Gaze in Relation to Glare



(a)



(b)

Figure VI.6 – **Lighting conditions:** the plot shows the distribution of a) the vertical illuminance at the vertical level at the position of camera C2 and b) the distribution of average luminance in the room for each lighting condition.

Table VI.3 – Average measurements of all participants' data.

Lighting condition	$\bar{E}_v$ [lux]	$\bar{L}_m$ [cd/m <sup>2</sup> ]	$\bar{L}_s$ [cd/m <sup>2</sup> ]	$\bar{\omega}_s$ [sr]	$\bar{\#} L_s$	sky
LC1: Clear sky, no sun inside	1200	300	4538	0.43	1.5	clear
LC2: Clear sky, sun on the wall	1800	600	2903	0.35	2.5	clear
LC3: Clear sky, sun on the desk	3000	1000	3919	0.33	4	clear
LC4: Clear sky, sun in the scene	5800	2500	45039	0.07	9	clear
LC5: Overcast sky, diffuse light	1000	400	2191	0.27	2	overcast
LC6: Artificial light	300	100	1064	0.08	1	-

$\bar{E}_v$  [lux]: Average illuminance at the vertical level  
 $\bar{L}_m$  [cd/m<sup>2</sup>]: Average average luminance  
 $\bar{L}_s$  [cd/m<sup>2</sup>]: Average luminance of the glare sources  
 $\bar{\omega}_s$  [sr]: Average glare source size  
 $\bar{\#} L_s$ : Average number of glare sources

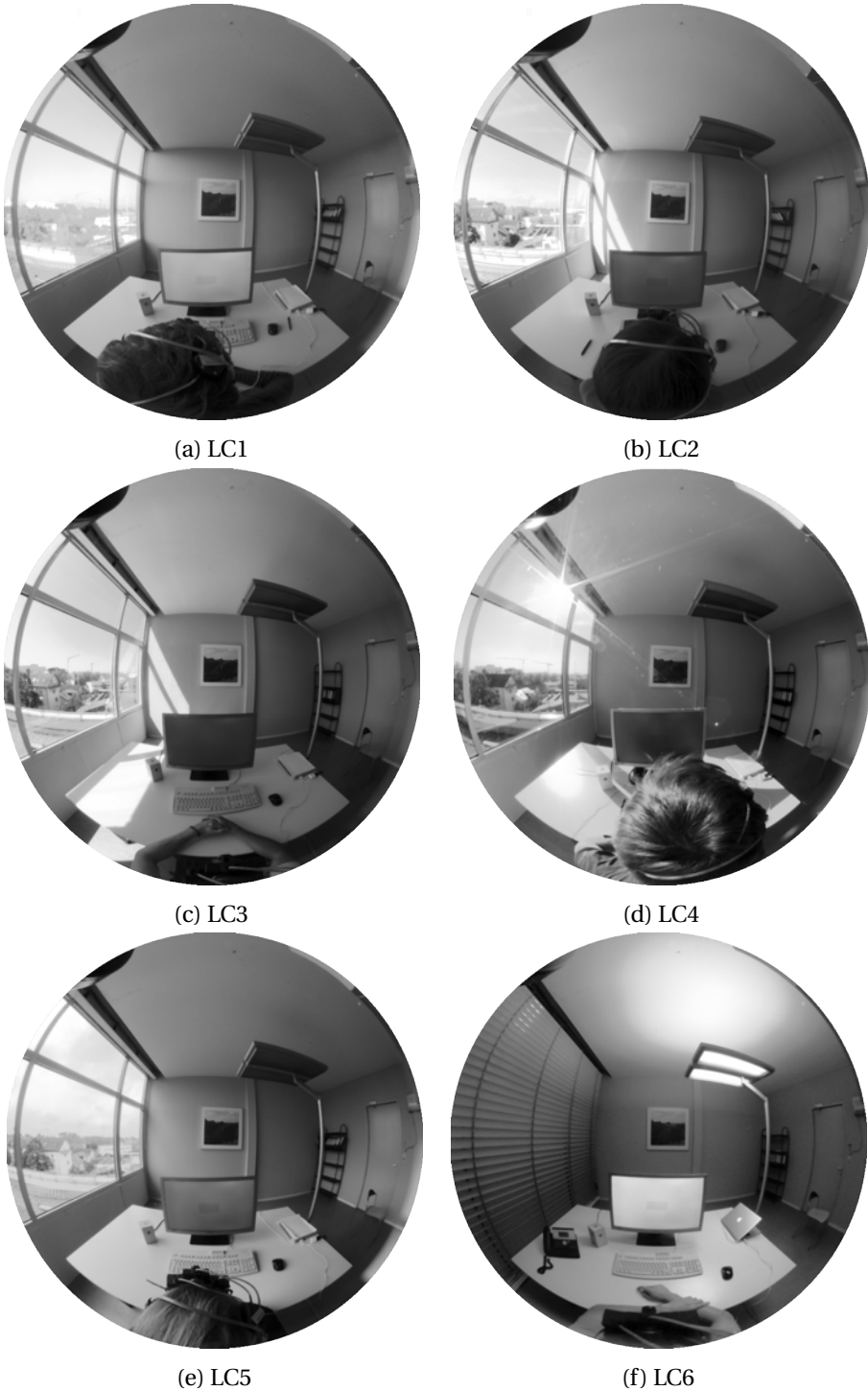


Figure VI.7 – **Six lighting conditions were considered in these experiments:** a) LC1: Clear sky with no direct sunlight, b) LC2: clear sky with direct sunlight on the wall opposite to the participant, c) LC3: clear sky with direct sunlight on desk, d) LC4: clear sky with sun in the scene, e) LC5: overcast sky, f) LC6: artificial light.



VI.1.4 Results: Gaze Behaviour in Different Lighting Conditions

To determine the influence of the lighting conditions on the gaze dynamics, the data was grouped according to the categorised lighting conditions (LC1-6) as a first step, and analysed statistically. The six lighting conditions are described in section VI.1.3. Additionally, averaged glare source luminance for the eight experimental phases are shown in table VI.4. Figure VI.8a, demonstrates glare source luminance and size in each lighting condition. The lighting conditions have different glare sources. LC4 is a lighting condition with sun in the scene, has the highest glare source brightness with a smaller size. The layout of the test-room is shown in figure VI.8b. The gaze origin axis, "the screen centre axis", directs straight ahead from the cameras' position towards the screen (Chapter IV describes how the gaze directions from participants' gaze position are translated into the camera coordinates and position). The cameras' positions are above the participants' head with a distance difference on the z-axis. In the plan the screen-centre axis and the axis dividing inside and outside, "outside axis", are shown. The outside axis is rotating 30° to the left from the head/camera position at 0°.

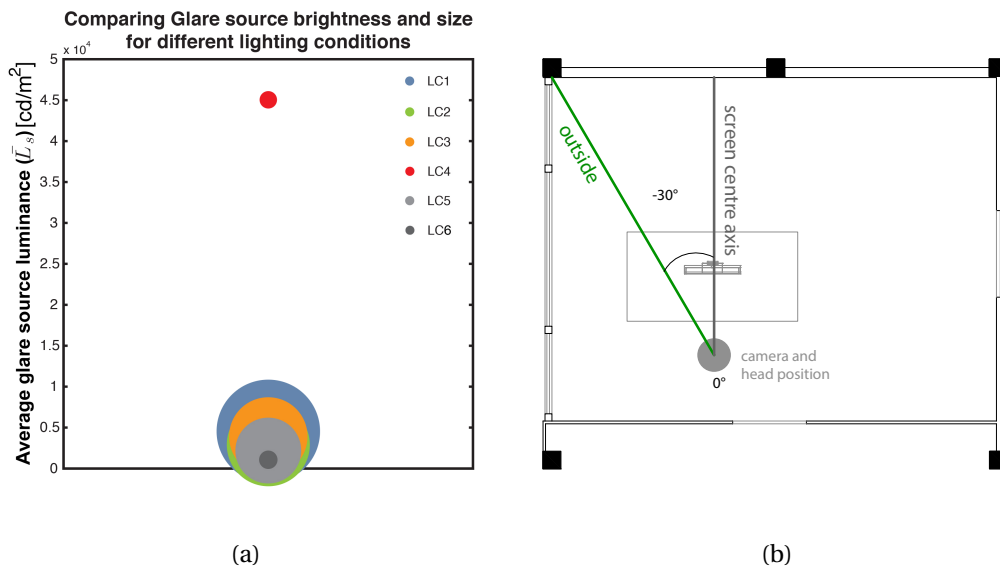


Figure VI.8 – a) the graph compares the average glare source size and brightness under different lighting conditions. The diameter of each circle is proportional to the average solid angle of the glare sources. b) the screen-centre axis and the outside axis are marked on the plan of the test-room.

Table VI.4 –  $\bar{L}_s$ : Average luminance value of glare sources found in each phase [cd/m<sup>2</sup>]

Lighting	Task-support 1				Task-support 2				Averaged
	Phase 1	Phase 2	Phase 3	Phase 4	Phase 1	Phase 2	Phase 3	Phase 4	
LC1	2209	1985	7520	2195	2930	8615	7750	3104	4538
LC2	2178	2104	2137.2	2109.5	3725	3629	3672	3672	2903
LC3	2162	2738	2366.3	2239.2	5400	5390	5501	5558	3919
LC4	32575	40843	28708	29092	56849	55810	57593	58847	45039
LC5	1901	1919	1757	1742.5	2517.5	2644	2626	2425	2191
LC6	1453	769	1456	1457	864	844	840	835	1064

## Chapter VI. Experimental Phase: Full Study

Figure VI.9(a-d) & VI.10(a-d) show the dominant gaze point of each participant during different phases of the tasks. The gaze orientations are noted with a horizontal rotation between  $-180^\circ$  and  $180^\circ$  around the room's vertical axis and vertical rotation between  $-90^\circ$  and  $90^\circ$  (see Figure ). The colours correspond to the six lighting conditions. The size of each data point corresponds to the size of the spatial frequency at that fixation point and thus the duration of gaze fixation. The screen-centre axis at  $0^\circ$  and the outside-axis at  $-30^\circ$  are marked in each graph. A downwards shift (negative vertical orientation) most noticeable in Figure VI.9a, is due to projection of the data from the camera position above the participants' head position.

Exploring this data it can be seen that horizontal and vertical gaze orientation as well as gaze distribution differs for different lighting conditions. The effect of task phases is different for on-screen task support but this effect is not seen for on-phone phases which have been done with a head-set and thus, no physical task-support object was in the scene. An overriding effect of task-support and task phases on gaze behaviour is another prominent observations. The gaze has focused on the screen Figure VI.9a & c or keyboard figure VI.9d despite the different lighting conditions.

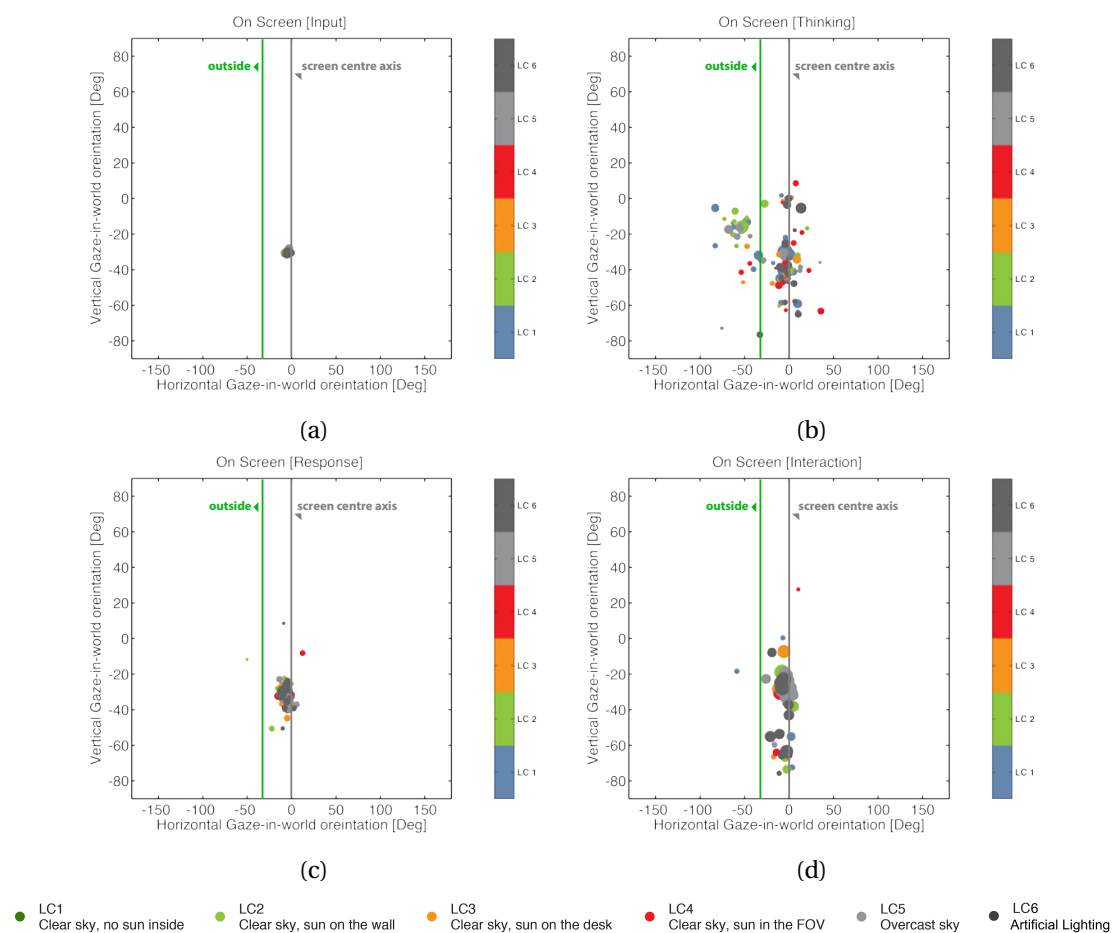


Figure VI.9 – Gaze dynamics & lighting conditions: grouped data for the 6 lighting conditions during phase a-d) while working with monitor

## VI.1. Experiment III: Investigating Gaze in Relation to Glare

In task phases that are independent from the task-support the gaze points that have clustered on the left side of the outside-axis compromises of 33% of the data points. From this cluster of data points 76% of the data points are in LC1 and LC2 categories. In other words, we can see that the gaze is more deviated towards the outside when the luminance adaptation level is lower in the FOV. When there are larger luminance variations in the field of view, such as in lighting conditions 3 and 4, the data points cluster more around the screen-centre axis. The overcast sky lighting condition LC5, and the electrical lighting lighting condition LC6, have the minimum effect on gaze orientations with the data points clustering mostly at the screen-centre axis.

The 3D representation of the data (Figure VI.11 a-h) show where the dominant gaze directions intersect with the geometry of the 3D space. The gaze fixation durations for each lighting condition can be seen best in these images. The fixation durations are mainly affected by the task-support. The gaze duration variations here are independent from the content of the view outside as the participants are exposed to similar view types.

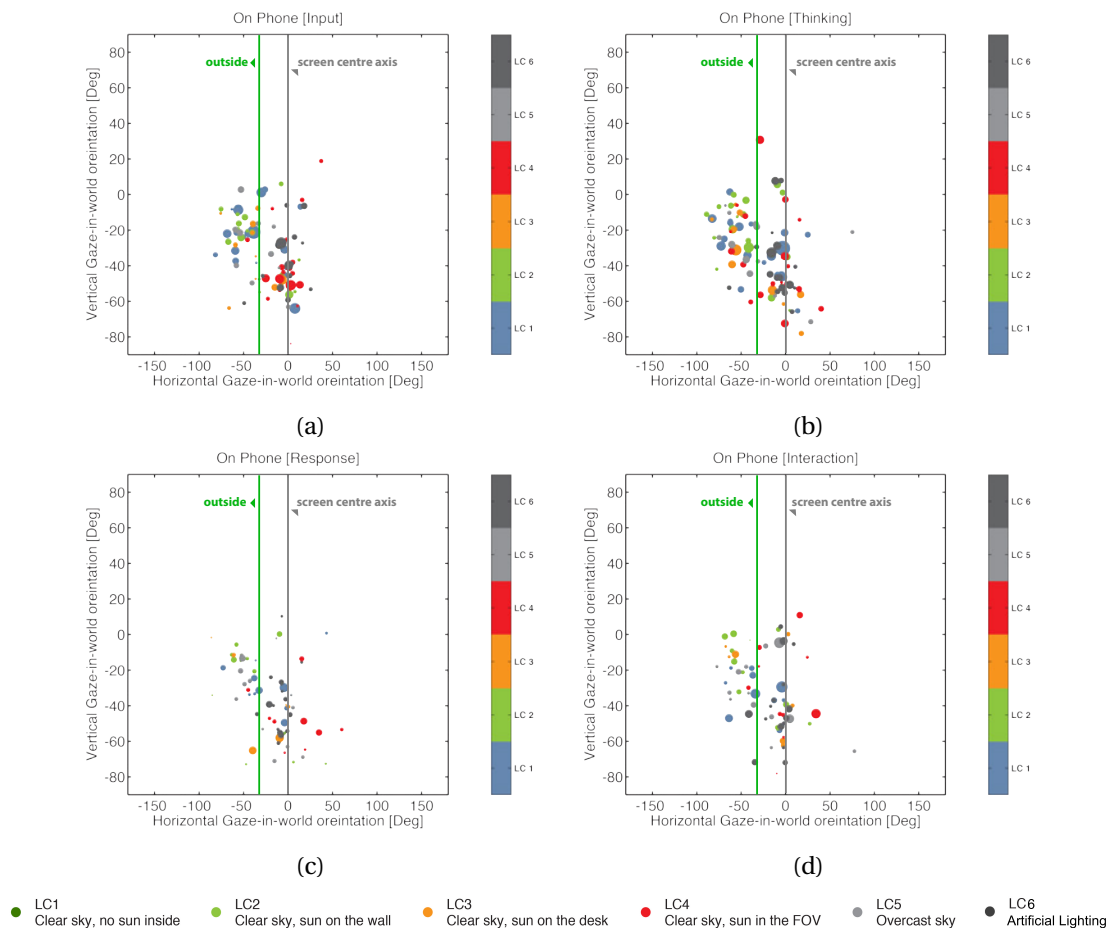
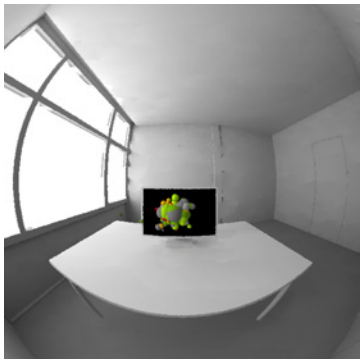
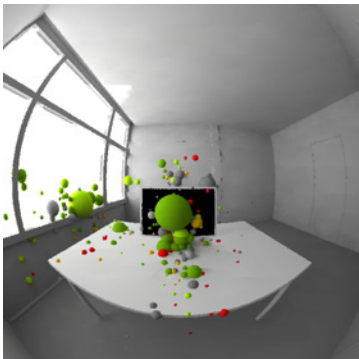


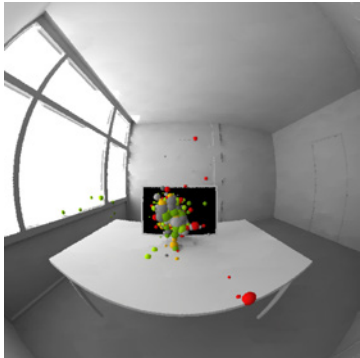
Figure VI.10 – Gaze dynamics & lighting conditions: grouped data for the 6 lighting conditions during phase a-d) while working with phone.



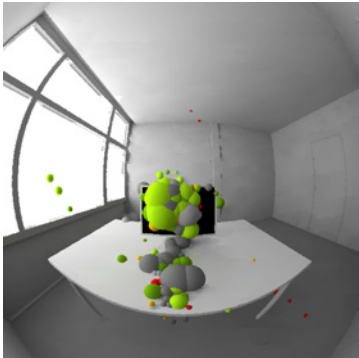
(a) On screen: *Input*



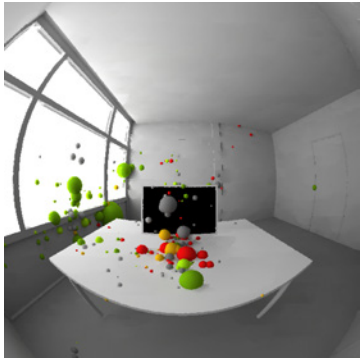
(b) On screen: *Thinking*



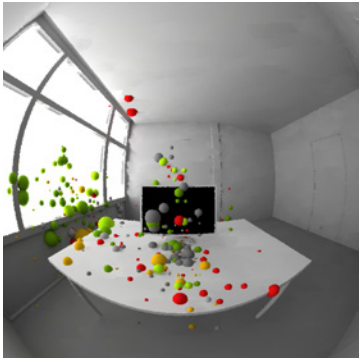
(c) On screen: *Response*



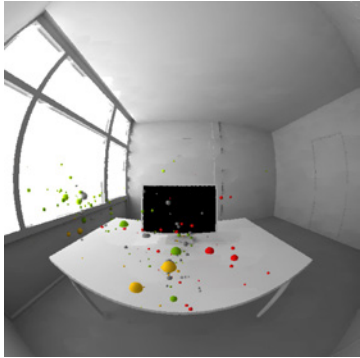
(d) On screen: *Interaction*



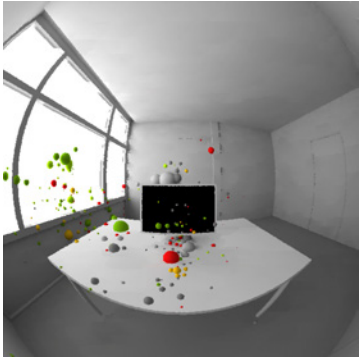
(e) On phone: *Input*



(f) On phone: *Thinking*



(g) On phone: *Response*



(h) On phone: *Interaction*

- LC1  
Clear sky, no sun inside
- LC2  
Clear sky, sun on the wall
- LC3  
Clear sky, sun on the desk
- LC4  
Clear sky, sun in the FOV
- LC5  
Overcast sky
- LC6  
Artificial Lighting

Figure VI.11 – **3D visualisation**: the colour correspond to the 6 lighting conditions and the size of the spheres correspond to the duration of the fixation on the same point.

**Adaptation Luminance Level & Gaze orientation**

The graph VI.12 shows horizontal gaze orientation on the  $x$ -axis and the vertical orientation on the  $y$ -axis. The  $z$ -axis is showing the illuminance at the eye level  $E_{vg}$  (equation III.2) which represents the adaptation level at the eye.  $E_{vg}$  is derived based on equation III.1 from the gaze-centred luminance images, thus representing the adaptation level at the eye with respect to the participants actual gaze direction. Each participant's gaze position during the two free exploration task phases (on screen and on phone *Thinking*) are shown with two data points.

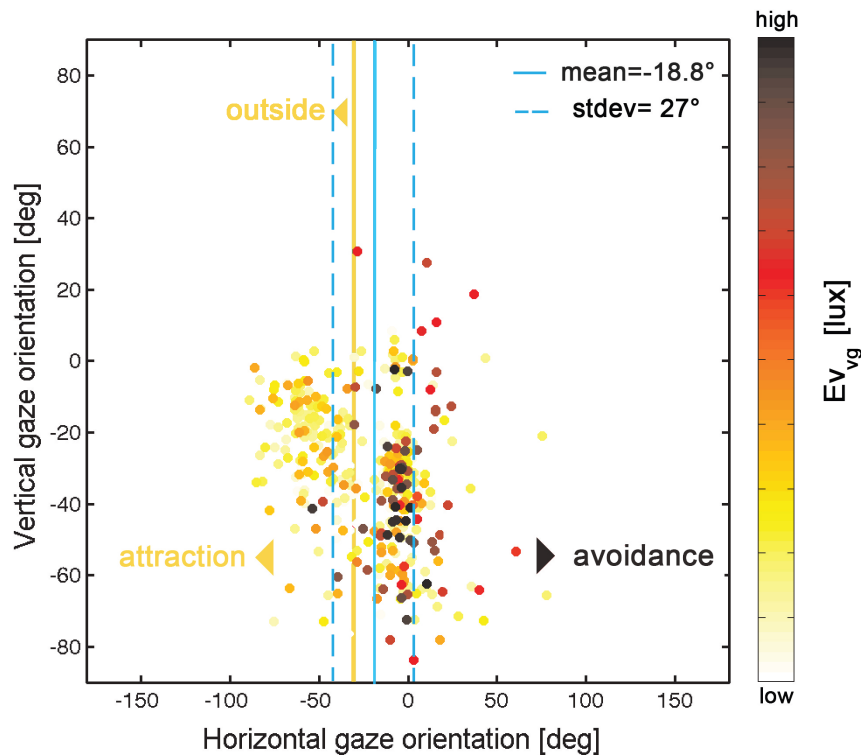


Figure VI.12 – **Gaze dynamics &  $E_v$** : Gaze orientation is shown in relation to  $E_v$  variation.

Previous results where the Gaze-driven approach and Fixed gaze-approach were compared (c.f. section VII.2), a prominent finding was that gaze is attracted to higher luminance values when the luminance adaptation levels are low. An intuitive assumption was that the higher luminance values are at the window side. Here we can see that the gaze is oriented towards the left in 82% of the cases and with 36% of the cases with full rotation towards the window and beyond the outside-axis. The gaze orientations on horizontal axis deviate to left with the mean value of  $-19^\circ$ . The initial assumption of "gaze attraction" to higher luminance values in exchange for view (window) is thus confirmed.

A "gaze avoidance" behaviour is, however, noticeable as adaptation luminance levels increases. As the illuminance levels at the eye  $E_{vg}$  increases the gaze directions orient inside the room as and stay

## Chapter VI. Experimental Phase: Full Study

around the screen-centre axis which are the indications of an avoidance behaviour. To quantify the effects of lighting conditions on gaze we performed a three-way ANOVA on three gaze responses as the dependent variables. The three gaze responses are horizontal gaze orientation, vertical gaze orientation and the gaze distribution. The gaze distribution is measured with radial standard deviation of the gaze points from the dominant gaze for each participant. The independent variables are daylight conditions (LC1-5), task-support (screen, phone) and task phases (*Input, Thinking, Response, Interaction*). To assess the practical significance of the results, the effect size was measured.

### Effect of Lighting Conditions on Horizontal Gaze Variance

Lighting conditions ( $F(4, 492)=2.9, P<0.05$ ) and task-phases ( $F(3, 492)=6.66, P<0.001$ ) have significant effects on horizontal gaze variance. There is no effect of task-support on the horizontal gaze variance and no interactions (all  $p>0.23$ ) (Table : VI.5). To assess the practical significance of the results we measured the effect size. The measure of effect magnitude is  $f=0.57$  for the lighting conditions and  $f=1.69$  for the task-phase both of which are classified as large ( $> 0.4$ ).

Table VI.5 – 3-way ANOVA on unequal sample sizes on horizontal variance

Source	SS	df	MS	F	p
x1:Daylit condition	30082.3	4	7520.6	2.9	0.0215
x2:Task-support	244	1	244	0.09	0.759
x3:Task phase	51730.9	3	17243.6	6.66	0.0002
x1.x2	5094.5	4	1273.6	0.49	0.7418
x1.x3	61650.1	12	5137.5	1.98	0.239
x2.x3	8215.3	3	2738.4	1.06	0.36
Error	1274309.6	492	2590.1		
Total	1421154.3	519			

Table VI.6 – 3-way ANOVA on unequal sample sizes on vertical variance

Source	SS	df	MS	F	p
x1:Daylit condition	2747	4	686.8	1.62	0.167
x2:Task-support	20.6	1	20.59	0.05	0.82
x3:Task phase	5923.6	3	1974.55	4.67	0.0032
x1.x2	445.4	4	111.34	0.26	0.9105
x1.x3	22403.5	12	1866.96	4.41	0
x2.x3	478.6	3	159.53	0.38	0.76
Error	208143.3	492	423.06		
Total	239621.1	519			

### Effect of Lighting Conditions on Vertical Gaze Variance

The vertical variance significantly differs ( $F(3, 492)=2.9, P<0.01$ ) for different task phases. More importantly, this difference is significantly different for different lighting conditions since there is an interaction between lighting condition and the vertical gaze variance ( $F(12, 492)=4.41, P<0.0001$ ) (Table

## VI.1. Experiment III: Investigating Gaze in Relation to Glare

: VI.6). The differences among means,  $f$ , is classified as large for both effects ( $f_1=1.1$  &  $f_2 =1.02$ , ( $> 0.4$ )). There is no significant effect of lighting conditions on the vertical gaze orientations ( $F(4, 492)=1.62$ ,  $P>0.05$ ).

### Effect of Lighting Conditions on Gaze Radial Standard Deviation

Lighting conditions ( $F(4, 492)=2.53$ ,  $P<0.05$ ) and task-support ( $F(1, 492)=6.07$ ,  $P<0.05$ ) have effect on the gaze distribution. There is also a weak interaction of lighting condition and task phase ( $F(1, 285.43)=1.56$ ,  $P<0.1$ ). In all other cases there is no significant effect (all  $p>0.09$ ) (Table : VI.7).

Table VI.7 – 3-way ANOVA on unequal sample sizes on radial standard deviation

Source	SS	df	MS	F	p
1:Daylit condition	1851.4	4	462.85	2.53	0.0395
x2:Task-support	1107.7	1	1107.74	6.07	0.0141
x3:Task phase	230	3	76.66	0.42	0.7389
x1.x2	469.3	4	117.33	0.64	0.6325
x1.x3	3425.2	12	285.43	1.56	0.0989
x2.x3	94.5	3	31.51	0.14	0.9149
Error	89856.7	492	182.64		
Total	96928.3	519			

## VI.2 Experiment IV: View Outside the Window

Daylight and view are two main components of an opening to the outside environment. Previous studies have shown that the view outside the window can bias the subjective assessments of discomfort glare. These studies indicate that there is a higher tolerance for discomfort caused by glare if the view outside of the window is more agreeable [46]. But the question is does view also have an effect on gaze behaviour?

Previously, our investigations on the effect of the view outside the window on gaze direction patterns for two similar view types (Figure: VI.13), showed no significant effect of the views on gaze behaviour. The two tested views differed minimally from each other. They both extended to a far distance with a mixture of artefacts, built environment and natural elements (mainly trees). To further investigate the dependencies of gaze behaviour and the view outside the window, we considered an additional two view-types in a new series of experiments.



Figure VI.13 – View Type 1: a mixture of nature and built environment on two orientations under overcast sky conditions.



Figure VI.14 – View Type 2 : a combination of containers and build environment in close distance under overcast sky conditions.



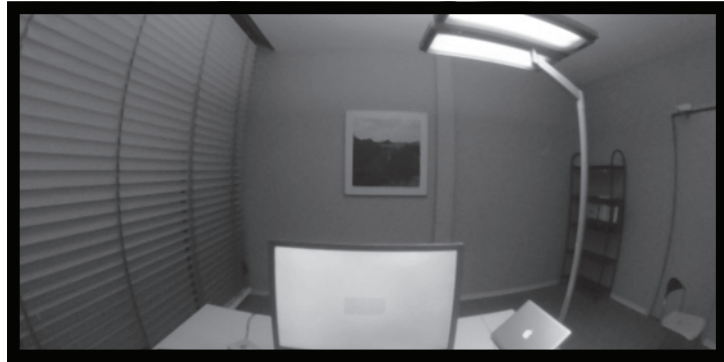


Figure VI.15 – View Type 3 : the window was blocked by a black cover and the venetian blinds were closed blocking light and view from the outside.

The previously tested South-West & West orientations were grouped into View Type 1 (Figure: VI.13).

This view type had the following qualities:

- Presence of objects in far distance,
- Complex view with a mixture of nature and artefacts,
- Trees as the main vegetation,
- Mixture of modern and vernacular architecture,
- High information content,
- A visible sky.

The second view type (Figure:VI.14) was oriented towards South-East. Some of the specifications of latter view type were:

- Presence of objects in close distance,
- Having low degree of complexity,
- Including objects that were poorly maintained,
- Grey and modern looking properties and dullness,
- Low information content,
- A visible sky.

The mentioned qualities for the two views can categorise them into "most appreciated" and "least appreciated" view types according to previous studies on view and human preference [61]. The two views (Figure: VI.13 & VI.14) were investigated under stable daylight conditions with overcast sky. The third view type was a "No view" condition under electrical lighting (Figure: VI.15). This view type had no visible view to the outside. The window was covered with a black cover to prevent the penetration of light and the venetian blinds were down. Nevertheless, it was obvious that there is a window on the left side of the room with probably a view to the outside.

### VI.2.1 Experimental Design

The experiments were designed based on a completely randomised factorial design [126]. Each participant was exposed to one of the three view-types. The between group effects are three view types (Figure: VI.16a) and the within group effects are two task-supports (computer screen and phone) (Table:VI.8). The layout and test procedure of this experiment is the same as the previous experiment described in section VI.1.

Table VI.8 – Experimental protocol with achieved sample sizes for all conditions

Within Groups Design:	Task-support 1: Computer screen Task-support 2: Phone	
Between Groups Design:	View type 1	N=15
View types	View type 2	N=16
	No view	N=17

**Participants.** The number of participants are shown in table VI.8. Three groups of participants (among them 10 female and 38 male) were recruited. The participants were randomly allocated to the three experimental conditions. Each participant performed an eight-phased office task with two task supports. The participation of the volunteers was approved and each participant gave an informed consent for attending the experiments.

### VI.2.2 Lighting Condition

The experiments were done under overcast lighting conditions for view-type1 and 2. The  $\bar{E}_v$  was 1000 lux for these conditions. The average glare source brightness was at 2191 cd/m<sup>2</sup> in size range of 0.27 sr. The view-type 3 condition was under electrical lighting. The  $\bar{E}_v$  was on average 300 lux and the average luminance at 100 cd/m<sup>2</sup>. The average glare source brightness was 1064 cd/m<sup>2</sup>. The glare source which was limited to the electrical light source was of 0.08 sr.

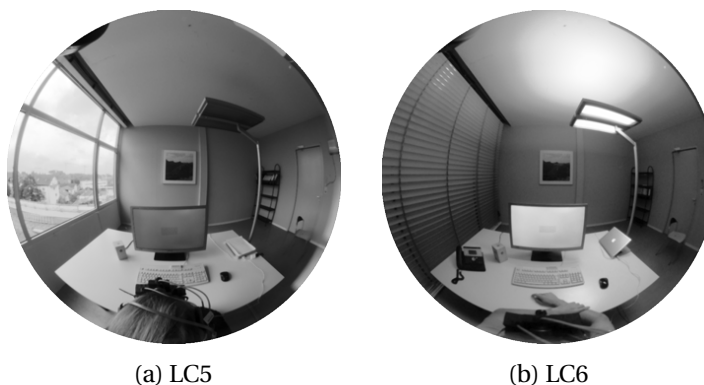


Figure VI.16 – **Lighting conditions:** a) overcast sky, b) electrical lighting

VI.2.3 Results: Gaze Dynamics & View Outside the Window

To investigate the effect of the three view types on gaze behaviour, first we looked at the gaze behaviour during different task phases. Graphs VI.17 (a-d) and VI.18 (a-d) show the dominant gaze of each participant during the eight task phases when working with computer and on phone. The  $x$ -axis represents horizontal gaze and the  $y$ -axis represents the vertical gaze orientation. The screen centre axis and the border axis between inside and outside are marked on the graphs. The data points are shown with circles. The circle diameter corresponds to the fixation duration and the colour represents the type of view: view type 1 green, view-type 2 grey, view-type 3 black.

Looking at the graphs below we can see that the data points cluster around the screen-axis when working with the computer and keyboard (Figure VI.17 a, c and d). The *Thinking* phase on the other hand leaves room for visual exploration independent from the effect of the task-support position. The prominent gaze behaviour under *Thinking* phase here is that mostly green and grey data points can be seen outside the window. Additionally, the data points are clustered differently for each view type condition.

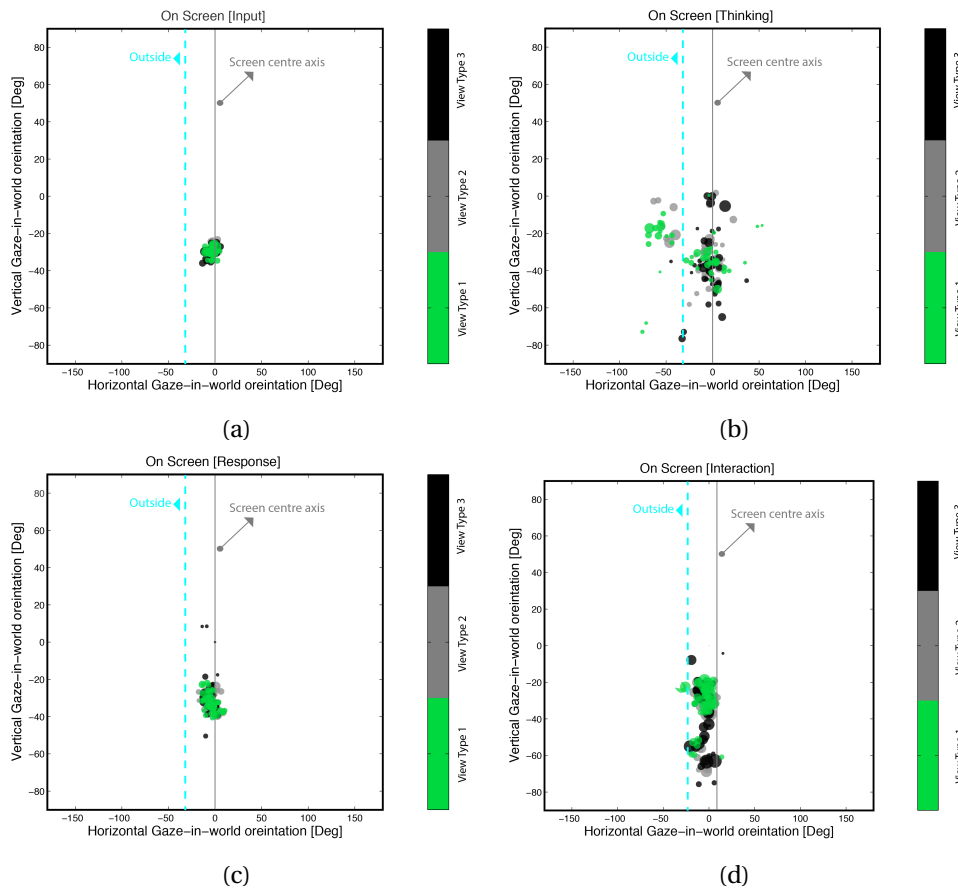


Figure VI.17 – Gaze patterns & view outside the window: a-d) while working with monitor

## Chapter VI. Experimental Phase: Full Study

During the on-phone phases, the phone object is not in the scene and the participants use a headset to perform the task phases. This allows for observation of gaze behaviour in relation to the three view types independent from the task-support.

One observable behaviour is that the gaze has stayed inside the room under electrical lighting conditions. The cluster of black data points are falling mainly around the screen axis. When performing task phases *Input*, *Response* and *Interaction* which require higher levels of cognitive thinking the data points are less spread in comparison to the *Thinking* phase. When performing the *Thinking* phase, we see more of a task independent behaviour. An interesting observation is that under view-type 3 with electrical lighting condition with no view outside, the general tendency of the gaze orientation is still towards the left where the window is located and there are several fixation points around the outside axis specially under *Thinking* phase. Another observable behaviour is that there are no gaze point farther inside the room under electrical lighting. The floor stand lamp that can be seen in Figure VI.16b is located on the left side. This observation can be in line with the gaze avoiding the higher luminance levels which we saw in previous sections.

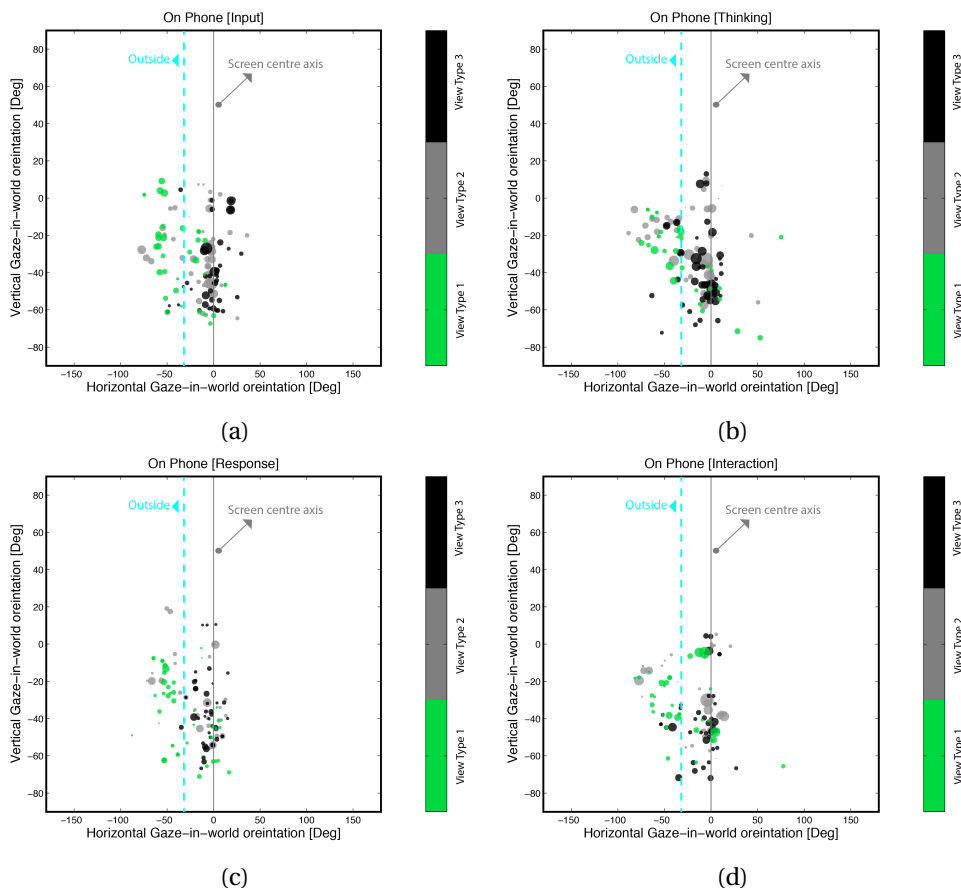


Figure VI.18 – Gaze patterns & view outside the window: a-d) while working with phone

## VI.2. Experiment IV: View Outside the Window

To observe the gaze behaviour independent from the task, the data from the *Thinking* phases are put together (Figure: VI.19). Exploring this data, different gaze behaviour for the three different view types, can be seen in horizontal and vertical orientations and the duration of the gaze fixations.

Gaze shifts differences on horizontal axis for view-type 1 is  $d=150.69^\circ$ , this value is  $d=139.19^\circ$  and  $d=100.19^\circ$  for, respectively, view-type 2 and 3. The shift difference  $d$  is calculated based on the difference between the maximum and minimum horizontal orientation. The fixation durations are shorter for the view-type 1 but there are larger shifts towards father parts inside the room and outside the window.

Additionally, clustering of data points in specific regions can be seen which is also different for the three view types. Three main clusters of data points can be seen in this graph. The three clusters correspond to three regions a1, a2 and a3 which respectively are the window, the screen position and the picture mounted on the opposite wall shown in Figure VI.20. In order to have a closer look on this clustering effect, the three view types are shown in separate graphs VI.21. Finally, from this graph it is not clear, though, if the gaze orients similarly towards inside and outside for view-type 1 and 2.

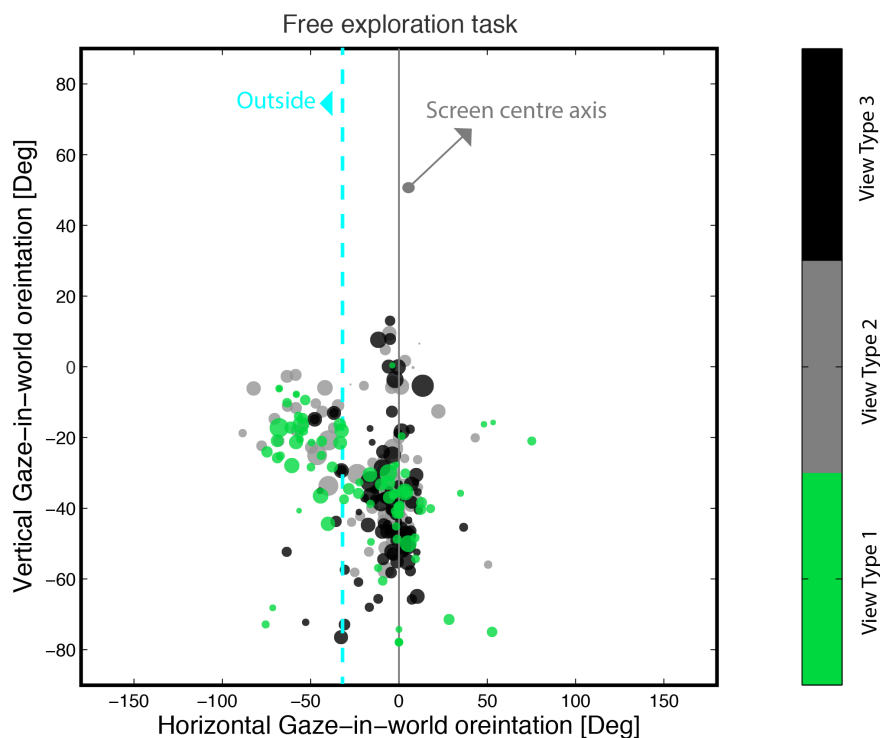


Figure VI.19 – **Gaze behaviour under free exploration tasks:** each data point represents one participants dominant gaze. the size of the data points corresponds to the fixation duration.

## Chapter VI. Experimental Phase: Full Study

Figure VI.21(a-c), demonstrates the gaze behaviour under each view-type condition. The three regions, a1-3, are marked with dashed circles on each graph showing the clustering of the gaze points. The circles' diameter corresponds to the number of data points in each region. These three regions correspond to: a1, the window, a2, the screen and a3 a picture mounted on the wall (Figure: VI.20).

Figure VI.21a shows the gaze distribution of view-type 1. Under this view-type 1, two main regions can be seen. The cluster size are similar for this two regions. Three fixation regions can be seen, under view-type 2 and view-type 3 conditions (Figure VI.21b & c). The number of gaze points falling on the screen region a2 is higher than region a1 and a3 for view-type 2 & 3. The gaze points are more fixating on the screen area with the largest number of gaze points under view-type 3.

Finally, the general tendency of the horizontal gaze orientations are towards the left. This mean value of horizontal orientation  $-20.56^\circ$  for view-type 1,  $-15.6^\circ$  for view-type 2 and  $-7.5^\circ$  for view type 2. The vertical gaze orientations has only varied minimally between the three view-types.



Figure VI.20 – **Gaze dynamics & view:** a panorama picture of the room from the point of view of the participant. The three prominent fixation regions a1- a3 are noted on the image.

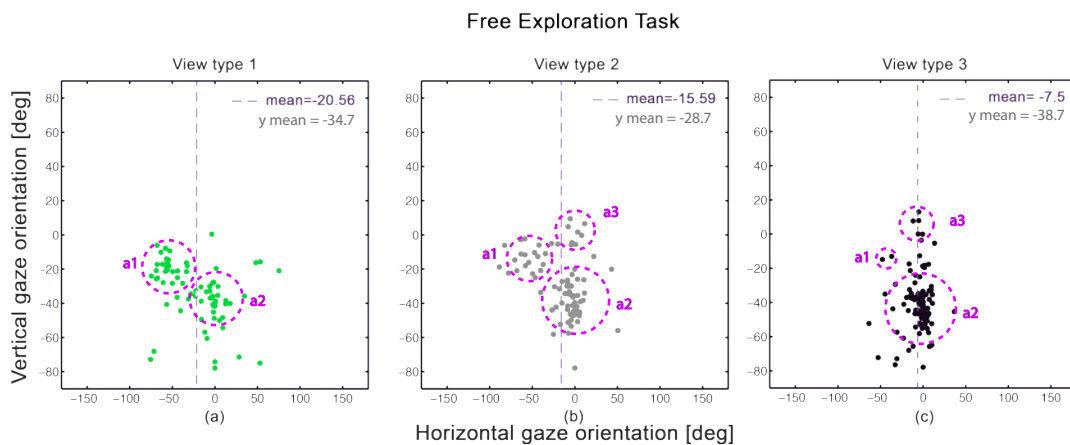


Figure VI.21 – **Gaze behaviour under free exploration tasks:** a) View-type 1, b) View-type 2, c) View-type 3.

## VI.2. Experiment IV: View Outside the Window

To quantify these observations one-way ANOVAs were done to compare gaze behaviour between each two view types. Additionally, we did a one-way ANOVA between the three views to conclude the prominent gaze behaviour differences between all the view types.

Table VI.9 shows the result on the horizontal gaze orientations. The F ratio and *P*-value from one-way ANOVA analysis on horizontal gaze orientations for the three view-types in comparison to each other. There is a horizontal gaze difference between view-type 1 and view-type 2 ( $F(1, 162)=4.6, P<0.1$ ).

The horizontal orientation is significantly different for view-types 1 and 2 in comparison to view-type 3 with no view ( $F(2, 162)=18.84, P<0.0001$ ) and ( $F(2, 162)=38.66, P<0.0001$ ). The boxplot in figure VI.22 shows the distribution of the data under each view-type condition. The 50% of the data falls inside the box between the 75 and 25 percentiles. The median, 75th and 25th percentile of the data and the min and max values are shown which gives a visual comparison of the differences between the three view-types.

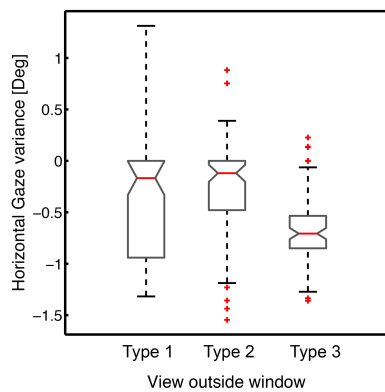


Table VI.9 – One-way ANOVA

	View types			
	1 & 2	1 & 3	2 & 3	all
F	4.662	18.84	38.66	16.11
P	0.033	$2.4 \times 10^{-5}$	$4.1 \times 10^{-9}$	$2.6 \times 10^{-7}$

Figure VI.22 – Horizontal.

The vertical orientation has been mainly effected by view-type 2 and 3  $F(2, 162)=10.78, P<0.01$  (table VI.10). The data distribution can be compared in Figure VI.23. The duration of fixations is signifi-

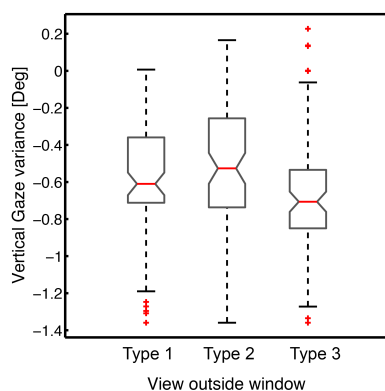
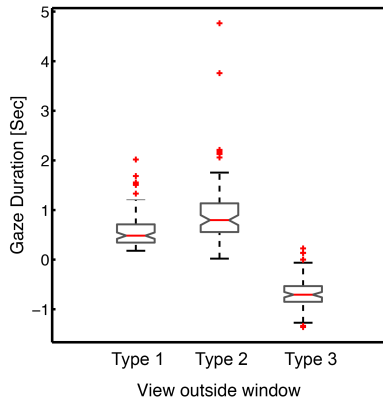


Table VI.10 – One-way ANOVA

	View types			
	1 & 2	1 & 3	2 & 3	all
F	3.56	2	10.78	5.44
P	0.0611	0.15	0.0013	.0049

Figure VI.23 – Vertical.

cantly different for all view-type conditions (all  $P < 0.0001$ ) (Table: VI.11). Figure VI.24 shows the data distribution for gaze durations.



**Table VI.11 – One-way ANOVA**

	View types			
	1 & 2	1 & 3	2 & 3	all
F	419.79	529.8	338.81	229.9
P	$7.7 \times 10^{-47}$	$6.1 \times 10^{-53}$	$1.5 \times 10^{-41}$	$9 \times 10^{-57}$

**Figure VI.24 – Duration.**

### VI.3 Summary & Discussion

A prominent finding on gaze orientation is that the gaze orients towards the window and only avoids the window in very high luminance levels. Gaze is oriented towards window in 82% of the cases with a general tendency of mean =  $-19^\circ$ . This result is independent from the dominant effect of variables such as change of view or task. Accordingly, the ANOVA results show that there is a significant effect of lighting conditions on horizontal gaze variance and gaze distribution. The size of the data points which is an indication of the duration of the fixations are better illustrated in Figure VI.11. Except for visually focused task where longer fixations have happened, no prominent pattern can be observed on gaze durations in relation to lighting conditions.

A prominent finding is importance of task-support position. In this study, each participant performed the office task sequence using two task-supports that are commonly used in offices to support the tasks: computer and phone. The results show that there is an effect of task-support that the gaze distribution has varied when using screen or phone. This effect has been similar for all lighting conditions and we see no interactions between task-support and lighting conditions for any of the gaze responses. Thus, task-support overrides any gaze behaviour due to light variations or presence of glare. The gaze is orientated towards the task position despite the presence of glare or change of lighting conditions. While orientated towards the task-support, the lighting conditions have only affected gaze in its vertical orientations when performing different task phases. The office task sequence performed by each participant included four task phases. The main components of a short period of office work were integrated in this office task sequence. The gaze behaviour was significantly different when performing these phases. There is a strong interaction between light conditions and task phases on vertical gaze



variance and a weak effect on the gaze distribution. In other words the vertical gaze orientations have been different for different task phases under different lighting conditions.

The overriding effect of task prevents the gaze from its natural response to the surround including lighting. An important conclusion is that if the task station (or work station) layout and position is not considered properly it could cause higher risks of visual discomfort.

Finally, the effect of the three view types was investigated on gaze behaviour. The main effects of the views on gaze orientations could be seen for free exploration *Thinking* phases. Three view types were considered in this study. The first view type had a view outside of the window. View-type 1 had a view content of a mixed nature and built environment and was extended to a far distance. View type 2 was oriented towards a close distance composition of artefacts including containers and stairs but with an open sky view. The third view type, view-type 3, was a blocked window with black cover and venetian blinds. The results show that gaze behaves differently under these three view conditions. Under view-type 1, there are shorter fixations and the gaze is spread into two main regions of interests: outside and screen regions. The gaze shifts are larger under view-type 1 conditions. The gaze fixations are longer under view-type 2 and view-type 3 conditions and the picture on the wall is a region of interest in presence of these view types. In conclusion, view-type 1 results in a more active gaze behaviour where the gaze is more dynamic and fixates only in shorter pauses in comparison to the two other views. The significant effect of view types on gaze behaviour indicates that the gaze relation to light and glare can not be seen without considering the view outside the window.



# VII Gaze-driven vs. Fixed-gaze Approach in Glare Evaluations

For each experimental trial consisting of 8 phases, gaze-centred luminance images were generated based on dominant gaze direction. In this chapter, the uncertainty of the developed gaze-centred luminance images is measured as a first step. Thereafter, the newly developed approach is compared to the fixed-gaze assumption.

The developed gaze-centred and fixed-gaze luminance images were at first step processed using an evaluation tool *Evalglare* for deriving variables of the discomfort glare models. This tool processes the HDR luminance images for possible glare sources.

The glare source detection algorithm adopted in the tool searches for pixels of luminance values  $x$ -times larger than the average luminance of a specified visual adaptation region, e.g. the monitor screen, based on a predefined threshold multiplier value. The tool then combines the detected glare pixels within a pre-defined search radius as one potential glare source. These parameters of threshold and search radius were set respectively to 10 and 0.2 rad [124].

In the case of gaze-centred images the the centre of the image was taken as the reference region with an opening radius value of 0.2 rad to cover the central vision (Figure: VII.1). The main outputs of the tool used in this study are illuminance at the vertical level  $E_v$  (equation III.1), luminance of the central vision  $L_f$  (equation III.2) and the discomfort glare risk prediction values based on DGI and DGP models. These three variables were used to compare the gaze-driven and fixed-gaze FOV approaches.

During the on-screen task the computer screen with an opening of 0.4 rad was considered as the reference region. During the *Thinking* phase, when the computer screen is off, the keyboard area is considered as the reference (Figure: VII.2a). During the on-phone tasks with no identifiable task area, the average luminance of the image was set as the reference (Figure:VII.2b).

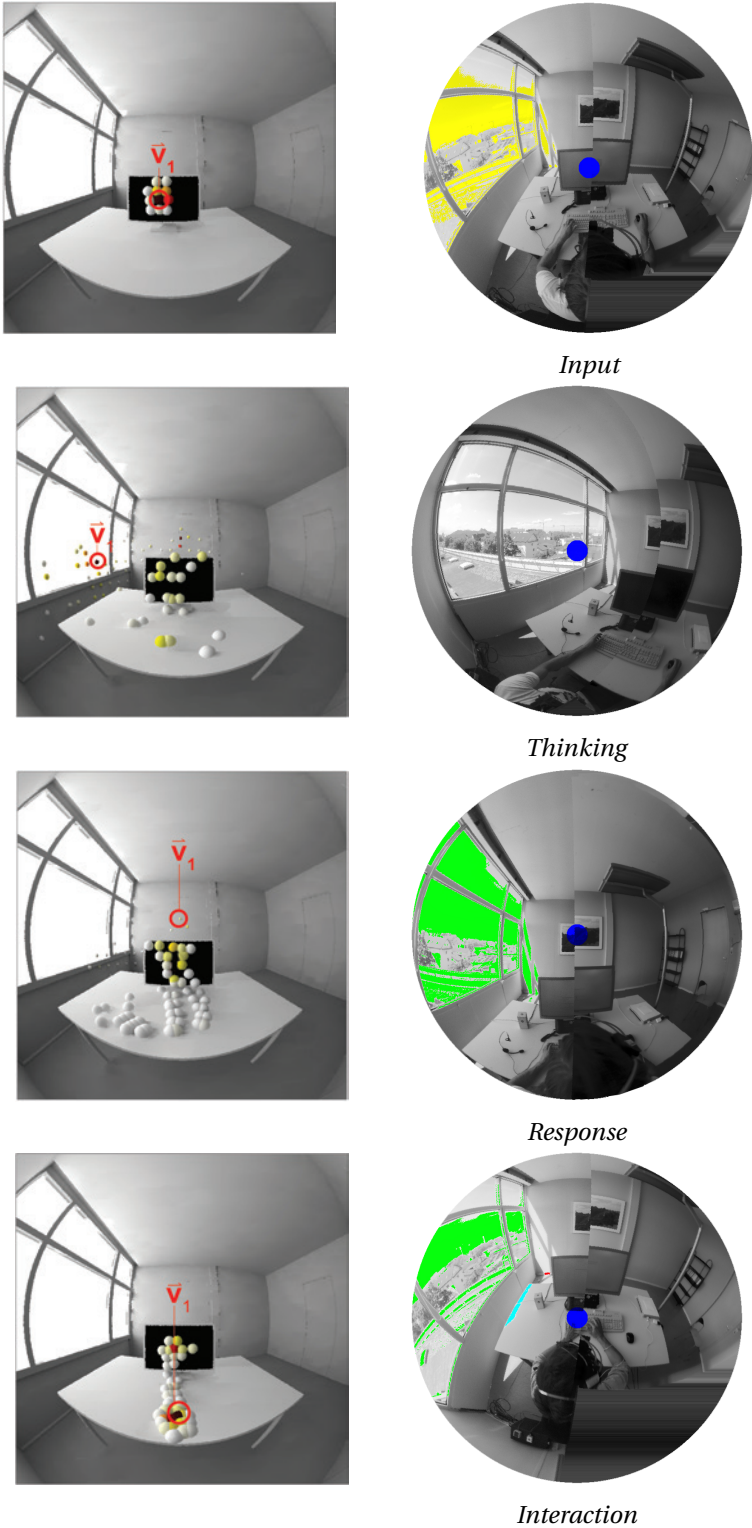


Figure VII.1 – Gaze-centred luminance images evaluated by *Evalglare*: left column) The gaze distribution of one participant during the four phases of the on-screen work is shown and the most dominant gaze  $\vec{v}_1$  is marked, right column) the gaze-driven FOV luminance image corresponding to  $\vec{v}_1$  in each phase as processed by *Evalglare*.

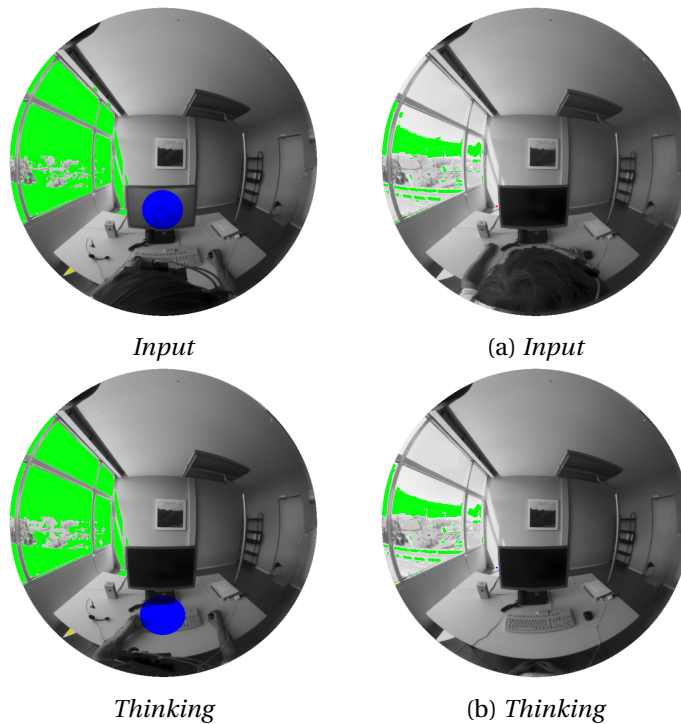


Figure VII.2 – **Fixed-gaze luminance images evaluated by *Evalglare***: a) the reference region are marked in blue; when the monitor was off during the *Thinking* phase, the keyboard region was set as reference, b) during the on-phone task the average luminance of the scene was considered as the threshold reference. This setting was the same for all the phases including the *Thinking* phase. The highlighted areas in are the potential glare sources.

## VII.1 Uncertainty Estimation

The uncertainty of gaze localisation in the luminance images can be caused within each step of the process. The uncertainties for deriving gaze-in-world data can be caused by initial camera resolutions, the process of deriving a head-centred, room referenced gaze directions. Luminance data collection and generating the gaze-centred luminance images are prone to uncertainties caused by device resolutions or calibration processes, camera positions, observational error, or random camera movements during the experimental trial. These uncertainties are addressed here.

### VII.1.1 EyeSeeCam - Gaze Uncertainty

The theoretical resolution of the EyeSeeCam device is at  $0.04^\circ \pm 0.01^\circ$  and thus negligible compared to other sources of error.

The deviation from the camera's optical axis was not considerable. This deviation was measured by localising the central dot in the calibration video from each participants and calculating the offset angle

between the recorded data and the video. This measurement was done using the camera calibration toolbox [125] (and more specifically function `normalise()`). The calibration allows for an error of maximum of  $1^\circ$  at the time of calibration, which applies to the central calibrated field and might be slightly larger for large eccentricities.

IMU sensors can produce drift errors for integrated signals over longer time periods. Thus, the drift correction is very important for accuracy and applied like following. Head orientations were measured from the scene video at multiple time points. The result of the quaternion integration at the time of the next available scene video measure was compared with the given absolute head orientation. Their difference was divided by the number of integration steps and added as additional rotation term between each step in a second run of integration over time. With the method the drift error was reduced to a negligible amount.

Uncertainty of head orientations mainly results from errors introduced by the lens, which – despite the correction – can accumulate to up to  $3^\circ$  in the far periphery. By avoiding eccentric key points during manual selection and by using an over constrained number of points (4 rather than 3) for the PnP protocol, we alleviated this issue and got an upper bound of  $2.5^\circ$  error for the individual point,  $1.25^\circ$  ( $\frac{2.5}{\sqrt{4}}$ ) for the set of points, taking the error of the PnP estimate ( $<1^\circ$ ) and drift into account, we then end up at a maximal error of  $1.9^\circ$ . A conservative estimate for the overall error of gaze-in-world is  $2.2^\circ$  ( $\sqrt{1^2 + 1.9^2}$ ). To be conservative, we chose analysis bins of  $5^\circ$  visual angle for all quantitative analysis, i.e. more than double this error, throughout. Possible systematic errors due to headband slippage were estimated from the reading-on-screen phase, and are unlikely to affect results.

### VII.1.2 Gaze-Centred Luminance Image Uncertainty

The cameras' initial measurement uncertainty is  $\pm 3\%$ . Additionally, the cameras are by 1.57% resulting in different values. Therefore an initial error of 5% can be estimated for the luminance measurements. The vignetting problem which is a reduction of an image's quality at the periphery, was avoided by cutting the edge of the main image by  $2^\circ$  when combining the two images.

The cameras were installed with the distance difference of 65 [mm] in CCD luminance cameras positions on the z-axis due to physical shape constraints. Also, the two cameras were not at the most ideal place, which is the participants' eye position. Installation of the structural system to hold the luminance cameras is inclined to measurement errors of angularity, perpendicularity and parallelism. Less likely random camera movements during the experimental trial could also cause uncertainties in the final outcome. These three error types change the camera point or direction of the optical axis.

Uncertainty estimation for these three error-types was done by simulating and reproducing these situations in actual and ideal scenarios under the extremely sensitive daylight condition with the sun in

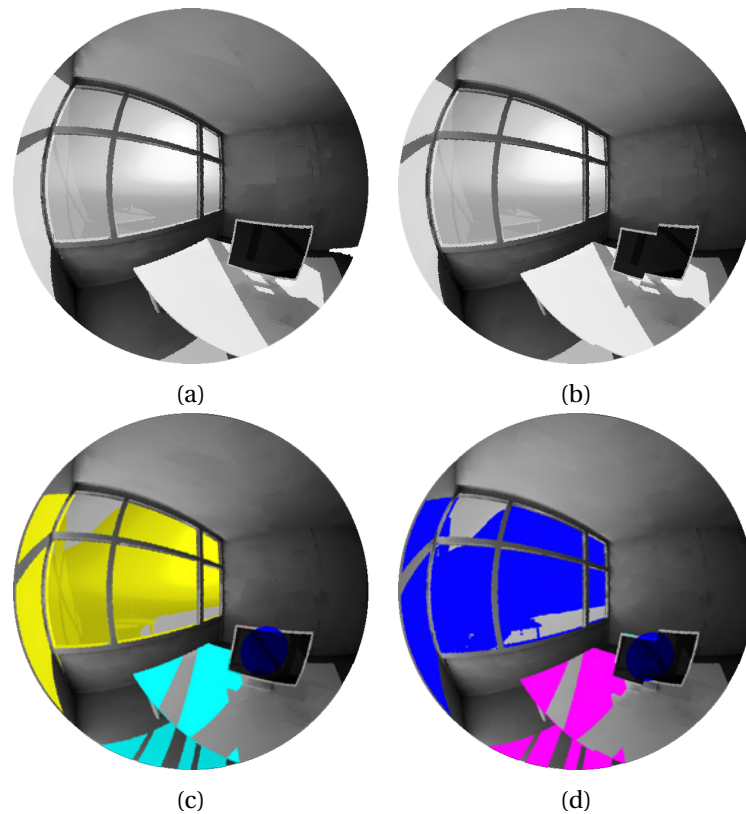


Figure VII.3 – **Camera position deference:** a) the Ideal position b) The 65 [mm] disposition, c-d) the images were processed using *Evalglare* and analysed using *Matlab*.

the FOV. This simulation process was done using *Radiance*. For each uncertainty scenario, two images were produced and a gaze-centred image was generated. The generated images were then processed and the luminance values between the two images were compared.

In extreme day lit conditions, the deference in cameras positions causes an error of 0.38% of luminance difference in comparison to an ideal scenrio. This estimation was done by simulating the ideal positioning of the cameras (Figure:VII.3b) and comparing it with the actual feasible physical positions with the fixed distance difference of 65 [mm] (Figure:VII.3b). sThe observational error was estimated by considering a maximum shift of a  $\pm 10$  [mm] in x and y direction or  $5^\circ$  of rotation around the z-axis for the type of structural installation used in the study. Observational error of 0.11% due to shifts and a maximum error of 8.6% due to rotations are estimated. This adds up to an overall error estimate of 9% in sensitive daylit condition with the sun in the FOV of the camera.

The disposition between the two cameras when sun is in the FOV, was checked in the sample pool and one case was eliminated dues to luminance camera's position difference in one case. Another four data samples were also deleted from the sample pool due to the dispositions between the camera and the participants' eye position.

## VII.2 Results: Gaze-driven Approach vs. Fixed-gaze Approach

### Visually Focused & Free Exploration Tasks

Figure VII.4 compares the illuminance at the vertical level  $E_v$  derived from dominant-gaze-centred luminance images and the fixed-gaze-centred luminance images under daylight conditions. The  $x$ -axis represents the values of the gaze-driven illuminance at the vertical eye level ( $E_{vg}$ ) and the  $y$ -axis the values of fixed-gaze illuminance at the vertical camera level ( $E_{vf}$ ) values. In the visually demanding *Input* phase (Figure:VII.4c), for the majority of the participants, the  $E_{vf}$  is greater than  $E_{vg}$  (63 cases).

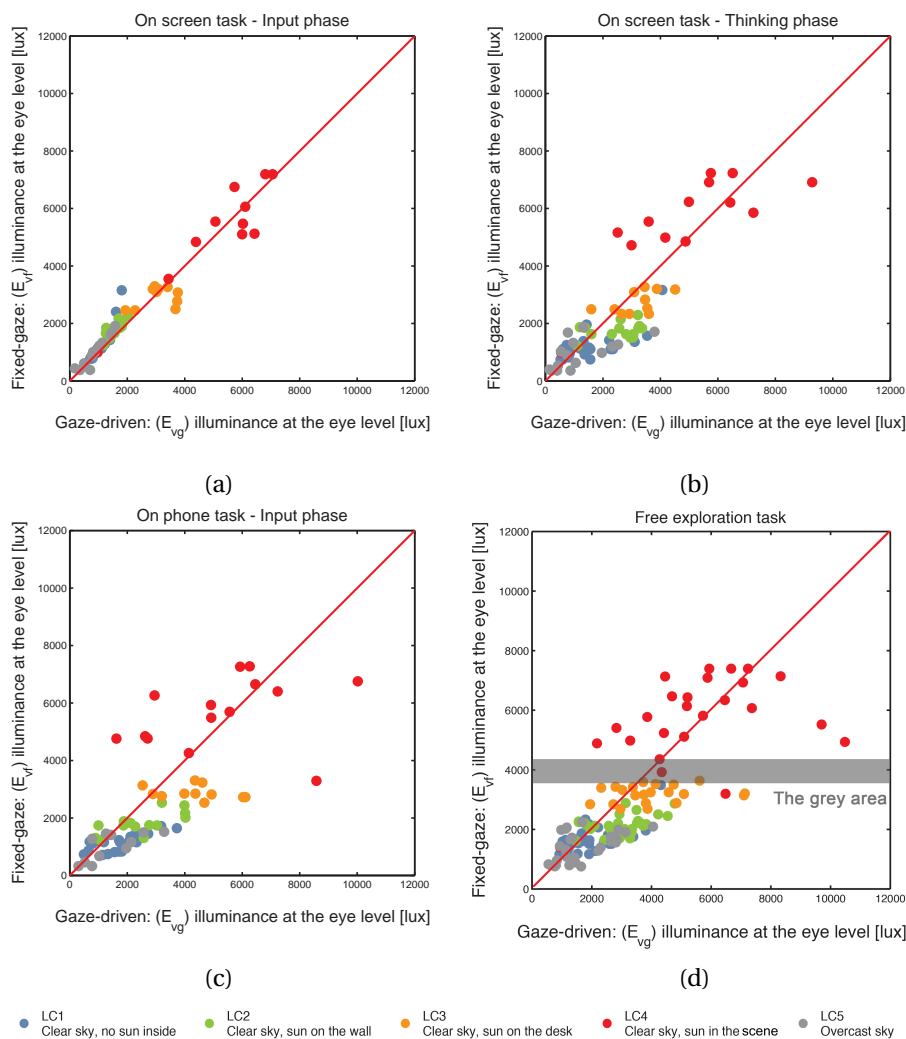


Figure VII.4 – **Illuminance at the vertical level for gaze-driven vs. fixed-gaze approach:** on-screen a) *Input* phase & b) *Thinking* phase, c) on-phone *Thinking* phase, d) free exploration phase which is the on-screen and on-phone *Thinking* phase combined; an observable a grey area is marked on the graph.



## VII.2. Results: Gaze-driven Approach vs. Fixed-gaze Approach

Considering that the on screen *Input* phase is restricted to and focused on the task-support area, the number of  $E_{vg}$  cases showing smaller values than  $E_{vf}$  is significantly high, thus indicating a small and robust effect on gaze orientation towards lower luminance adaptation levels. In contrast, during the free exploration *Thinking* phase, there are considerable differences between the actual illuminance level at the eye  $E_{vg}$  and the one predicted by the fixed-gaze assumption (Figure:VII.4a). This effect also applies to the situation when the task phase has been performed during the session where the phone is used as the task-support (Figure: VII.4b). The free exploration task phases invites participants to explore the surroundings independently of the task-support and can give us a better understanding of the effect of lighting conditions on gaze orientations. Figure: VII.4d shows  $E_{vg}$  and  $E_{vf}$  during the *Thinking* phases. Exploring the data we can see that the gaze-driven and fixed-gaze approaches behave differently as the illuminance at the vertical level rises. Here, we can observe prominent gaze behaviour: as the  $E_v$  values increase, there is a shift of  $E_{vg}$  to the lower values. In other words, the gaze is oriented towards the lower luminance levels (inside the room) by 64%, thus the vertical illuminance at the vertical level is lower than the vertical illuminance at the fixed camera position. This effect is opposite for lower vertical illuminance levels where the gaze is oriented towards the higher luminance levels (outside of the window) by 65%. To illustrate this we have shown the data in two groups above and below an observable grey area. This grey area represents a region where no data has been collected due to experimental set up which has been restricted to two view outside the window. The median ( $m_{above}=(4993, 5924)$  &  $m_{below}=(2089, 1513)$ ) and the standard deviation ( $std_{above}=(2112, 1098)$  &  $std_{below}=(1391, 755.6)$ ) show the general tendency of each group (Figure:VII.5a). The boxplot (Figure:VII.5b) shows the significant reduction of the median values for  $E_{vg}$  illuminance levels above the grey area in comparison to the lower values below the grey area

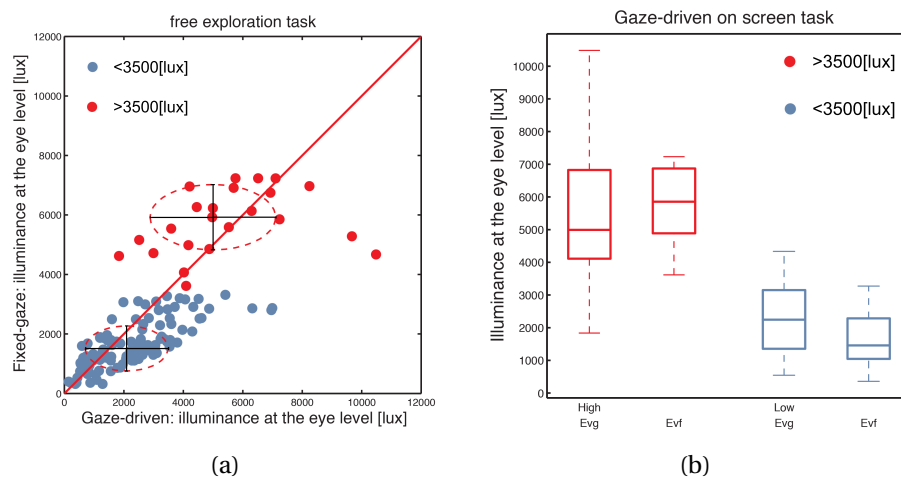


Figure VII.5 – **The graphs demonstrate gaze-driven vs. fixed-gaze  $E_v$  approach:** a) the median and standard deviation of gaze-driven values  $E_{vg}$  and fixed FOV values  $E_{vf}$  for above and below the grey area are shown, b) the graph is a box plot comparing the distribution of the  $E_{vg}$  and  $E_{vf}$  for higher and lower values than the grey area.

## Chapter VII. Gaze-driven vs. Fixed-gaze Approach in Glare Evaluations

To quantify the difference between the two approaches, a two-way ANOVA was performed on illuminance at the vertical level ( $E_v$ ) as the dependent variable. The independent variables are the measurement approaches (gaze-driven  $E_{vg}$  and fixed-gaze  $E_{vf}$ ) and the five daylit conditions (LC1-5). We found no evidence that the assumption of homogeneity was violated ( $P=0.26$ , Levene's test) and thus used an ANOVA for further analysis. As the number of samples was not equal for each lighting

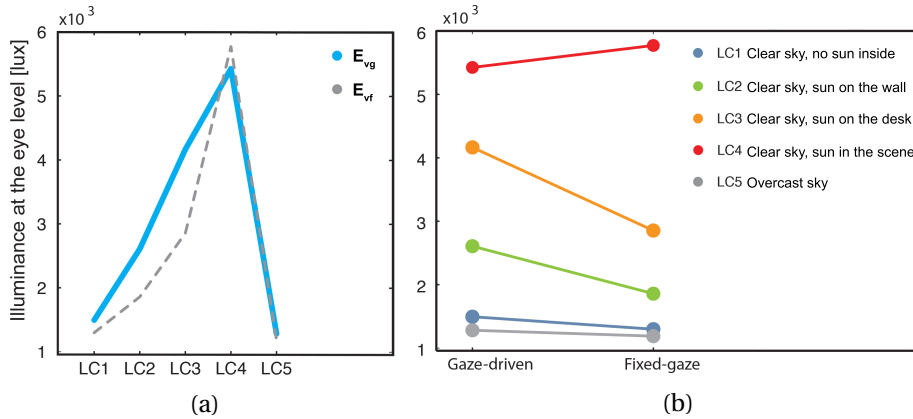


Figure VII.6 – **Interaction plots:** a) Interaction diagram corresponding to  $E_v$  for gaze-driven and fixed-gaze approach, b) Interaction diagram for  $E_v$  corresponding to different lighting conditions: The lines are not parallel, which means that there is an interaction between the two factors.

condition, we randomly selected samples using a stratified simple sampling without replacement. The two-way ANOVA results ( $F(1, 200) = 13.75$ ,  $P < 0.001$ ) show that a gaze-driven approach is significantly different from a fixed-gaze approach (Table: VII.1). Figure VII.6a illustrates the difference between the gaze-driven and the fixed-gaze approach. The change of  $E_v$  under different lighting conditions is apparent ( $F(4, 200) = 193.19$ ,  $P < 0.001$ ). Importantly, there is a significant interaction ( $F(4, 200) = 4.28$ ,  $P = 0.0024$ ) between the two approaches (Figure VII.6b): for the high luminance condition (LC4), the gaze-driven approach shows lower luminance than the fixed-gaze approach, while for the lower luminance conditions the pattern is reversed. The former situation supports the notion that gaze preferentially selects medium luminance regions and avoids extremes. In line with this, condition LC5 (overcast sky) shows the minimal difference between the two approaches. Attraction to higher luminances could indicate the attraction to window which has higher luminance values. In order to investigate this notion, the gaze orientations in each lighting condition is studied in section VI.1.4.

Table VII.1 – Two-way ANOVA results

Source	SS	df	MS	F	p
Approach	$1.0 \times 10^7$	1	$1.0 \times 10^7$	13.75	0.0003
Daylit-condition	$5.8 \times 10^8$	4	$1.4 \times 10^8$	193.19	0
Interaction	$1.3 \times 10^7$	4	$3.2 \times 10^6$	4.28	0.0024
Error	$1.5 \times 10^8$	200	$7.6 \times 10^5$		
Total	$7.6 \times 10^8$	209			

**Gaze-driven vs. Fixed-gaze Approach for Central Vision Luminance**

The luminance at the central vision is compared for the gaze-driven and fixed-gaze approach during the visual exploration *Thinking* phases. In the on-screen phase (Figure: VII.7a) the  $x$ -axis is the luminance [ $\text{cd}/\text{m}^2$ ] of the central vision derived from the gaze-centred luminance images. The central vision region is defined with an opening of 0.2 rad with a small margin. The  $y$ -axis is the luminance [ $\text{cd}/\text{m}^2$ ] the task area (monitor screen) with an opening of 0.4 rad based on the assumption that the gaze is fixed on the task area. During the on-phone phases (Figure: VII.7b), since there is no fixed task area present, the average luminance of the room represents the fixed-gaze measurement on the  $y$ -axis .

We can see a prominent gaze behaviour which is in line with the findings in the previous section: the gaze fixates on lower luminance values during lighting condition LC4 in 71% of the cases and LC3 in more 50% of the cases for both task phases. Nevertheless, the gaze fixation on brighter region can be seen in lighting conditions 1, 2. Additionally, it can be seen that the difference between the fixation preferences is very large with the data being on much lower values in case of lighting condition LC4 and much higher values in case of lighting condition 1,2. No significant trend is observable in case of the over cask sky conditions, LC5.

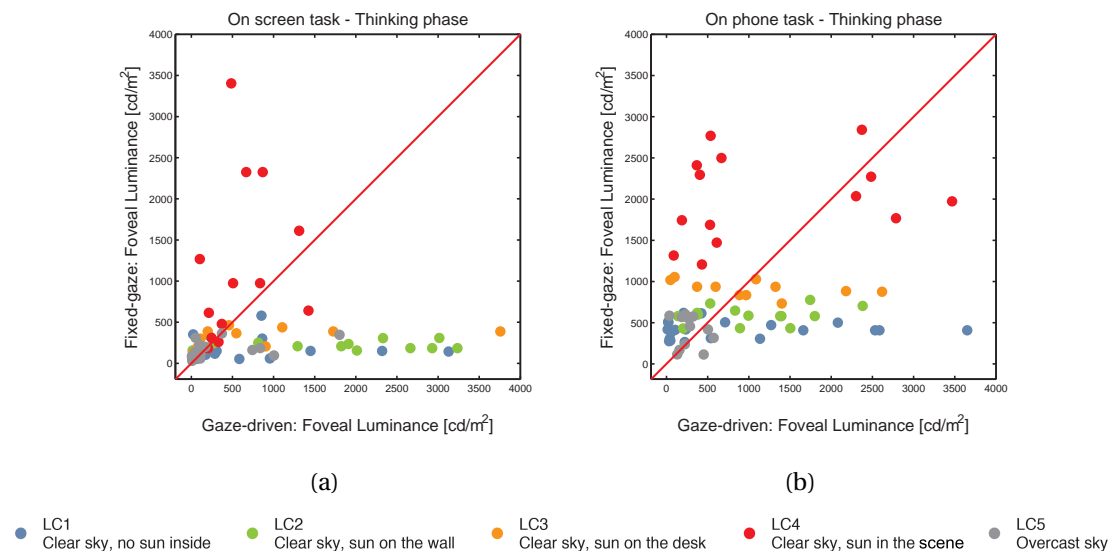


Figure VII.7 – **Gaze-driven vs. fixed-gaze approach for central vision:** luminance at the central vision [ $\text{cd}/\text{m}^2$ ] during *Thinking* phase a) when working on screen, b) when working on-phone.

**Gaze-driven vs. Fixed-gaze Approach for Daylight Glare Metrics**

The gaze-driven approach for glare prediction metrics DGP and DGI in comparison to the fixed-gaze approach are evaluated in this section. Figure VII.8(a-b) show the results of DGP calculations comparing the two approaches and Figure VII.9(a-b) show the DGI results.

## Chapter VII. Gaze-driven vs. Fixed-gaze Approach in Glare Evaluations

---

Gaze-driven DGP as shown in the equation VII.1, is dependent mainly on  $E_v$ . The first graph, Figure VII.8a, shows that gaze-driven approach in 80% results in lower DGP values than the fixed-gaze DGP during the *Input* phase. In the second graph, Figure VII.8b, we can see that 75% of the cases are towards higher DGP values while being towards lower DGP values in 78% of the cases in lighting condition LC4 with sun in the field of view. The mean and standard deviation of the LC4 in comparison to the other lighting conditions are also shown. This result show that the general tendency for all lighting conditions is towards higher DGP values. Using the gaze-driven approach, DGI prediction values are lower than for the fixed FOV approach in 82% of the cases. This deviation is similar for all lighting conditions. DGI as shown in equation VII.1, is dependent mainly on the glare source luminance variations over the background luminance (the average luminance of the image without the glare sources).

Despite DGP value being different for the two approaches in different lighting conditions for *Thinking* phases, for a task driven office setting DGP results show very high correlation ( $R_2=0.98$ ) between the two approaches for all lighting conditions. Conversely, the DGI results for the same condition has a much lower correlation value between the two approaches, ( $R_2=0.58$ ). The higher dependencies of DGI on the glare sources explain the sensitivity of DGI on gaze orientations.

The gaze-driven approach results in different DGP and DGI predictions when the gaze is not focused on the task. It is important to compare these results with the subjective assessments in order to understand whether gaze-driven DGP and DGI values correlates better with the participants' subjective assessment of the glare situation.

A prominent conclusion is that if a choice to direct the gaze exists, the glare prediction of the space would generate different results. It is hence important to understand the gaze behaviour in relation to light and to understand the gaze behaviour in the space before making any glare predictions and deciding on the daylight strategy of the space.

$$DGI = 10 \cdot \log\left(0.5 \sum_{i=1}^n \frac{L_{s,i}^{1.6} \cdot \Omega_{s,i}^{0.8}}{L_b + .07\omega_{s,i}^{0.5} \cdot L_{s,i}}\right) \quad (VII.1)$$

$$DGP = 5.87 \cdot 10^{-5} \cdot E_v + 9.18 \cdot 10^{-2} \times \log\left(1 + \sum_i \frac{L_{s,i}^2 \cdot \omega_{s,i}}{E_v^{1.87} \cdot P_i^2}\right) + 0.16 \quad (VII.2)$$

$L_{s,i}$  Luminance of a glare source

$\omega_{s,i}$  Solid angle of glare source  $i$  subtend at the eye

$\Omega_{s,i}$  Solid angle of source modified for position factor

$L_b$  Luminance of the background

$E_v$  Illuminance at the vertical eye level

$P_i$  Position index

## VII.2. Results: Gaze-driven Approach vs. Fixed-gaze Approach

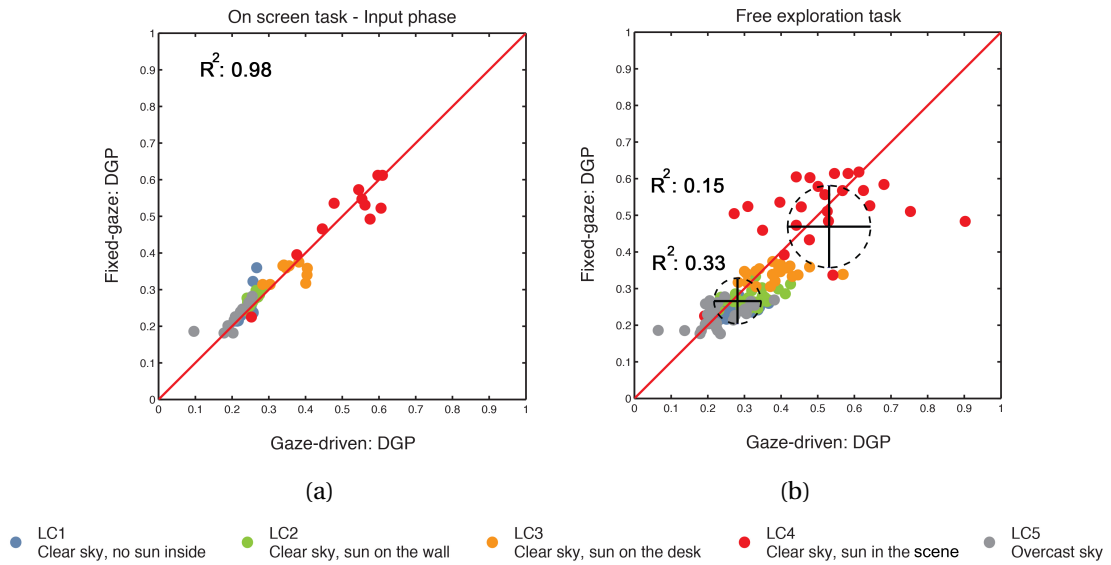


Figure VII.8 – Gaze-driven vs. fixed-gaze approach for DGP: a) *Input* phase on-screen task and b) *Thinking* phase on-screen task.

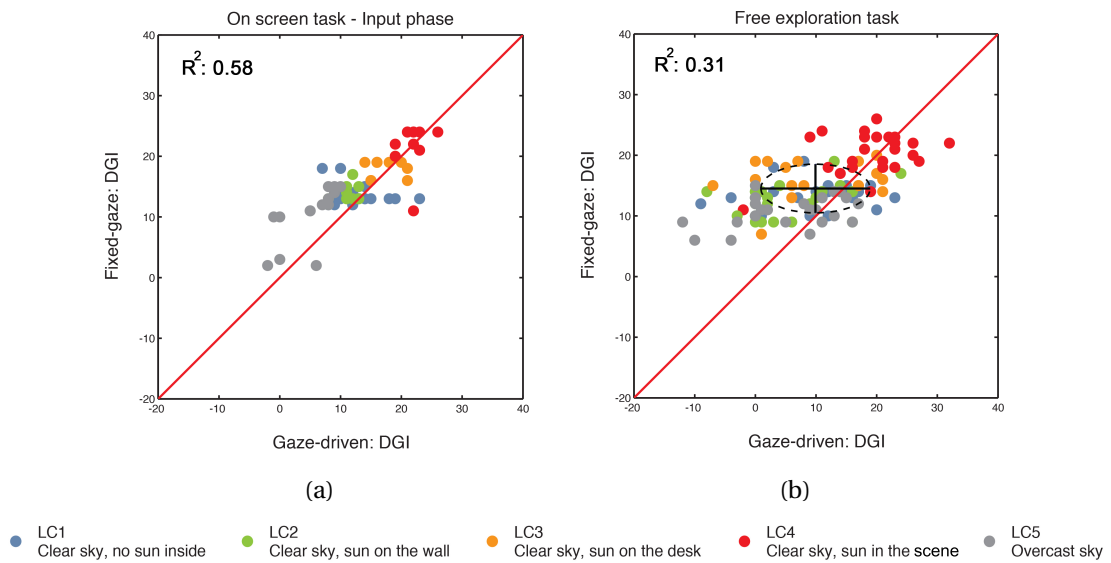


Figure VII.9 – Gaze-driven vs. fixed-gaze approach for DGI: a) *Input* phase on-screen task and b) *Thinking* phase on-screen task.

### VII.3 Summary & Discussion

In order to validate this method, gaze-driven approach and fixed-gaze approach were compared. Using the newly developed gaze-driven approach the gaze-centred luminance images were derived for 80 participants during daylight conditions. These luminance images represent the luminance distribution in FOV with respect to the dominant fixation point of the participant at the time of the experiment. The actual luminance values, hence are derived for each phase of the experimental trial for each participant. The participants performed an eight phased office task using two different task support in the final experiments. In total eight gaze-centred image and eight fixed-gaze images per experimental trial were processed using a *Radiance*-based tool: *Evalglare* to derived the photometric quantities. To quantify the difference between the two approaches, several statistical tests were performed on illuminance at eye level and foveal luminance values as independent variables.

Despite gaze being focused on the task area under visually demanding tasks, i.e. the on-screen *Input* phase, the results show that the gaze is deviated towards lower luminance levels resulting in smaller illuminance at the eye level. Nevertheless, the differences between the two approaches are insignificant and the visual task overrides light-induced gaze shifts.

The observation of results under the free exploration phases, *Thinking* phases, however, demonstrate a significant difference between the two approaches. The difference between the two approaches is larger for higher adaptation luminance levels where the gaze avoids extreme regions with higher luminance values and rests on the medium luminance regions.

Importantly, the interaction between the two approaches and the five daylight conditions is significantly high which re-emphasises the notion that the dynamic gaze behaves different from the fixed-gaze assumption under the different lighting conditions.

The comparison between the two approaches for DGP and DGI metrics also shows different prediction values for free exploration phases. Otherwise, when focused on the task area, DGP values does not change for the gaze-driven approach whereas DGI shows stronger sensitivity to the gaze behaviour. What precedes a glare evaluation is determining the gaze point and direction wether is it towards the task or any other point in the space. Understanding the gaze behaviour in relation to light, hence is eminent to the glare evaluation of the space.

Primarily, the comparison between the two approaches conclude that gaze avoids extremes for medium luminance regions when brighter glare sources exist in the FOV. The gaze attraction is, otherwise always on brighter regions. This finding is in line with the gaze behaviour in different lighting conditions.

# VIII Conclusion

"Do not follow where the path may lead. Go instead where there is no path and leave a trail."

*Ralph Waldo Emerson*

## VIII.1 Achievements

A novel gaze-driven approach was developed for dynamic discomfort glare assessments. A gaze-driven approach for discomfort glare assessments, on one hand, is a method for better understanding the gaze behaviour in relation to light, and on the other hand, is a novel and quantitative approach to investigate discomfort glare that corresponds to building occupant gaze responses. The newly developed approach creates a foothold for assessment of discomfort glare based on gaze responses. The future vision for this project is to support reliable predictions of building occupant responses to the indoor lighting conditions in order to support the design of workplaces.

The gaze-driven approach was developed in this study by integration of the luminance images for recording light variation coupled with mobile eye-tracking methods for recording gaze responses. As result gaze-centred luminance images were generated. A gaze-centred luminance image is an accumulation of luminance values perceived at eye which make an accurate measurement of luminance distribution in the FOV possible. Using this approach a gaze response to the actual variation of light in the FOV can be observed.

The developed gaze-driven approach was done in three major steps. The first step was to compute the gaze directions in the real scene (gaze-in-world) from the data recorded by an eye-tracker. The second step was to identify the dominant gaze directions, i.e. fixation points over the scene. The final step was to derive the gaze-centred luminance images based on the dominant gaze directions. Each of these steps were comprised of several stages which are described in this thesis.

The newly developed approach was fully realised in four user assessment experiments where the

relevant data for producing gaze-driven glare assessments were collected. The first two of these experiments served as pilot studies to proof the adopted principles and to determine an optimised experimental strategy. As outcome, an optimised experiential strategy was developed to derive all the necessary variables while minimising the nuisances. Finally, an extensive series of experiments were performed with a refined experimental strategy to include gaze, glare, lighting exposure, and subjective assessment measures and to observe the main hypotheses of the study:

Hypothesis 1) Dynamic gaze measurements are different than the fixed-gaze measurements

Hypothesis 2) Luminance distribution has an effect on gaze behaviour

Hypothesis 3) The view outside the window has an effect on gaze behaviour

Six different lighting conditions with a thorough consideration of variables such as view outside the window and office task were considered in these experiments. An office task sequence was designed carefully so as to include the main components of a real office work with a well-defined engagement range in order to encourage a realistic work flow where both visual and cognitive performance is required. This office task sequence was prepared and programmed for use with different task-supports. Also, a questionnaire was developed with inclusion of socio-demographic data, mood, context recognition, glare rating and acceptance/comfort ratings. The following parameters were extracted for each participant, task and phase of the experiment:

- 1) HDR luminance images for a 270° record of luminance values
- 2) The gaze direction parameters from the eye-tracking records
- 3) The subjective assessment data

The Collected data was processed with the gaze-driven approach to derive gaze-centred data. The gaze-centred luminance images were then compared with the fixed-gaze approach. Finally the effect of lighting conditions and view outside the window on the gaze shifts was statistically tested.

### VIII.2 Main Findings and Discussion of Results

The first pilot study delivered a proof-of-principle. This study showed that orientation relative to different light conditions has a measurable impact on gaze behaviour for different office tasks, without considering the control of the view outside the window in particular. In the second pilot study we investigated gaze direction distributions under two different lighting conditions while the participants were performing standardised office tasks. This study served two purposes: first, to investigate the possible bias towards the view outside the window for three different task-support (monitor, paper and phone) under glare-free, overcast sky orientations (West vs. South-West); second, to investigate the effect on gaze direction of being exposed to two very different lighting conditions for the same



tasks. The results from the two pilot studies thus allowed for selection of tasks and settings for the final experiment as well as precise control of light conditions, and delivered a proof of concept on the relation between lighting and gaze direction.

### **Gaze -driven vs. Fixed-gaze Approach for discomfort glare assessments**

The newly developed approach was compared to the fixed-gaze assumption. The results show that there is a significant difference between the two approaches. This difference is larger for higher luminance levels where the gaze avoids extreme regions with higher luminance levels and rests on the medium luminance regions. In presence of the lower luminance adaptation levels, the gaze is attracted to brighter regions in the scene. The interaction between the two approaches and the five daylight conditions is highly significant indicating that the dynamic gaze behaves differently from the fixed-gaze assumption under the different lighting conditions.

The gaze-driven and fixed-haze predictions result in different prediction results for the two glare metric DGP and DGI for the free exploration phases. What can be seen when comparing the two approaches for deriving the DGP and DGI values, is that in extreme glare conditions with sun in FOV the gaze-driven values are always lower for the two metrics. The clear gaze avoidance in this situations and the effect of gaze direction on the result, hence, can not be neglected. Moreover, when the adaptation luminance levels are low, gaze-driven DGP results in slightly higher DGP values and DGI results in significantly lower values. The main differences between the two metrics come from their initial formula, where one is dependent on the adaptation levels in terms of illuminance at the eye level and the other is dependent on the contrast between the glare and the background.

Conversely, for a task-orientated office setting, gaze-driven approach does not affect the DGP predictions as the assumption of fixed gaze direction of task is a correct assumption. Understanding the gaze behaviour in relation to light and defining the layout of the task-station, However, precedes the glare evaluation. Moreover, It is important to compare these results with the subjective assessments in future steps to have understand the relation between the gaze behaviour and the glare perception.

### **Gaze Dynamics in Different Lighting Conditions and Views**

Lighting conditions have a measurable impact on gaze behaviour for different realistic office tasks. A prominent finding is that the gaze orients towards the window and only avoids the window in very high luminance levels.

The results based on the analysis of variance on horizontal gaze variance significantly differ in different lighting conditions. There is a smaller effect for vertical gaze variance. The angular range of both head and eye movements in a horizontal orientation are much larger than in a vertical orientation. There-

## Chapter VIII. Conclusion

---

fore, the horizontal gaze variance is likely to measure gaze behaviour in relation to the independent factors with more sensitivity. Nevertheless, there is a strong interaction between lighting conditions and task phases on vertical gaze variance meaning that the vertical gaze orientations have differed significantly under different lighting conditions for different tasks. The spread, or distribution of the gaze orientations, also differs significantly under different lighting conditions. Observing the gaze dynamics during the visual exploration phase where the participants had no visual task constraints highlights the significant effects of lighting conditions on gaze variances.

### Conclusion

Gaze-driven approach generates accurate luminance values that have been perceived at the experimental phases. The comparison of the newly developed approach with a fixed-gaze assumption produces several outcomes.

As a first observation we could see that the effect of lighting conditions (or other independent variables such as view), can mainly be observed in the *Thinking* phases. This rule has been adopted in all analysis phases of this study: in order to observe the effect of the independent variables on gaze behaviour we have looked at the *Thinking* phases of the experiment.

Secondly, we observe that the two chosen task-supports and the defined task phases have created a range of visually demanding task phases to exploration phase where the effect of the independent variables can be observed on gaze responses while simulating an office task sequence that resembles an everyday office work. The developed office task sequence for the study has created a good basis to study the gaze behaviour in relation to light in offices.

And finally, the most prominent outcome is that in offices the office task activity is the one of the main drives for gaze behaviour. This highlights the importance of the position of the working station including all its supporting elements such as the computer screen, phone, desk etc., in the layout of the workspaces. Task overrides the effect of other variable on gaze behaviour, therefore prevents the gaze from its natural behaviour to the surround. Understanding the natural behaviour of gaze in relation to light and positioning of the task with respect to that is a prerequisite for minimum glare exposure. The observations on gaze behaviour in relation to light show that gaze tolerates higher luminance values in exchange for view. Previous studies with subjective assessment [46] had shown that the office workers accept higher glare risk in exchange for view outside the window. In their studies on relation between glare and view, Tuaycharoen and Tregenza have shown that the subjects declare less discomfort glare in presence of a bright window with an interesting view. Gaze behaviour in relation to light is in line with this previous finding. Additionally, different view-types generate different gaze behaviour. Thus, understudying the gaze behaviour in relation to light in indoor environments can not be done without taking the view into consideration.

### VIII.3 Application and Use in Perspective

Maximising daylight access while maintaining a glare-free indoor environment is an ongoing challenge for daylighting design. The most recent methods for predicting glare in daylighting design rely on analyses of high dynamic (HDR) range images. HDR images are an accumulation of luminance values, which creates a basis for luminance-based metric analysis. In daylighting design phase the HDR images are created by advanced physically-based renderings of simulated 3D model of the architectural space which is done by using tools such as *Radiance* [120]. These images are rendered and produced from a fixed point of gaze and gaze direction.

There are three questions that come into mind before starting the rendering session for glare evaluations:

- (1) Which gaze point?
- (2) Which gaze direction should be evaluated?

and more importantly

- (3) What is the gaze response to the luminance levels from an initial gaze point and direction?

The findings of this study show that there is a significant statistical relation between the luminance variations and shift of gaze directions. These findings demonstrate a certain attraction and avoidance gaze behaviour. The gaze is attracted to view and tolerates higher luminance levels and avoids extreme luminance levels. More importantly, in a workspace, the gaze is attracted to the devices that support the task that is being performed. The layout and arrangement of the work station, hence, plays an important role on the ultimate perception of the luminous space and its degree of visual comfort or discomfort.

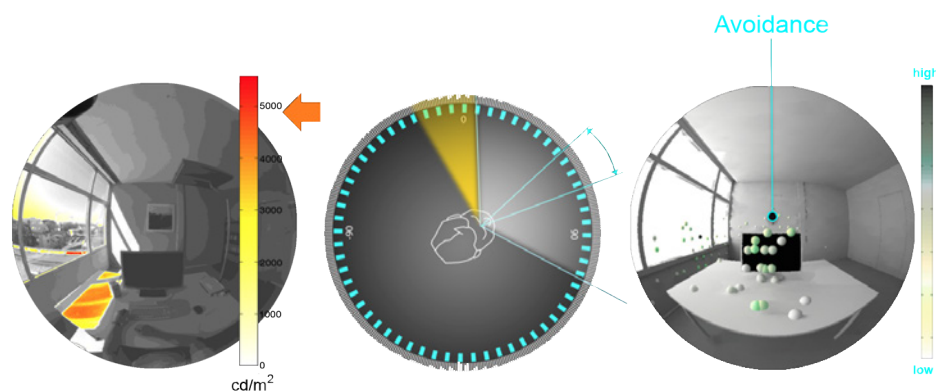


Figure VIII.1 – **Gaze avoidance:** significant statistical relation between the luminance variations and shift of gaze as a foothold for further development of a gaze direction model

The findings of this study and the developed approach can serve as a foothold for further development of a gaze responsive model (Figure:VIII.1). This model can predict "gaze responsive comfort zones" based on an initial gaze point and direction. The gaze responsive comfort zones are areas in space that

are more attractive or comfortable for gaze in terms of the luminous environment impact. Foremost, the challenge is to define a relation between view outside and the glare impact in a certain adaptation luminance level on gaze orientations (Figure: VIII.2). The ultimate goal is to introduce a range of gaze directions within which a space suitable for a glare-free daylighting exist.

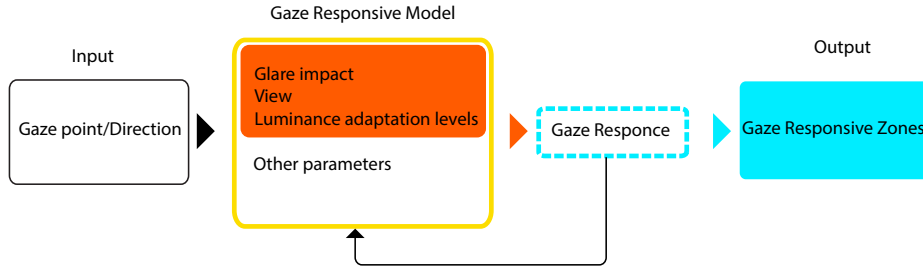


Figure VIII.2 – **Gaze avoidance**: a concept for a gaze responsive model to predicts the gaze response to independent variables glare impact and view.

A preliminary and conceptual representation of this model is shown in Figure:VIII.3a-b. This representation is a simplified model of the gaze response to "glare impact". The glare impact is defined as a linear combination of  $L_s, \omega_s$  divided by  $P$  for glare source  $l$  (see equation VIII.1).

As an input an initial gaze point and gaze direction is introduced to the model. An HDR image is produced produced from the initial gaze point and direction using *Radiance*. Processing of the HDR images using *Evalglare* results in calculation of several photometric quantities. Glare impact is used as a constant coefficient in a linear model to determine the angular gaze shift.

$$Glare\ Impact = \sum_{l=1}^n \frac{L_{s,l} \cdot \omega_{s,l}}{P_l} \tag{VIII.1}$$

The gaze shift is defined then by generating a rotation matrix.

A rotation matrix compromises of a matrix of angular rotations  $\gamma$ ,  $\beta$  and  $\alpha$  around the three axis from a defined gaze point.  $\gamma$  is a counter-clockwise rotation about the  $x$ -axis,  $\alpha$  is counter-clockwise rotation about the  $z$ -axis and  $\beta$  is a counter-clockwise rotation about the  $y$ -axis. The angular gaze shift here is based on  $\gamma$  and  $\alpha$  rotations and not  $\beta$ . The latter represents a head tilt. The assumption here is that there is no head tilt around the  $y$ -axis. The coordinate system here is defined in a way that  $y$ axis is straight from the gaze point, the positive  $x$ -axis is points to the right.

Finally, for each gaze vector a rotation matrix is generated (equation array VIII.3, VIII.4, VIII.4). The rotation matrix is used to shift the gaze vectors between the initial gaze point and the centre of the glare source. Each gaze direction was rotated about the respective relevant axes where the origin is the initial gaze position. An arbitrary initial shift angle was also considered in this model. The gaze responses which are shifted away from the centre of the glare sources based on the glare impact value are shown with a cyan sphere. Each sphere is a gaze point at the intersection of the gaze direction with

the geometry.

$$\mathbf{R}_x(\gamma) = \begin{vmatrix} 1 & 0 & 0 \\ 0 & \cos\gamma & -\sin\gamma \\ 0 & \sin\gamma & \cos\gamma \end{vmatrix} \quad (\text{VIII.2})$$

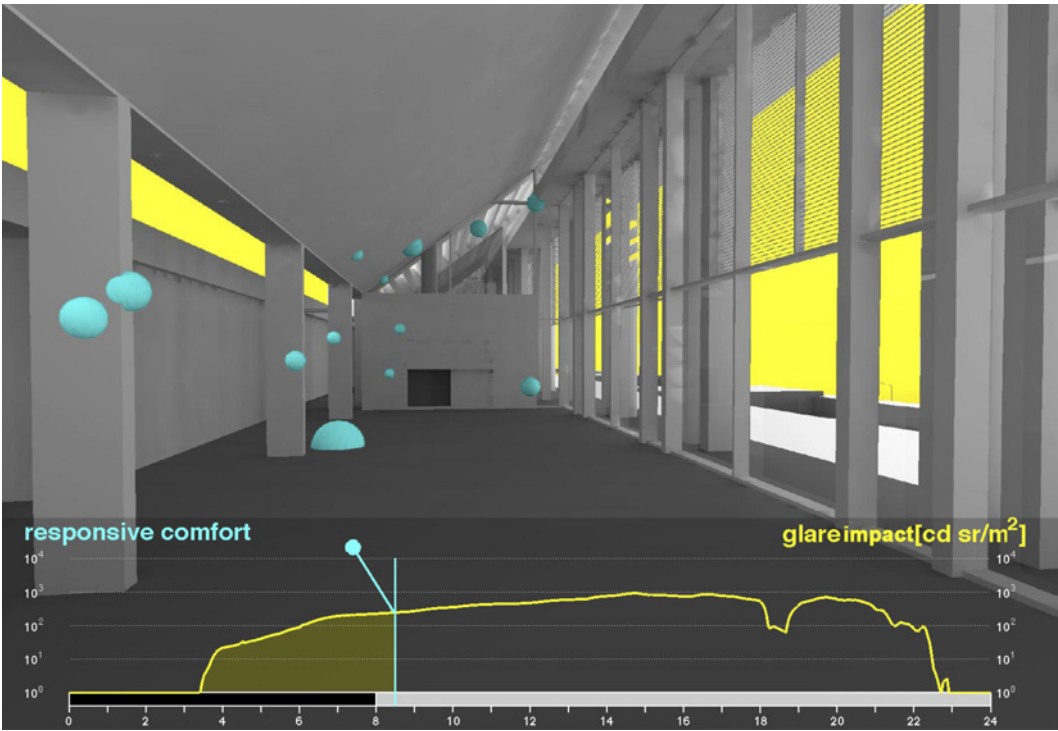
$$\mathbf{R}_y(\beta) = \mathbb{1} \quad (\text{VIII.3})$$

$$\mathbf{R}_z(\alpha) = \begin{vmatrix} \cos\alpha & -\sin\alpha & 0 \\ \sin\alpha & \cos\alpha & 0 \\ 0 & 0 & 1 \end{vmatrix} \quad (\text{VIII.4})$$

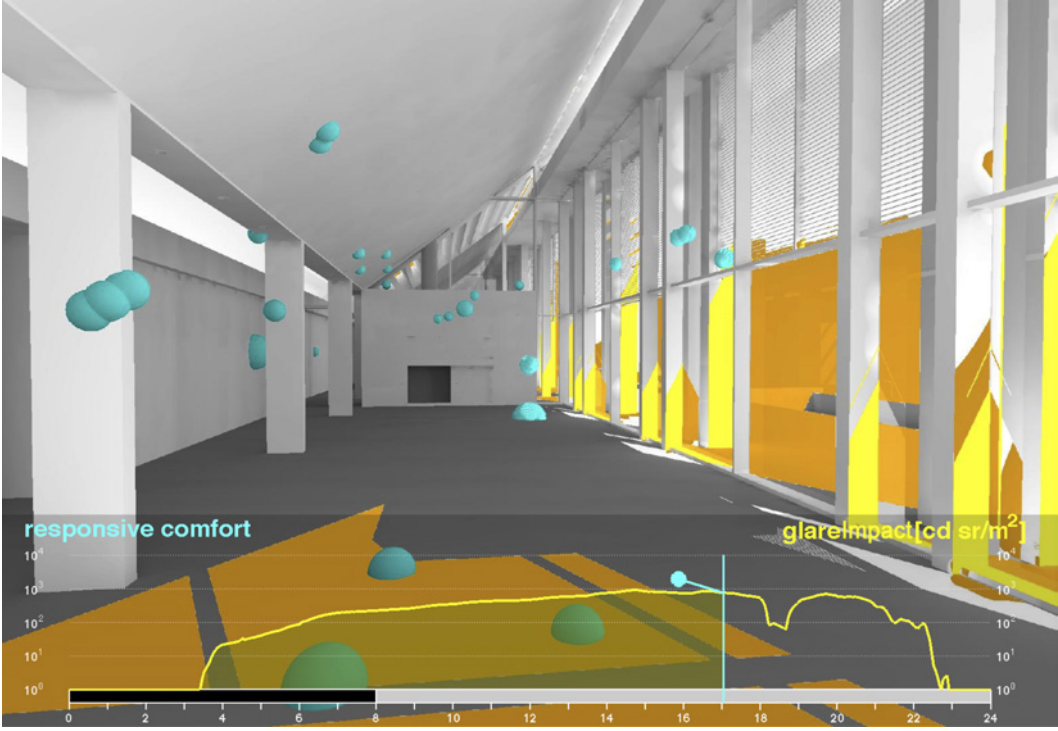
Where  $\gamma$  is a counter-clockwise rotation about the  $x$ -axis,  $\beta$  is a counter-clockwise rotation about the  $y$ -axis,  $\alpha$  is counter-clockwise rotation about the  $z$ -axis. It is important to note that  $R(\alpha, \beta, \gamma)$  performs the roll first, then the pitch, and finally the yaw.

The developed routine and the adopted tools are as follow:

- 1) Physically-based HDR renderings of space over time (*Radiance*)
- 2) Processing the HDR rendering (*Evalglare*)
- 3) Reading the data into *Matlab* (*Matlab*)
- 4) Glare impact is calculated (*Matlab*)
- 5) Arbitrary gaze vectors are derived based on the centre of glare sources (*Radiance*)
- 6) Rotation matrix is generated (*Matlab*)
- 7) Gaze responses are derived (*Matlab*)
- 8) Gaze responses are visualised (*Radiance*)



(a)



(b)

Figure VIII.3 – **Future perspective:** Gaze shifts as a response to the glare impact at different times of the day. The cyan spheres represent the gaze direction intersection with the geometry. The potential glare sources are highlighted in yellow. The variations in the glare source colour correspond to the glare source intensity.

### VIII.3. Application and Use in Perspective

Figure VIII.3 (a-b) show the illustrated results where the glare impacts are highlighted and the gaze responses to each glare source is shown with a cyan sphere where the intersection point of gaze and the geometry of the space. The figures present the variation of the glare impact over time. The gaze direction as response to each impact value is shown as a vector at each point. Figure VIII.4 is showing the same graphs at different days simulated over month June at latitude of 64° N and longitude of 21° W. The location was chosen based on the representational reasons at the time.

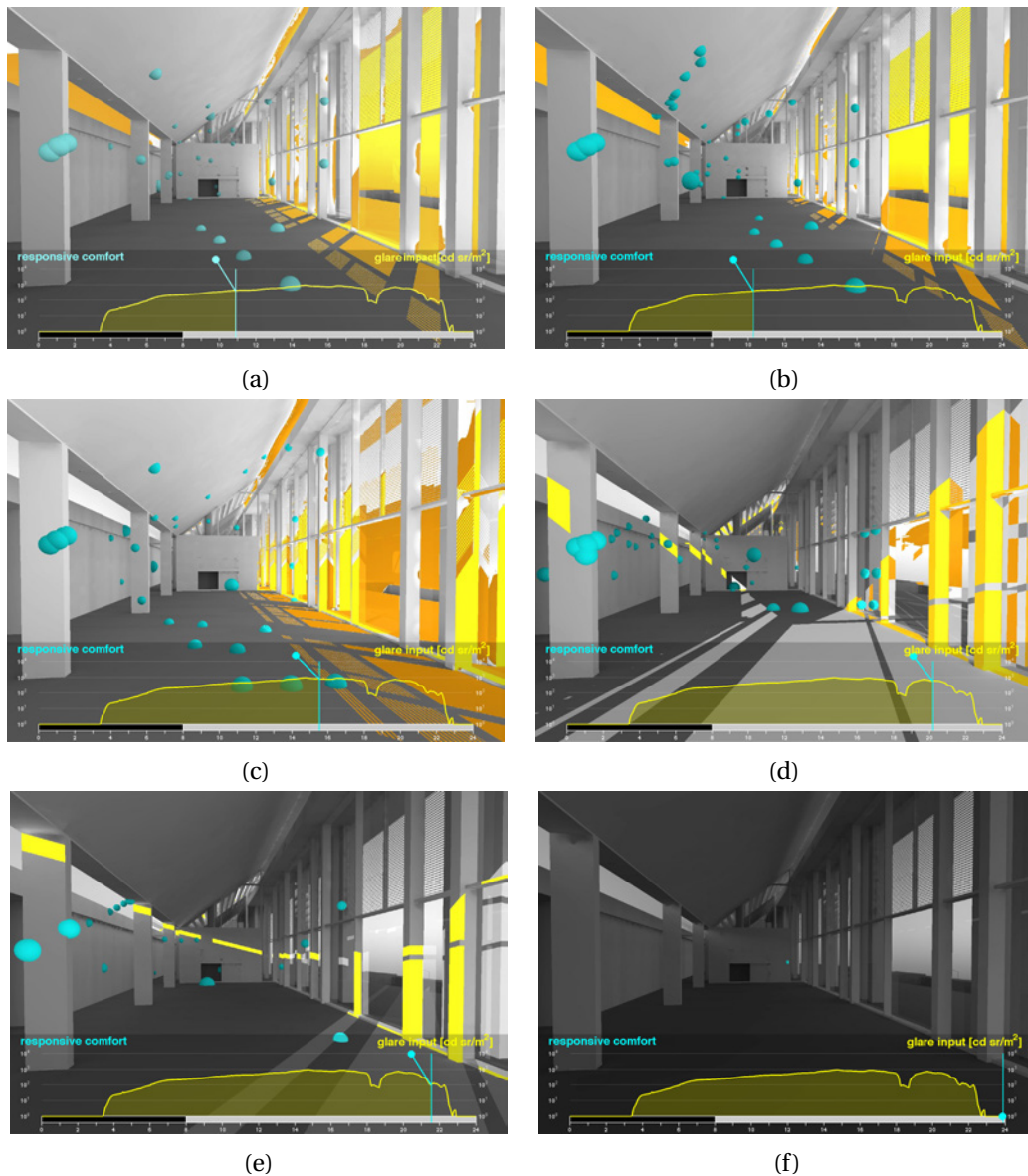


Figure VIII.4 – **Future perspective:** Gaze response to glare impact are visualised over time.

### VIII.4 Future steps

The present study has provided the proof of principle that gaze direction cannot be ignored or assumed to be fixed when evaluating glare for visual discomfort. This work has led to the achievement of an innovative approach for understanding gaze behaviour in relation to glare. A foothold has been created for dynamic discomfort glare assessments toward a gaze responsive design. In a comprehensive set of experiments influence of 6 different lighting conditions, view outside the window and task on gaze was investigated. The performed experiments, with a large sample size for high statistical significance, are a basis for further future investigation and developments.

Several enhancement possibilities based on the findings of this study can be considered before reaching solid developments.

For further improvement of the developed gaze-driven approach we need to overcome several limitations of the current study. Namely, sensitivity analyses on determining glare detection parameters, e.g. glare source threshold and search radius, and the spatial dispersion frequency for dominant gaze identification. Overcoming the error caused by the camera positions by adopting newer technologies would refine the final luminance measures. Moreover, the adoption of gaze tracking technologies that interfere minimally with participants' natural behaviour should be considered

The final results presented in this study considered the illuminance at the eye level as the eye adaptation level and an independent variable of light. Obviously, more investigation on the effect of light variations on gaze shifts, with focus on other photometric parameters that are relevant to visual discomfort, is needed. The luminance distribution in different parts of the FOV and their effect on is one of these measures. Several measures of lighting conditions were tested in this study and will be considered in the final version of this thesis. Moreover, other visual system characteristics, such as contrast sensitivity or behaviours such as blinks and pupil oscillations, should be studied in order to have a better understanding of visual system responses to light variations in the FOV.

In future steps, the two approaches will be evaluated against subjective assessments of discomfort glare. This evaluation will demonstrate whether a gaze-driven luminance estimation in relation to the subjective assessments gives a better prediction for risk of discomfort glare situations than when using the fixed view assumption.

Finally, an essential issue is trying to understand the iterative mechanism of the gaze shift in relation to light. Gaze-shifts and light variations are inter dependent meaning that with each shift of gaze the eye is exposed to a new luminance field and the re-adaptation could lead to a new gaze response. The intuitive understanding of this mechanism suggests that gaze shifts in order to find a comfortable adaptation luminance level.



The integration of a dynamic gaze parameter into the glare prediction models can strengthen the prediction power of these models for a more accurate glare risk evaluation.

The developed approach demonstrates the need to integrate observed gaze direction patterns into visual comfort assessments. Gaze direction is an important parameter for glare risk evaluation and integration of a dynamic gaze parameter into the glare prediction models strengthens the prediction power of these models for a more accurate glare risk evaluation. To reach this end we need to overcome several limitations of the current study. Namely, sensitivity analyses on determining glare detection parameters, e.g. glare source threshold and search radius, the spatial dispersion frequency for dominant gaze identification.



# Appendices



# **A Questionnaire**



**Vom Versuchsleiter auszufüllen:**

System:

Zeit:

Versuchspersonennummer:

Q <sub>1</sub>	Q <sub>2</sub>	R	Q <sub>3</sub>	Q <sub>4</sub>	eye

**Einverständniserklärung:**

Hiermit bestätige ich, dass ich über folgendes Aufgeklärt wurde:

1. Die Teilnahme ist freiwillig und kann jederzeit ohne Angabe von Gründen abgebrochen werden, ohne dass sich daraus negative Konsequenzen ergeben.
2. Die erhobenen Daten werden vertraulich behandelt und nur vom damit betrauten wissenschaftlichen Personal verarbeitet.
3. Ich stimme der Veröffentlichung der aus den Daten gewonnenen Erkenntnisse zu.
4. Ich wurde über den Ablauf der Versuche aufgeklärt.

Mit meiner Unterschrift bestätige ich, dass ich an diesem Nutzerakzeptanztest zur Bewertung von Blendungsempfinden bei verschiedenen Verschattungssystemen und Ausblicken teilnehmen möchte.

Name: \_\_\_\_\_

Unterschrift: \_\_\_\_\_

Freiburg im Breisgau, den, \_\_\_\_\_

**Fragen zu Ihrer Person**

**1. Tragen Sie bei büroähnlichen Arbeiten normalerweise eine Brille oder Kontaktlinsen?  
Wenn ja, bitte ankreuzen:**

Kontaktlinsen (auch wenn selten bitte ankreuzen)

Brille (auch wenn selten bitte ankreuzen)

**2. Sind sie Links- oder Rechtshänder?**

Rechtshänder

Linkshänder

**3. Geschlecht?**

weiblich

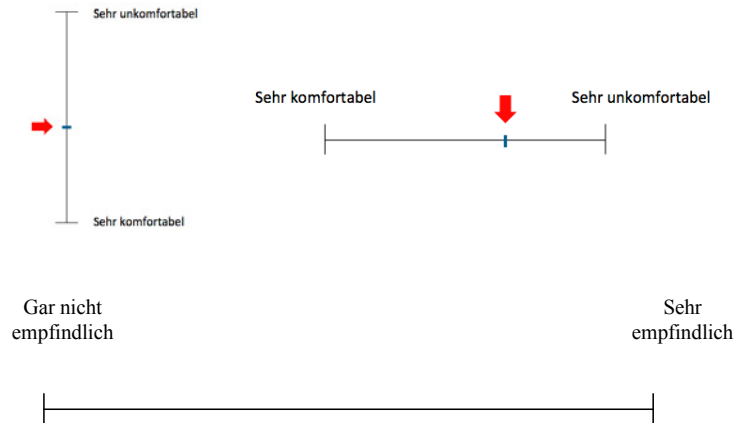
männlich

**4. Alter?**

\_\_\_\_\_ Jahre

**5. Halten sie sich für empfindlich gegenüber hellerem Licht?**

Beispiel für die Beantwortung dieses Fragentyps:



**6. Welche Kategorie beschreibt ihren Job am besten?**

- |                                      |  |
|--------------------------------------|--|
| <input type="checkbox"/> Verwaltung  | <input type="checkbox"/> Technisch, Wissenschaftlich |
| <input type="checkbox"/> Sekretär/in | <input type="checkbox"/> Leitend                     |
| <input type="checkbox"/> Student     | <input type="checkbox"/> Andere: _____               |

**9. Haben Sie momentan eine der folgenden gesundheitlichen Einschränkungen?**

Wenn ja, bitte ankreuzen:

- |  |  |
|--|--|
| <input type="checkbox"/> Leichte Erkältung | <input type="checkbox"/> Augentränen                   |
| <input type="checkbox"/> Leichte Schmerzen | <input type="checkbox"/> Konzentrationsschwierigkeiten |
| <input type="checkbox"/> Unwohlsein        | <input type="checkbox"/> Andere: _____                 |

**10. Wie unglücklich oder glücklich fühlen Sie sich im Moment?**

Sehr unglücklich      sehr glücklich

**11. Wie ruhig oder aufgeregt fühlen Sie sich im Moment?**

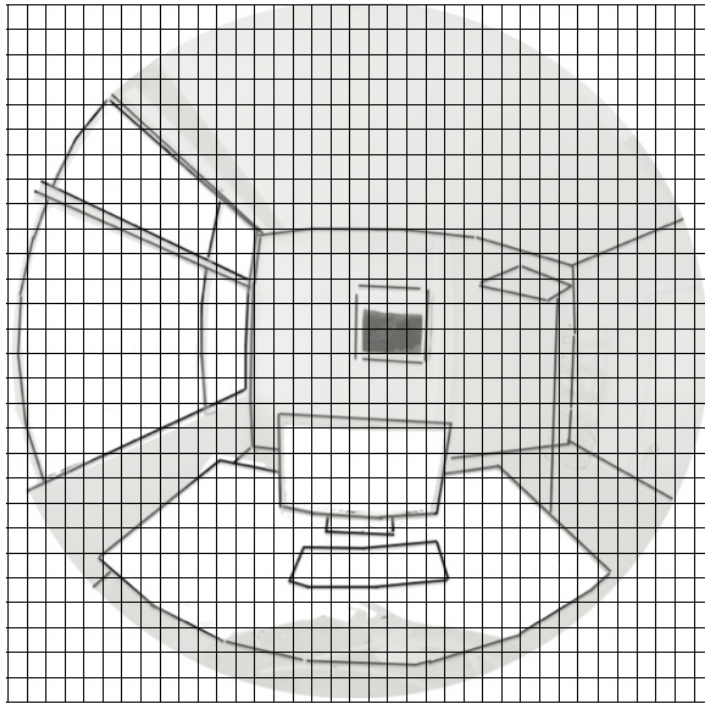
Sehr ruhig      sehr aufgeregt

**12. Wie selbstbestimmt fühlen Sie sich im Moment?**

Selbstbestimmt      fremdbestimmt



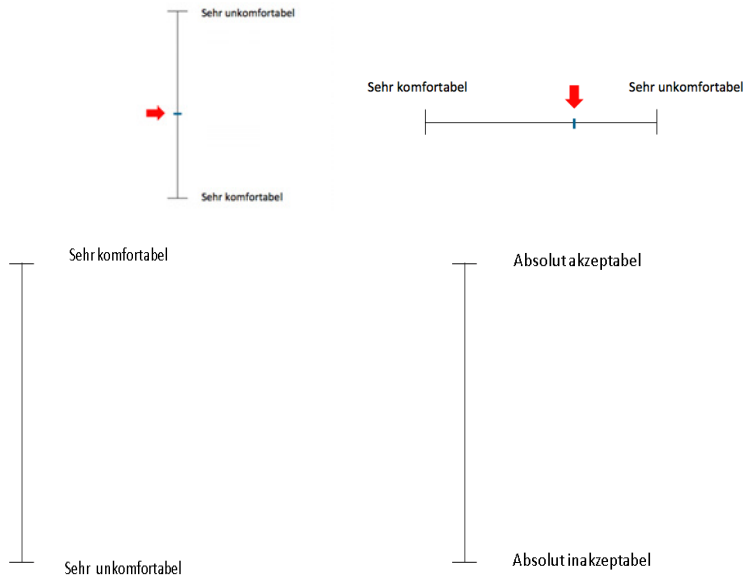
13. Bitte markieren Sie die Teile des Rasters, die den Teilen dieses Raumes (nicht auf dem Bild) entsprechen, in denen Sie die Blendung unbehaglich bzw. inakzeptabel finden. Bitte markieren sie dabei soviel von der Blendquelle wie möglich.



13. Bitte markieren Sie alle Optionen, die Belichtungssituation in diesem Büro beschreiben (Mehrfachnennungen möglich)

- düster
- dämmrig
- angenehm
- hell
- Blendung

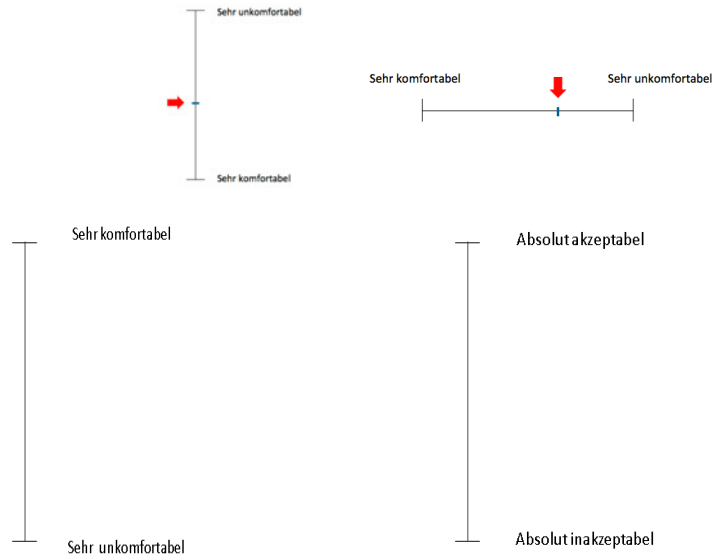
15. Bitte bewerten Sie die Beleuchtung des Raumes, unter der Annahme, dass Sie Ihre alltägliche Büroarbeit unter diesen Beleuchtungsbedingungen verrichten müssten."



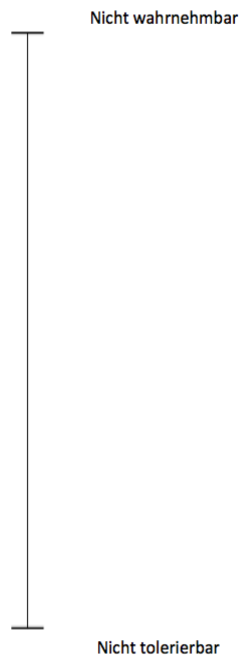
16. Bitte markieren Sie den Grad der Blendung den Sie gerade empfinden.



17. Bitte bewerten Sie die Beleuchtung des Raumes, unter der Annahme, dass Sie Ihre alltägliche Büroarbeit unter diesen Beleuchtungsbedingungen verrichten müssten."



18. Bitte markieren Sie den Grad der Blendung, den Sie während der Aufgabe empfanden.





# **B Office task sequence**

**On paper example**



Text Number 2

Roberto Cabeza von der Duke University in North Carolina hat gemeinsam mit einem koreanischen Kollegen Hinweise darauf entdeckt, wo im Gehirn Déjà-vus entstehen. Wie leicht es ist, Menschen falsche Erinnerungen einzupflanzen, zeigte auch die amerikanische Psychologin Elizabeth Loftus schon in den neunziger Jahren. Sie brachte ihre Versuchspersonen dazu, detaillierte Erinnerungen an ein unangenehmes Kindheitserlebnis zu entwickeln. Dabei half ein Familienmitglied der Probanden, das heimlich mit der Psychologin kooperierte. Beispielsweise der ältere Bruder, der eine angeblich alte Geschichte aufbrachte: Die Versuchsperson sei mit fünf Jahren einmal in einem Kaufhaus verlorengegangen, ein älterer Herr im Flanellhemd habe sie dann an der Hand genommen und zur schon verzweifelt suchenden Mutter zurückgebracht. Kurz darauf fielen den so Genarrten sogar Details wie die Stimme des Helfers im Flanellhemd wieder ein. Dabei hatte das Ereignis niemals stattgefunden, die Erinnerungen waren erzeugt.

Am Ende dieser Aufgabe hören Sie einen Ton. Bitte blättern Sie dann um.



Wie ist Ihre Meinung zu dem Inhalt des Textes?

Sie haben jetzt die Möglichkeit, für ein paar Minuten über den Text nachzudenken

Am Ende dieser Aufgabe hören Sie einen Ton. Bitte blättern Sie dann um.

Was glauben Sie, wie einfach es ist, anderen eine fiktive Erinnerung glaubhaft zu machen?

Sehr einfach

Einfach

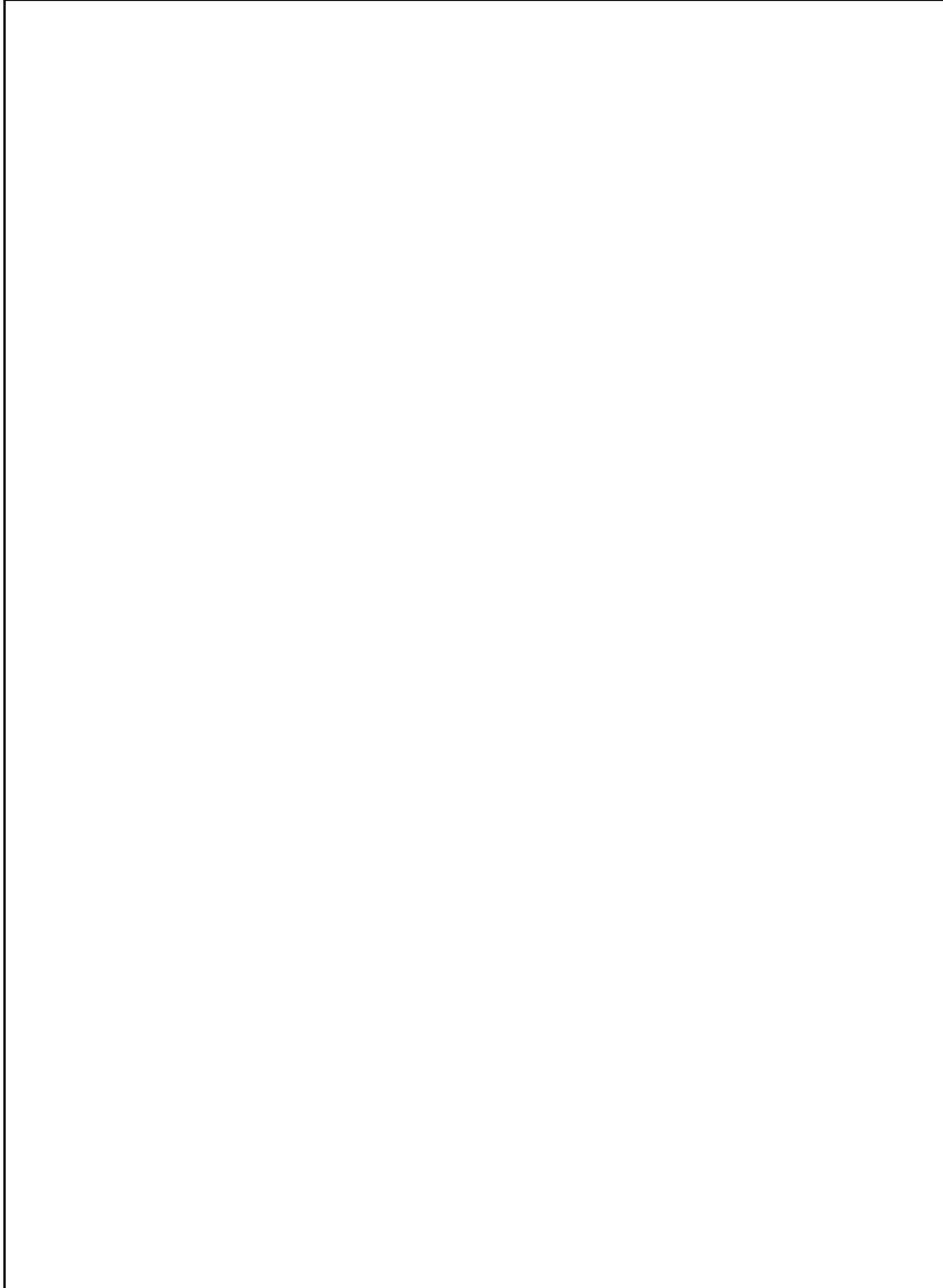
Nicht so einfach

Schwer

Am Ende dieser Aufgabe hören Sie einen Ton. Bitte blättern Sie dann um.

Bitte schreiben Sie Ihre Meinung über den Inhalt des Textes auf.

Schreiben Sie dazu Ihren Text in den Rahmen unterhalb. Sie haben dazu 3 Minuten Zeit.

A large, empty rectangular box with a thin black border, intended for the participant to write their opinion on the text's content within a three-minute time limit.

Ende dieser Testphase



## **C Nomenclature**



All the symbols relating to the parameters and variables used in this thesis are listed here as a nomenclature list.

$BGI$	British Glare Index
$CGI$	CIE Glare Index
$C_l$	Luminance contrast
$D$	Distance between eye and plane of glare source [mm]
$DGI$	Daylight Glare Index
$DGI_N$	New Daylight Glare Index
$DGP$	Daylight Glare Probability
$\bar{DGP}$	Averaged DGP of the data sample
$df$	Degree of freedom
$e_{1-4}$	Model-specific parameters
$E_d$	Direct vertical illuminance at the eye due to all glare sources [lux]
$E_i$	Indirect illuminance at the eye ( $E_i = \pi \times L_b$ ) [lux]
$E_v$	Illuminance at the vertical level
$E_{vg}$	Illuminance at the eye (gaze) level
$E_{vf}$	Illuminance at the vertical level at the fixed camera position
$\bar{E}_v$	Averaged illuminance at the vertical level of the data sample
$F_{avg}$	Average luminance of the window, floor, ceiling and glare sources
$F$	F ratio
$f$	Effect size
$\hat{\mathbf{g}}$	Gaze (gaze-in-world) direction
$g$ -value	Solar energy transmittance of glass: total solar heat gain / incident solar radiation [-]
$H$	Vertical distance between source and gaze direction [mm]
$k$	number of sample groups means
$L_a$	Adaptation Luminance
$L_{adapt}$	Average vertical unshielded luminance in the FOV [ $\text{cd}/\text{m}^2$ ]
$L_b$	Luminance of the background excluding the glare sources
$L_c$	Luminance of the ceiling [ $\text{cd}/\text{m}^2$ ]
$L_{ext}$	Average vertical unshielded luminance of the exterior [ $\text{cd}/\text{m}^2$ ]
$L_f$	Luminance of the floor [ $\text{cd}/\text{m}^2$ ]
$L_j$	Luminance of pixel $j$ [ $\text{cd}/\text{m}^2$ ]
$L_l$	Luminance of pixel $l$ [ $\text{cd}/\text{m}^2$ ]
$L_m$	Average luminance [ $\text{cd}/\text{m}^2$ ]
$\bar{L}_m$	Average luminance of the data sample [ $\text{cd}/\text{m}^2$ ]
$L_r$	Luminance of a reference area [ $\text{cd}/\text{m}^2$ ]
$L_s$	Luminance of a glare source [ $\text{cd}/\text{m}^2$ ]

## Appendix C. Nomenclature

---

$\bar{L}_s$	Average luminance of glare sources of the data sample [cd/m <sup>2</sup> ]
$L_{s,i}$	Luminance of a glare source $i$
$L_{s,j}$	Luminance of a glare source $j$
$L_{s,l}$	Luminance of a glare source $l$
$L_w$	Luminance of the window [cd/m <sup>2</sup> ]
$L_{window}$	Average vertical shielded luminance of the window [cd/m <sup>2</sup> ]
$m$	Mean of each data sample group
$m_i$	Mean of the whole data sample
$MS$	Mean square
$\bar{m}$	The centre of distribution
$P_i$	Position Index of source $i$
$P_l$	Position Index of source $l$
$P_1$	Point 1 at the camera position
$P_2$	Gaze vector intersection point with the geometry
<b>Q</b>	Quaternion rotation operator
$r$	Search radius implemented in glare detection algorithms
$R_x$	Rotation matrix around $x$ -axis
$R_y$	Rotation matrix around $y$ -axis
$R_z$	Rotation matrix around $z$ -axis
$SS$	Sum of squares
$\hat{v}$	Gaze vector from the camera point of view
$VCP$	Visual Comfort Probability
$UGR$	Unified Glare Rating
$U$ -value	Overall heat transfer coefficient [W/m <sup>2</sup> K]
$\vec{w}$	Head-fixed axis
$x_{multiplier}$	Threshold multiplier to detect glare sources in glare detection algorithms
$\alpha$	Rotation angle around $z$ -axis
$\beta$	Rotation angle around $y$ -axis
$\gamma$	Rotation angle around $x$ -axis
$\theta_j$	Angle between pixel $j$ and the optic axis [rad]
$\theta$	Elevation angle between -90° & 90° [deg]
$\theta_g$	Vertical gaze orientation[rad]
$\rho_{ceiling}$	Total reflectance of ceiling in visible spectrum
$\rho_{floor}$	Total reflectance of floor in visible spectrum
$\rho_{wall}$	Total reflectance of wall in visible spectrum
$\sigma$	Angle between the gaze direction and the line between the eye the glare source
$\sigma_m$	square root of average sum of squares of all sample means



---

$\tau_{\perp}$	total transmission of glazing in visible spectrum for perpendicular angle of incidence [-]
$\tau$	Angle between the vertical plane of gaze direction and the glare source
$\phi$	Azimuth angle between $-180^{\circ}$ & $180^{\circ}$ [deg]
$\phi_g$	Horizontal gaze orientation [rad]
$\omega_c$	Solid angle of ceiling area subtended at the eye [sr]
$\omega_f$	Solid angle of floor area subtended at the eye [sr]
$\omega_j$	Solid angle of pixel $j$ [sr]
$\omega_{pN}$	Solid angle of the glare source modified to include window configuration and observation position
$\omega_s$	Solid angle of source subtended at the eye [sr]
$\Omega_s$	Solid angle of source modified for position factor
$\omega_{s,i}$	Solid angle of glare source $i$ subtend at the eye [lux]
$\omega_{s,j}$	Solid angle of glare source $j$ subtend at the eye [lux]
$\omega_{s,l}$	Solid angle of glare source $l$ subtend at the eye [lux]
$\bar{\omega}_s$	Averaged solid angle subtended at the eye of all detected glare sources [sr]
$\omega_w$	Solid angle of window subtended at the eye [sr]
$\bar{\#} L_s$	Average number of detected glare source



# Bibliography

- [1] Barbara Matusiak. The impact of lighting/daylighting and reflectances on the size impression of the room. full-scale studies. *Architectural Science Review*, 47(2):115–119, 2004.
- [2] Mary Guzowski. *Daylighting for sustainable design*. McGraw-Hill New York, NY, 2000.
- [3] Jennifer A Veitch. Psychological processes influencing lighting quality. *Journal of the Illuminating Engineering Society*, 30(1):124–140, 2001.
- [4] G Newsham, C Arsenault, J Veitch, A Tosco, and C Duval. Task lighting effects on office worker satisfaction and performance, and energy efficiency. *Leukos*, 1(4):7–26, 2005.
- [5] Werner K E Osterhaus. Discomfort glare assessment and prevention for daylight applications in office environments. *Solar Energy*, 79(2):140–158, 2005.
- [6] A R Webb. Considerations for lighting in the built environment: Non-visual effects of light. *Energy and Buildings*, 38(7):721–727, July 2006.
- [7] George C. Brainard, John P. Hanifin, Jeffrey M. Greeson, Brenda Byrne, Gena Glickman, Edward Gerner, and Mark D. Rollag. Action spectrum for melatonin regulation in humans: Evidence for a novel circadian photoreceptor. *The Journal of Neuroscience*, 21(16):6405–6412, August 2001.
- [8] Steven W. Lockley, Erin E. Evans, Frank A. Scheer, George C. Brainard, Charles A. Czeisler, and Daniel Aeschbach. Short-wavelength sensitivity for the direct effects of light on alertness, vigilance, and the waking electroencephalogram in humans. *Sleep*, 29(2):161–168, February 2006.
- [9] C Cuttle. Identifying the human values associated with windows. *International Daylighting*, 5:3–6, 2002.
- [10] JJ Kim and J Wineman. Are windows and views really better? a quantitative analysis of the economic and psychological value of views. *Report, University of Michigan*, 2005.
- [11] Anca D Galasiu and Jennifer A Veitch. Occupant preferences and satisfaction with the luminous environment and control systems in daylit offices: a literature review. *Energy and Buildings*, 38(7):728–742, 2006.

## Bibliography

---

- [12] Basel Infrac AG Bern TEP Energy GmbH, Prognos AG. Analysis of energy consumption by specific use/analyse des schweizerischen energieverbrauchs 2000-2013 nach verwendungszwecken. BFE, 2014.
- [13] M Bodart and A De Herde. Global energy savings in offices buildings by the use of daylighting. *Energy and Buildings*, 34(5):421–429, 2002.
- [14] Mithra Moezzi and John Goins. Text mining for occupant perspectives on the physical workplace. *Building Research & Information*, 39(2):169–182, 2011.
- [15] Benjamin T Vincent, Roland Baddeley, Alessia Correani, Tom Troscianko, and Ute Leonards. Do we look at lights? using mixture modelling to distinguish between low-and high-level factors in natural image viewing. *Visual Cognition*, 17(6-7):856–879, 2009.
- [16] A Nuthmann and W Einhäuser. A new approach to modeling the influence of image features on fixation selection in scenes. *The New York Academy of Scientists*, In press.
- [17] Philipp M. Sury, Sylvia Hubalek, and Christoph Schierz. *A first step on eye movements in office settings: Eine explorative Studie zu Augenbewegungen im Büroalltag*, volume 51. GRIN Verlag, 2010.
- [18] S Kokoschka and P Haubner. Luminance ratios at visual display workstations and visual performance. *Lighting research and Technology*, 17(3):138–144, 1985.
- [19] Peter Robert Boyce. *Human factors in lighting*. Crc Press, 2014.
- [20] Martin G Helander and Lijian Zhang. Field studies of comfort and discomfort in sitting. *Ergonomics*, 40(9):895–915, 1997.
- [21] Werner Osterhaus. Design guidelines for glare-free daylight work environments. In *Presentation at 3rd VELUX Daylighting Symposium, Rotterdam*, 2009.
- [22] Martine Velds. *Assessment of lighting quality in office rooms with daylighting systems*. PhD thesis, Delft University of Technology, 1999.
- [23] International Commission On Illumination (CIE). INTERNATIONAL LIGHTING VOCABULARY. *Central Bureau of the Commission Internationale de l'Eclairage, Kegelgasse*, 27, 1989.
- [24] M Luckiesh and S K Guth. Brightness in visual field at borderline between comfort and discomfort (BCD). *Illuminating engineering*, 1949.
- [25] Wonwoo Kim, Hyunjoo Han, and Jeong Tai Kim. The position index of a glare source at the borderline between comfort and discomfort (BCD) in the whole visual field. *Building and Environment*, 44(5):1017–1023, 2009.
- [26] SK Guth. Light and comfort. *Industrial medicine & surgery*, 27(11):570–574, 1958.

- [27] Robert D Clear. Discomfort glare: What do we actually know? *Lighting Research and Technology*, 2012.
- [28] T Iwata, N Somekawa, M Shukuya, and K Kimura. Subjective response on discomfort glare caused by windows. *Proceedings of the 22nd Session of the CIE, Division*, 3:108–109, 1991.
- [29] W Kim and Y Koga. Effect of local background luminance on discomfort glare. *Building and Environment*, 39(12):1435–1442, 2004.
- [30] CODE CIBSE. Code for interior lighting. *London: The Chartered Institution of Building Services Engineers*, 1994.
- [31] Sylvia Hubalek and Christoph Schierz. Lichtblick–photometrical situation and eye movements at vdu work places. In *CIE Symposium*, volume 4, pages 322–324, 2004.
- [32] J Alstan Jakubiec and Christoph F Reinhart. The ‘adaptive zone’—a concept for assessing discomfort glare throughout daylight spaces. *Lighting Research and Technology*, 44(2):149–170, 2012.
- [33] J Winter. Typical eye fixation areas of car drivers in inner-city environments at night. In *LUXEU-ROPA*, 2013.
- [34] Ingrid Heynderickx, J Ciocoiu, and Xiaoyan Zhu. Estimating eye adaptation for typical luminance values in the field of view while driving in urban streets. *Light & Engineering*, 21(4), 2013.
- [35] Steve Fotios, Jim Uttley, and Naoya Hara. Critical pedestrian tasks: Using eye-tracking within a dual task paradigm. In *Proceedings of the CIE Centenary Conference “Towards a New Century of Light”*, pages 234–240. Sheffield, 2013.
- [36] S Fotios, J Uttley, C Cheal, and N Hara. Using eye-tracking to identify pedestrians’ critical visual tasks. part 1. dual task approach. *Lighting Research and Technology*, page 1477153514522472, 2014.
- [37] Johannes J Vos. Reflections on glare. *Lighting Research and Technology*, 35:163–176, 2003.
- [38] P Stone. A model for the explanation of discomfort and pain in the eye caused by light. *Lighting Research and Technology*, 41(2):109–121, 2009.
- [39] Johannes J Vos. Glare today in historical perspective: Towards a new cie glare observer and a new glare nomenclature. *International Commission On Illumination (CIE)*, 133(1):38–42, 1999.
- [40] Marie-Claude Dubois. Shading devices and daylight quality: an evaluation based on simple performance indicators. *Lighting Research and Technology*, 35(1):61–76, March 2003.
- [41] Pedro Correia da Silva, Vítor Leal, and Marilyne Andersen. Influence of shading control patterns on the energy assessment of office spaces. *Energy and Buildings*, 50:35–48, 2012.
- [42] Glenn A Fry and Vincent M King. The pupillary response and discomfort glare. *Journal of the Illuminating Engineering Society*, 4(4):307–324, 1975.

## Bibliography

---

- [43] S M Berman, M A Bullimore, R J Jacobs, I L Bailey, and N Gandhi. An objective measure of discomfort glare. *Journal of Illuminating Engineering Society*, 1994.
- [44] PA Howarth, G Heron, DS Greenhouse, IL Bailey, and SM Berman. Discomfort from glare: The role of pupillary hippus†. *Lighting Research and Technology*, 25(1):37–42, 1993.
- [45] Jan Wienold and Jens Christoffersen. Evaluation methods and development of a new glare prediction model for daylight environments with the use of CCD cameras. *Energy and Buildings*, 38(7):743–757, July 2006.
- [46] N Tuaycharoen and PR Tregenza. View and discomfort glare from windows. *Lighting Research and Technology*, 39(2):185–200, 2007.
- [47] Michael Sivak, Michael Flannagan, Michael Ensing, and Carole J Simmons. Discomfort glare is task dependent. Technical report, 1989.
- [48] Olov Östberg, Peter T Stone, and Robert A Benson. *Free magnitude estimation of discomfort glare and working task difficulty*. University of Göteborg, Department of Psychology, 1975.
- [49] Susanne Fleischer, Helmut Krueger, and Christoph Schierz. Effect of brightness distribution and light colours on office staff. In *The 9th European Lighting Conference Proceeding Book of Lux Europa*, pages 77–80, 2001.
- [50] T Iwata and M Tokura. Position index for a glare source located below the line of vision. *Lighting Research and Technology*, 29(3):172–178, 1997.
- [51] Ian Ashdown. Sensitivity analysis of glare rating metrics. *Leukos*, 2(2):115–122, 2005.
- [52] Ali A Nazzal. A new daylight glare evaluation method. *Journal of Light & Visual Environment*, 24(2):19–27, 2000.
- [53] Michelle Eble-Hankins. *Subjective impression of discomfort glare from sources of non-uniform luminance*. PhD thesis, University of Nebraska, 2008.
- [54] M Rubiño, A Cruz, JA Garcia, and E Hita. Discomfort glare indices: a comparative study. *Applied optics*, 33(34):8001–8008, 1994.
- [55] Martine Velds. User acceptance studies to evaluate discomfort glare in daylit rooms. *Solar energy*, 73(2):95–103, 2002.
- [56] K Fisekis and M Davies. Prediction of discomfort glare from windows. *Lighting Research and Technology*, 35:360–371, 2003.
- [57] Wonwoo Kim and Yasuko Koga. Glare constant gw for the evaluation of discomfort glare from windows. *Solar Energy*, 78(1):105–111, 2005.
- [58] P Chauvel, JB Collins, R Dogniaux, and J Longmore. Glare from windows: current views of the problem. *Lighting research and Technology*, 14(1):31–46, 1982.

- [59] R G Hopkinson. Glare from daylighting in buildings. 3(4):206–215, 1972.
- [60] Jan Wienold. Dynamic daylight glare evaluation. In *Proceedings of Building Simulation*, pages 27–30, 2009.
- [61] Hester Hellenga. *Daylight and view: The influence of windows on the visual quality of indoor spaces*. PhD thesis, Technische Univeriteit Delft, Netherlands, 2013.
- [62] Jan Wienold. *Daylight glare in offices*. PhD thesis, Fraunhofer-Verl., Stuttgart, 2010.
- [63] Percy W. Cobb and Frank K. Moss. Glare and the four fundamental factors in vision. *Trans. Illum. Eng. Soc*, 23:1104–1120, 1928.
- [64] M.B. Hirning, G.L. Isoardi, S. Coyne, V.R. Garcia Hansen, and I. Cowling. Post occupancy evaluations relating to discomfort glare: A study of green buildings in brisbane. *Building and Environment*, 59:349–357, January 2013.
- [65] Kevin Van Den Wymelenberg and Mehlika Inanici. A critical investigation of common lighting design metrics for predicting human visual comfort in offices with daylight. *LEUKOS*, 10(3):145–164, 2014.
- [66] M.B. Hirning, G.L. Isoardi, and I. Cowling. Discomfort glare in open plan green buildings. *Energy and Buildings*, 70:427–440, February 2014.
- [67] Ralph Galbraith Hopkinson and John Bryan Collins. *The ergonomics of lighting*. 1970.
- [68] Mark Stanley Rea. *The IESNA lighting handbook: reference & application*. Illuminating Engineering Society of North America, New York, NY, 2000.
- [69] K. Parpairi, N. V. Baker, K. A. Steemers, and R. Compagnon. The luminance differences index: a new indicator of user preferences in daylit spaces. *Lighting Research and Technology*, 34(1):53–66, March 2002.
- [70] JJ Meyer, D Francioli, and H Kerhoven. A new model for the assessment of visual comfort at vdt-workstations. In *Proc. of the Xth Annual International Occupational Ergonomics and Safety Conference: Advances in Occupational Ergonomics and Safety*, volume 1, pages 233–238, 1996.
- [71] M. Van Den Wymelenberg Inanici. The effect of luminance distribution patterns on occupant preference in a daylit office environment. *Leukos*, 7:103–122, 2010.
- [72] L. Loe, K.P. Mansfield, and E. Rowlands. Appearance of lit environment and its relevance in lighting design: Experimental study. *Lighting Research and Technology*, 26(3):119–133, January 1994.
- [73] D.K. Tiller and J.A. Veitch. Perceived room brightness: Pilot study on the effect of luminance distribution. *Lighting Research and Technology*, 27(2):93–101, June 1995.

## Bibliography

---

- [74] Mehlika Inanici and M Navvab. The virtual lighting laboratory: Per-pixel luminance data analysis. *Leukos*, 3(2):89–104, 2006.
- [75] RJ Krauzlis. Eye movements. *Fundamental Neuroscience*, pages 775–792, 2008.
- [76] Dario D Salvucci and Joseph H Goldberg. Identifying fixations and saccades in eye-tracking protocols. In *Proceedings of the 2000 symposium on Eye tracking research & applications*, pages 71–78. ACM, 2000.
- [77] Bernard Marius't Hart and Wolfgang Einhäuser. Mind the step: complementary effects of an implicit task on eye and head movements in real-life gaze allocation. *Experimental brain research*, 223(2):233–249, 2012.
- [78] Mark D. Fairchild, Garrett M. Johnson, Jason Babcock, and Jeff B. Pelz. Is your eye on the ball?: Eye tracking golfers while putting. *Unpublished manuscript, Rochester Institute of Technology*, 2001.
- [79] Guy Buswell, Thomas. How people look at pictures:a study of the psychology of perception in art. Technical report, Chicago: Universityof Chicago Press., 1935.
- [80] Alfred Yarbus, L. *Eye movements and vision*. New York: Plenum Press., 1967.
- [81] Laurent Itti, Christof Koch, and Ernst Niebur. A model of saliency-based visual attention for rapid scene analysis. 20(11):1254–1259, 1998.
- [82] John M. Henderson, James R. Brockmole, Monica S. Castelhana, and Michael Mack. Visual saliency does not account for eye movements during visual search in real-world scenes. *Eye movements: A window on mind and brain*, pages 537–562, 2007.
- [83] Vidhya Navalpakkam and Laurent Itti. Modeling the influence of task on attention. *Vision Research*, 45(2):205–231, January 2005.
- [84] Wolfgang Einhäuser, Ueli Rutishauser, and Christof Koch. Task-demands can immediately reverse the effects of sensory-driven saliency in complex visual stimuli. *Journal of Vision*, 8(2):2, 2008.
- [85] Antonio Torralba, Aude Oliva, Monica S. Castelhana, and John M. Henderson. Contextual guidance of eye movements and attention in real-world scenes: the role of global features in object search. *Psychological review*, 113(4):766, 2006.
- [86] C. A. Rothkopf, D. H. Ballard, and M. M. Hayhoe. Task and context determine where you look. *Journal of Vision*, 7(14):16–16, December 2007.
- [87] Jeremy M. Wolfe. Guided search 4.0. *Integrated models of cognitive systems*, pages 99–119, 2007.
- [88] Marc Pomplun. Saccadic selectivity in complex visual search displays. *Vision Research*, 46(12):1886–1900, June 2006.



- 
- [89] Michael Land and D. N. Lee. Where we look when we steer. 369(6483):742–744, June 1994.
- [90] Mary Hayhoe and Dana Ballard. Eye movements in natural behavior. *Trends in Cognitive Sciences*, 9(4):188–194, April 2005.
- [91] M Land, N Mennie, and J Rusted. The roles of vision and eye movements in the control of activities of daily living. *Perception*, 28(11):1311–1328, 1999.
- [92] Michael F. Land and Peter McLeod. From eye movements to actions: how batsmen hit the ball. *Nature neuroscience*, 3(12):1340–1345, 2000.
- [93] Mary Hayhoe, Neil Mennie, Brian Sullivan, and Keith Gorgos. The role of internal models and prediction in catching balls. In *Proceedings of the American Association for Artificial Intelligence*, 2005.
- [94] Howlett Boyce Hunter C. The benefits of daylight through windows. pages 88–88, 2003.
- [95] Myriam B. C. Aries, Jennifer A. Veitch, and Guy Newsham. Windows, view, and office characteristics predict physical and psychological discomfort. *Journal of Environmental Psychology*, 30(4):533–541, December 2010.
- [96] P Leather, M Pyrgas, D Beale, and C Lawrence. Windows in the workplace: Sunlight, view, and occupational stress. *Environment and Behavior*, 30(6):739–762, 1998.
- [97] Jeong Tai Kim, Ju Young Shin, and Geun Young Yun. Prediction of discomfort glares from windows: Influence of the subjective evaluation of window views. *Indoor and Built Environment*, page 1420326X11423157, 2011.
- [98] Hester Hellinga and Truus Hordijk. The d&v analysis method: A method for the analysis of daylight access and view quality. *Building and Environment*, 79:101–114, 2014.
- [99] Erich Schneider, Thomas Villgrattner, Johannes Vockeroth, Klaus Bartl, Stefan Kohlbecher, Stanislavs Bardins, Heinz Ulbrich, and Thomas Brandt. EyeSeeCam: An eye movement-driven head camera for the examination of natural visual exploration. *Annals of the New York Academy of Sciences*, 1164(1):461–467, 2009.
- [100] Ernst Neufert and Peter Neufert. *Architects' data*. John Wiley & Sons, 2012.
- [101] H J Herrmann and S Scheuer. Requirements for new technologies becoming part of on-screen works as well as directions for their implementation, especially in standardization activities. 2004.
- [102] Bernard Marius't Hart, Johannes Vockeroth, Frank Schumann, Klaus Bartl, Erich Schneider, Peter Koenig, and Wolfgang Einhäuser. Gaze allocation in natural stimuli: Comparing free exploration to head-fixed viewing conditions. *Visual Cognition*, 17(6-7):1132–1158, 2009.

## Bibliography

---

- [103] P R Boyce, J A Veitch, G R Newsham, C C Jones, J Heerwagen, M Myer, C M Hunter, and J.A. Boyce Veitch. Lighting quality and office work: two field simulation experiments. *Lighting Research & Technology*, 38(3):191–223, 2006.
- [104] Mandana Sarey Khanie, Josef Stoll, Sandra Mende, Jan Wienold, Wolfgang Einhäuser, and Marilynne Andersen. Uncovering relationships between view direction patterns and glare perception in a daylit workspace. In *LUXEUROPA*, number EPFL-CONF-188436, 2013.
- [105] C. Hubalek Schierz. LichtBlick – photometrical situation and eye movements at VDU work places. 2005.
- [106] ISO/9241-303:2011, ergonomics of human-system interaction, part 303: Requirements for electronic visual displays. Technical report, 2011.
- [107] G. Legge. *Psychophysics of reading in normal and low vision*. Lawrence Erlbaum Associates Inc., Mahwah, New Jersey, 2006.
- [108] ISO. ISO/9241-12:1998, ergonomic requirements for office work with visual display terminals (vdts) , part 12: Presentation of information. Technical report, 1998.
- [109] Mandana Sarey Khanie. *Light & visual comfort in office environment: towards a model for required minimum contrast on monitorscreen*. Chalmers tekniska högsk., Göteborg, 2010.
- [110] RG Hopkinson. The multiple criterion technique of subjective appraisal. *Quarterly Journal of Experimental Psychology*, 2(3):124–131, 1950.
- [111] R G Hopkinson. Evaluation of glare. *Illuminating engineering*, 1957.
- [112] Fredrik Lange and Magnus Söderlund. Response formats in questionnaires: Itemized rating scales versus continuous rating scales. *SSE/EFI Working Paper Series in Business Administration*, (2004):13, 2004.
- [113] AO Grigg. Some problems concerning the use of rating scales for visual assessment. *Journal of the Market Research Society*, 22(1), 1980.
- [114] Donald G Gardner, Larry L Cummings, Randall B Dunham, and Jon L Pierce. Single-item versus multiple-item measurement scales: An empirical comparison. *Educational and Psychological Measurement*, 58(6):898–915, 1998.
- [115] Boas Shamir and Ronit Kark. A single-item graphic scale for the measurement of organizational identification. *Journal of Occupational and Organizational Psychology*, 77(1):115–123, 2004.
- [116] Moshe M Givon and Zur Shapira. Response to rating scales: a theoretical model and its application to the number of categories problem. *Journal of Marketing Research*, pages 410–419, 1984.

- [117] Leonie Geerdinck. Graduation report: Glare perception in terms of acceptance and comfort. 2012.
- [118] Kevin W Houser and Dale K Tiller. Measuring the subjective response to interior lighting: paired comparisons and semantic differential scaling. *Lighting Research and Technology*, 35(3):183–195, 2003.
- [119] Mn Inanici. Evaluation of high dynamic range photography as a luminance data acquisition system. *Lighting Research and Technology*, 38(2):123–136, June 2006.
- [120] Greg Ward-Larson and Rob Shakespeare. *Rendering with radiance: the art and science of lighting visualization*. Morgan Kaufmann Publishers Inc., San Francisco, CA, USA, 1998.
- [121] Mark Stanley Rea and IG Jeffrey. A new luminance and image analysis system for lighting and vision i. equipment and calibration. *Journal of the illuminating Engineering Society*, 19(1):64–72, 1990.
- [122] L. Bellia, A. Cesarano, F. Minichiello, and S. Sibilio. Setting up a CCD photometer for lighting research and design. *Building and Environment*, 37(11):1099–1106, 2002.
- [123] Mehlika N. Inanici. *Transformations in architectural lighting analysis: Virtual lighting laboratory*. PhD thesis, The University of Michigan, 2004.
- [124] Mandana Sarey Khanie, Jan Wienold, and Marilyne Andersen. A sensitivity analysis on glare detection parameters (remote presentation). In *13th International Radiance Workshop 2014*, 2014.
- [125] Jean-Yves Bouguet. Camera calibration toolbox for matlab, 2004.
- [126] Roger E Kirk. Experimental design: Procedures for the behavioural sciences (brooks/cole: Belmont, ca). CA, USA, 1968.
- [127] Jack B. Kuipers. *Quaternions and rotation sequences : a primer with applications to orbits, aerospace, and virtual reality*. Princeton Univ. Press, Princeton, NJ, 1999.
- [128] Denis G Pelli and Katharine A Tillman. The uncrowded window of object recognition. *Nature neuroscience*, 11(10):1129–1135, 2008.
- [129] Mandana Sarey Khanie and Marilyne Andersen. Towards a refined understanding of comfort in workspaces. In *Swiss–Emirati Friendship Forum: UAE-Swiss Research Day 2011*, number EPFL-POSTER-166734, 2011.
- [130] Mandana Sarey Khanie, Josef Stoll, Sandra Mende, Jan Wienold, Wolfgang Einhäuser, and Marilyne Andersen. Investigation of gaze patterns in daylight workplaces: using eye-tracking methods to objectify view direction as a function of lighting conditions. In *Proceedings of CIE Centenary Conference" Towards a New Century of Light"*, number EPFL-CONF-186132, pages 250–259. CIE Central Bureau, 2013.

## Bibliography

---

- [131] Gregory J. Ward. The RADIANCE lighting simulation and rendering system. In *Proceedings of the 21st annual conference on Computer graphics and interactive techniques, SIGGRAPH '94*, pages 459–472, New York, NY, USA, 1994. ACM.
- [132] Michael Bach. The freiburg visual acuity test—automatic measurement of visual acuity. *Optometry and vision*, 73:49–53, 1996.





Feb 01- Nov 02 **Amod Architecture and Urbanism Consultant**  
Internship

**Tehran, Iran**

Projects:  
Recycle Park, Municipal Districts 7, Tehran, Iran

#### **WORKSHOP AND SEMINARS**

Sep	10	<b>Reality Studio, UN-Habitat</b>	<b>Nairobi, Kusumu, Kenya</b>
Sep	09	<b>LUX Europa</b>	<b>Istanbul, Turkey</b>
Dec	08&12	<b>Stockholm Lighting Days</b>	<b>Stockholm, Sweden</b>
Oct	08	<b>nordic LIGHTING + DESIGN conference</b>	<b>Helsinki, Finland</b>
Sep	07	<b>Design In the Dark</b> Sint-Lucas School of Architecture Universal Design for visual impaired	<b>Gent, Belgium</b>
Sep	06	<b>Lights in Alingsås</b> , Interacting with people Project: The Housing State: Östlyckan Bostadsområdet Design Leaders; Jöran Linder, Erik Olsson	<b>Alingsås, Sweden</b>
Mar	06	<b>AGS, the Alliance for global Sustainability</b> AGS Annual Meeting in Bangkok: "Parallel session on Energy/ Food, Water/Risk, and Governance/Education"	<b>Bangkok, Thailand</b>

#### **LANGUAGE**

English	Bilingual Proficiency
Persian	Native Proficiency
Swedish	Full Professional Proficiency
German	Limited Working Proficiency
French	Elementary Proficiency
Arabic	Elementary Proficiency

#### **REFERENCE**

Marilyne Andersen; PhD, Professor, École polytechnique fédérale de Lausanne (EPFL)

E marilyne.andersen@epfl.ch  
T +41(0)21 693 08 83

Jan Wienold; PhD, Fraunhofer ISE

E jan.wienold@epfl.ch  
T +41(0)21 693 0849

Monica Billger; PhD, Professor, Chalmers University of Technology

E monica.billger@chalmers.se  
T +46 (0)31 772 23 83

Kai Pippo; Creative Director, Principal; PLDA

E kai.piippo@ljusarkitektur.se  
T +46 (0)70 855 81 51